Marine carbonate factories: Review and update

JOHN J. G. REIJMER 🅔

Carbonate Sedimentology Group (CSG@CPG), Geosciences Department, College of Petroleum Engineering & Geosciences, King Fahd University of Petroleum & Minerals, Dhahran 31261, Kingdom of Saudi Arabia (E-mail: J.J.G.Reijmer@vu.nl)

ABSTRACT

The carbonate factories model, as defined at the beginning of the century, provides a subdivision of marine carbonate sediment production-systems based on the style of carbonate precipitation. The main factors controlling marine carbonate precipitation are light, water temperature, nutrients, salinity, substrate and carbonate saturation. Site-specific controls influencing the systems comprise ocean currents, upwelling and non-upwelling systems, ocean-atmosphere systems, atmospheric systems, shallow-water dynamics, and terrestrial sediment and water input.

Each factory has its own sediment-production window linking optimal sediment production with selected environmental controls. Sediment production in the tropical factory (T-factory) is light and temperature-dependent and negatively impacted by nutrients. Sediment production and export depends on the size of the shallow-water areas within the photic zone. The cold-water-coral factory (CWC-factory) is nutrient-dependent, but light-independent. Sediment production relates to nutrient supply enabling the growth of the cold-water corals. The cool-water factory (C-factory) displays a strong link to nutrients and water temperature, with parts that are light-dependent, for example, sediment production in kelp dominated environments. The sediment mineralogy and sediment production area within the high-energy hydrodynamic zone govern sediment distribution with sediment behaviour comparable to siliciclastics. The microbial/mud-mound factory (M-factory) is nutrient-dependent and to some extent temperature and light-independent. Sediment production and export is referred to here as slope shedding and links to the main sediment production on the upper slope. The planktic factory (P-factory) depends on variations in light, temperature and nutrients resulting in fluctuating pelagic fall-out.

Platform morphologies and slope profiles are also factory specific: T-factories show a rimmed flat-topped platform with adjacent exponential slopes or a carbonate ramp morphology; CWC-factories display mound morphologies with steep slopes; C-factories are associated with open shelf systems and Gaussian shaped slope profiles; while M-factories are characterized by individual steep-sided mounds or flat-topped platforms with deepened margins and a linear shaped slope profile. The P-factory provides biotic grains to all environments and at times, like for the Cretaceous, may dominate sedimentation patterns in the basin realm.

The sequence stratigraphic patterns substantially differ between factories. The T-factory being light-dependent is characterized by higher sediment production when the platform tops are flooded (highstand shedding). It displays decoupled sediment wedges with the partial infill of accommodation in the shallow-water realm and major sediment export towards the slopes and surrounding basins. The CWC-factory is marked by *in situ* production and deposition with limited sediment export forming single CWC spots or

sediment accumulation ridges. The C-factory has a siliciclastic equivalent style of sediment distribution with lowstand-dominated, shelf edge wedges and a shaved-off shelf during sea-level highstands. Slope shedding marks the M-factory in which sediment production occurs within the upper slope realm of the flat-topped platforms both during highstands and lowstands in sea-level. This allows for fairly continuous sediment production exhibiting minor impact of sea-level changes, but with progradation, aggradation and retrogradation of the system being only limited by local environmental changes. P-factory sediment production may vary in accordance with variations in sea-level, providing time-lines and systems tracts boundaries in the pelagic realm.

In summary, each factory is branded by an individual set of features, for example, production window, sediment production and export, morphologies and slopes. It is this unique set of variables marking each factory that determines the factory-dependent response to small-scale and large-scale environmental changes through space and time as shown in the sequence stratigraphic development.

Keywords Carbonate factories, platform morphologies, sediment export, sediment production, sequence stratigraphy, slope systems.

INTRODUCTION

One of the main advances in carbonate sedimentology achieved during the last three decades, is the distinction of different carbonate factories. These are groups of carbonate-producing organisms that operate under a specific set of environmental conditions, and as a result have a particular sedimentological and stratigraphic imprint. A carbonate factory classification system thus provides a set of characteristics, ranging from the micro-texture to the overall stratal geometries, which enable predictions away from known data points.

The aim of this paper is to provide a review and update of the carbonate factories that operate and operated in the marine realm, including both the benthic and planktic organisms. Although several different types of factories will be reviewed, the one preferred in this paper is based on the work by Schlager (2000, 2003, 2005).

The following key characteristics of the carbonate factories will be dealt with: (i) the environmental parameters influencing carbonate production; (ii) the mineralogy, grain-size and texture; (iii) growth strategy and associated morphology and architecture; (iv) slope morphologies; and (v) sequence stratigraphic characteristics. The factories will be illustrated, where possible, with key examples from both the recent and ancient.

HISTORY OF RESEARCH ON CARBONATE FACTORIES

Pioneering work in the 1950s on the Bahamas by the SHELL Oil Company laboratory group at Miami led by Robert N. Ginsburg still has an impact on present-day thinking of carbonate depositional models. The group started the trend of describing grain-size patterns and particle distributions, and linking them to distinct depositional environments along the Bahamian platforms (e.g. Ginsburg *et al.*, 1958). Since those times, the classification of carbonate sedimentary systems has been done along many lines. The classic carbonate classification schemes by Folk (1959, 1974) and Dunham (1962) strictly go by their depositional texture. The occurrence of the type of allochems, their abundance and packing; in combination with the type and percentage of matrix, for example micrite versus sparite, determines the classification of the carbonate sediments and indirectly relates to the energy level of the depositional environment. The discussion on aforementioned classification schemes and their use in describing carbonate facies is ongoing (e.g. Lokier & Al Junaibi, 2016).

Lees & Buller (1972) used a classification system based on assessment of the dominant benthic grain types occurring on modern temperate and warm–water shelves. Lees (1975) over time evaluated the influence of salinity and

temperature on carbonate sediments and related them to the grain type associations. Nelson (1988) discussed the occurrence of non-tropical shelf carbonates located at higher latitudes, >30° north or south, with a mean annual surface-water isotherm below 20°C. Hence, Nelson (1988) considered those found outside the zone with hermatypic coral reefs separated by a mean annual surface-water isotherm of 20°C.

Carannante *et al.* (1988) used a similar approach and defined a series of carbonate lithofacies ranging from coral reef facies (chlorozoan) to chloralgal (chlorozoan without hermatypic corals), rhodalgal (with abundant encrusting coralline algae) and molechfor with benthic foraminifera, molluscs, echinoids, bryozoans and barnacles. These lithofacies were linked to latitude and depth-dependent variations in water temperature although other factors, for example, water salinity, nutrient content and light penetration, were also considered to be important. Over time, more and more grain associations were added, that were associated with variations in seawater temperature, as summarized by Kindler & Wilson (2010), emphasizing the difficulty of capturing the natural variance through strict subdivisions.

Rao (1996) and Betzler *et al.* (1997a) discussed the occurrence of temperate or warm-temperate carbonates deposited in transitional warm-temperate zones linking the tropical and polar regions. James (1997) summarized the particle types and introduced the heterozoan and photozoan association concept; terminology that currently is widely used. In the James (1997) classification, the heterozoan association covered the cool-water carbonates occurring in modern marine settings with seawater temperatures mostly below 20°C, exhibiting heterotrophic feeding strategies. The photozoan association comprises carbonates deposited in eutrophic to oligotrophic settings covering warm-water environments characterized by green calcareous algae and corals, but also by inorganically produced ooids, muds and cements. However, recent studies of ooids illustrate that microbes play an essential role in their formation (Pacton *et al.*, 2012; Edgcomb *et al.*, 2013; Diaz *et al.*, 2014, 2015; Diaz & Eberli, 2019). For the Gulf of California, Halfar *et al.* (2000, 2004, 2006a,b) demonstrated that boundaries between heterozoan and photozoan associations are gradual and that various transitional facies are present related to variations in temperature and nutrient levels.

The study on depositional profiles of carbonate platforms by Pomar (2001), distinguished three main groups of carbonate-producing biota associated with their dependence upon light: (i) euphotic biota appearing in the light flooded zone in shallow, wave-agitated areas; (ii) oligophotic biota in reduced light conditions frequently encountered in deeper, commonly non-wave-agitated areas; and (iii) biota that are photo-independent and can occur throughout all water-depth ranges. Pomar (2001) also argued for a link between the aforementioned groups in carbonate-producing biota and possible platform morphologies. However, tropical and microbial marine carbonate systems with comparable flat-topped morphologies, for example Great Bahama Bank (Ginsburg *et al.*, 1958) for tropical systems and Sierra de Cuera (e.g. Bahamonde *et al.*, 2004) for microbial systems, are not in accordance with this model. The same holds for present-day tropical systems with morphologies varying from carbonate ramps (for example, Arabian/Persian Gulf) to flat-topped morphologies (for example, Bahamas) and large-scale atolls (for example, Maldives). On the other hand, bottom communities may modify water circulation when building barrier reefs or may stabilize the sediment surface at the sea bottom by trapping and binding sediment grains through organic films (Ginsburg & Lowenstam, 1958). As discussed for Tahiti by Blanchon *et al.* (2014), the transition from a fringing to a barrier reef system may also occur in response to a rise in sea-level flooding the antecedent Pleistocene slope and reef-flat platform accompanied by a switch in the coral-assemblage to faster growing species.

Heterozoan associations may also develop in nutrient-rich, shallow or deep tropical marine waters (James, 1997). Pomar (2001) argued that depth-dependent variations in carbonate producing biota mainly relate to light conditions, but also noted that other environmental parameters control the bathymetric distribution of benthic carbonate systems like salinity, temperature, current or wave action, and turbidity. Michel *et al.* (2011) and Klicpera *et al.* (2015) for the Mauritanian shelf, Humphreys *et al.* (2016) and Reymond *et al.* (2016) for the Galapagos Islands and Reijmer *et al.* (2012a,b) for Panama demonstrated that local upwelling introducing nutrient-rich cold waters to shallow settings forces tropical carbonate producing biota to shift from a photozoan to a heterozoan association.

A different approach to classifying carbonates was proposed by Schlager (2000, 2003, 2005) who introduced the carbonate factory concept, which is based on the style of carbonate precipitation (Fig. 1). Three different modes were proposed, based on the basic types of carbonate precipitation defined by Lowenstam & Weiner (1989), ranging from: (i) abiotic; and (ii) biotically induced (mud-mound / microbial factory or M-factory); to (iii) biotically controlled with heterotrophic (cool-water factory or C-factory) and autotrophic styles (tropical or T-factory). Schlager also discussed the factory-dependent production profiles and platform morphologies (Fig. 2).

The objective of this review is to discuss recent insights in the carbonate factory classification concept and to merge the system-inherent precipitation styles of the individual carbonate factories with their platform morphologies, variations in sediment production and export, sediment composition (grain sizes and mineralogy), differentiations in platform slopes and sequence stratigraphic applications. The review focuses on present-day examples, but discusses related ancient counterparts whenever appropriate. It should be noted that: (i) the present-day is characterized by particular conditions being an interglacial in an ice-age, and thus is different from most of the Phanerozoic; (ii) as a result for some ancient examples,

for example intra-cratonic intra-shelf basins and microbial dominated platforms, present-day analogues are virtually absent, which is the reason why, for these cases, mostly ancient examples are cited; and (iii) the bias of the author, who aims to inspire other workers to further improve current understanding of marine carbonate factories.

ENVIRONMENTAL CONTROLS

Major environmental controls

A number of environmental parameters direct the different modes of carbonate precipitation in present-day environments (Table 1). In marine and freshwater aquatic settings, besides the biotically controlled and biotically induced mode, the abiotic mode also is present. However, during the production of whitings, which up to now have been considered as abiotic muds, microbes most likely play a mediating role (e.g. Robbins & Blackwelder, 1992; Yates & Robbins, 1998; Thompson, 2000; Pratt, 2001).

The diversity in the biotically controlled precipitation modes is guided by a set of factors that determine environmental variations. The most important factors are: (i) light; (ii) temperature; (iii) nutrients; (iv) salinity; (v) substrate; and (vi) carbonate saturation (Table 1). The
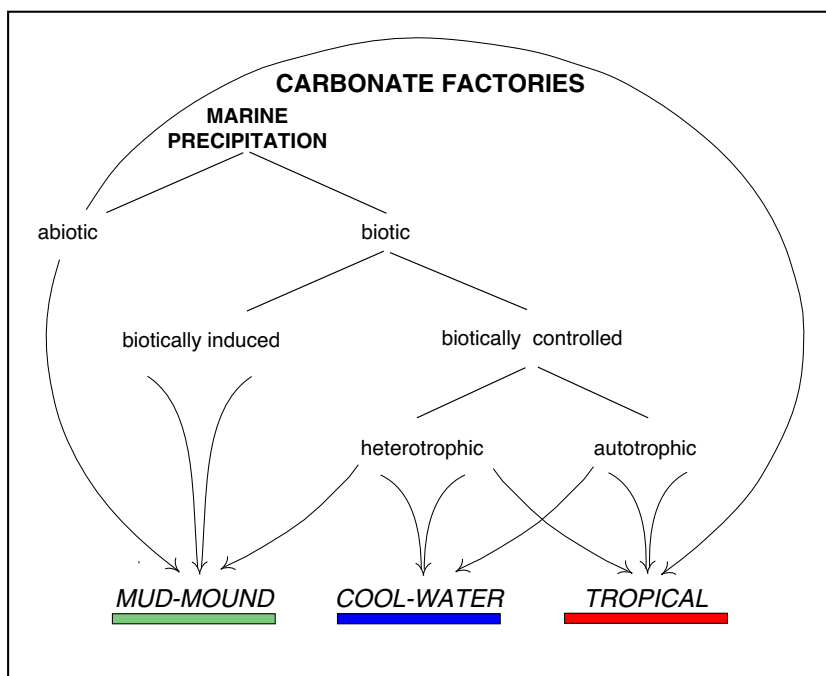
Fig. 1. The original carbonate factory model of Schlager (2003) showing marine precipitation modes and associated carbonate factories. The tropical factory (T-factory) is characterized by biotically controlled precipitation through tropical autotrophic organisms or heterotrophic organisms with autotrophic symbionts. The cold-water factory (C-factory) displays biotically controlled precipitation by heterotrophic organisms. The mud-mound factory (M-factory) is dominated by biotically induced precipitation. Abiotic precipitates may occur in the M-factory and the T-factory. Redrawn from Schlager (2003, 2005).
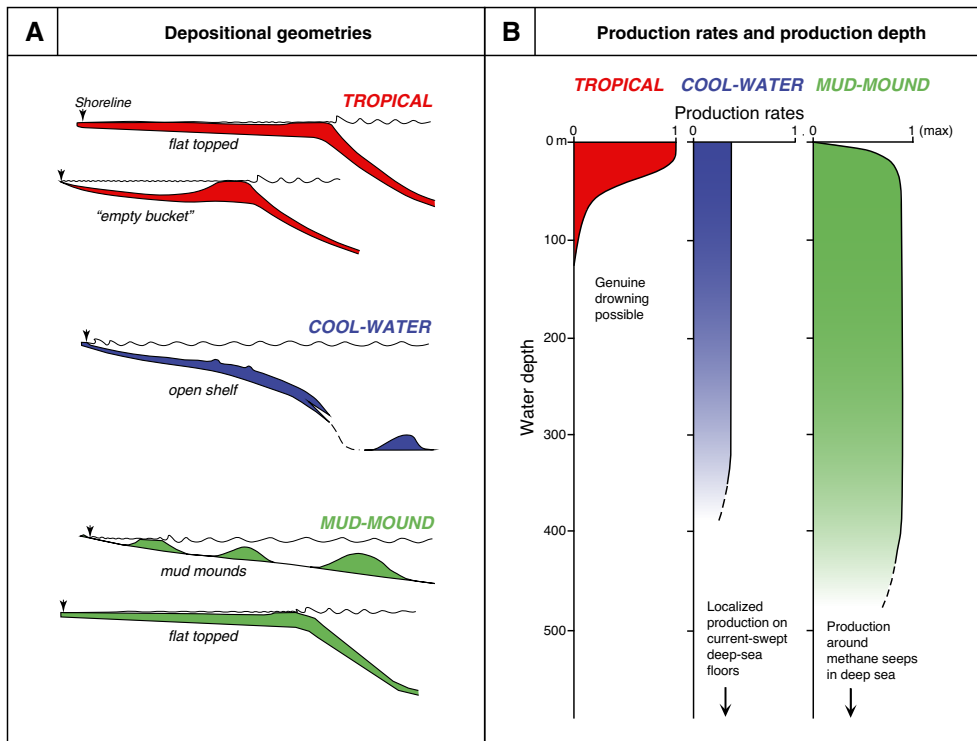
Fig. 2. (A) Depositional geometries of the carbonate factories, and (B) production rates and depth windows for the various carbonate factories. Modified from Schlager (2003, 2005). Production window of the light-dependent T-factory is restricted to the upper water column, but with very high production rates. Production rates of the C-factory is independent of light, lower than for the T-factory but over a wider depth range. The same holds for the M-factory. After Schlager (2003, 2005).

restrictions for the style of carbonate precipitation and associated sediment production windows are set by these factors. The prevalence of specific factors may regulate the development of certain biota, which ultimately will determine the evolution and morphological expression of the individual carbonate systems.

Table 1. Environmental controls directing the different modes of carbonate precipitation.

Main environmental controls	Site-specific environmental controls
Light	Ocean currents
Water temperature	Upwelling and non-upwelling systems
Nutrients	Ocean-atmospheric systems
Salinity	Atmospheric regimes
Substrate	Shallow-water dynamics
Carbonate saturation	Terrestrial sediment and water input

Light

Light is considered to be one of the most significant environmental controls. The extent of light-related zonation varies within the oceans depending on the depth of the euphotic zone and the clarity of the waters (Hallock & Schlager, 1986; Hallock, 2005; Schlager, 2005). Hence variations in the clarity of the euphotic zone may constrain the spatial and bathymetric development of the reef and consequently the vitality of the carbonate factory and sediment productivity. At present, the depth of the euphotic zone varies from as shallow as 20 m for the Arabian/Persian Gulf, Singapore and western Caribbean, to 40 m for the Great Barrier Reef and the Yucatan shelf, and maximum values of almost 150 m for Pacific atolls (Schlager, 2005, p. 16).

Growth forms of corals are regulated by depth of the light-saturated zone and euphotic zone with branching corals dominating the uppermost levels, head corals in intermediate water depths and platy corals occurring at the deepest low light levels (Reiss & Hottinger, 1984; Hallock &

Schlager, 1986; Hallock, 2005). The coral growth form and water-depth distribution were also used to evaluate the carbonate platform progradation of various Miocene carbonate platforms such as the Llucmajor platform (Mallorca, Spain; Pomar, 1991) and the Mut Basin (Bassant *et al.*, 2005). It has been suggested that elevated ultraviolet radiation levels may damage the symbiotic photosynthetic algae and the coral tissues in shallow to deep water depths (Lewis, 2001).

Light also impacts the growth rates of the photosynthetic, carbonate-secreting benthos like large benthic foraminifera (Hallock, 1985; Hohenegger, 2005) as well as calcareous green algae like *Halimeda*, *Penicillus* and *Udotea* (Bosence, 1989). Carbonate production by epibionts related to the growth of *Thalassia* or other seagrass substrates can also be significant (Nelson & Ginsburg, 1986; Bosence, 1989; Perry & Beavington-Penney, 2005). *Thalassia* also could be linked to lime mud production on carbonate platforms while providing a habitat for various calcifying organisms (Enríquez & Schubert, 2014).

Water temperature
As discussed by Lees & Buller (1972) the diversities of the biotic association on modern temperate and warm–water shelves are strongly linked to temperature. Moving from the equator to higher latitudes, skeletal and non-skeletal assemblages change in response to changing environmental conditions while each carbonate-secreting species has its own optimum growth window along the temperature scale (Lees, 1975). Hence, tropical and cool-water assemblages differ significantly and various transitional assemblages have been documented (e.g. Carannante *et al.*, 1988; Rao, 1996; Betzler *et al.*, 1997a; Halfar *et al.*, 2000, 2004; Halfar *et al.*, 2006b). The distribution and occurrence of water temperature ranges rely on (palaeo-)ocean circulation patterns and (palaeo-)latitudinal position, and hence determine the distribution of specific organisms across the globe through time. For cool-water (heterozoan) carbonates, Michel *et al.* (2018) demonstrated that advantageous oceanographic conditions for heterozoan carbonate production occur in regions with high marine productivity, while light-related carbonate platform ecosystems (for example, rhodalgal platforms) prevail within subtropical and warm-temperate latitudes. These authors also proposed to separate the phototrophic seagrass/red algal and the heterozoan platform systems because they are linked to different environmental parameters, namely light versus nutrients.

Nutrients
The third important factor in controlling the carbonate precipitation mode are nutrient levels, for example, phosphate and nitrate. High nutrient levels excite the development of filamentous algae, barnacles and certain taxa of bryozoans, and at the same time reduce calcification rates (e.g. Halfar *et al.*, 2004, 2006b; Reijmer *et al.*, 2012a).

Mutti & Hallock (2003) defined a set of thresholds for the development of carbonate facies associations, and variations in ocean water temperatures and nutrient availability. Variations in nutrient gradients in low latitude environments incorporated: (i) oligotrophic settings with coral reefs in which nutrient limitation is the primary control for biota development; (ii) mesotrophic environments with coral-algae and macroalgae (including calcareous green algae), known to occur in upwelling zones, in which competition was believed to regulate occurrence of biota; (iii) eutrophic sites with heterotrophs in which light was seen as the limiting factor for biota development; and (iv) hypotrophic with bacteria as the dominant benthos; a system regulated by the supply of oxygen. Variations in the nutrient gradient not only modify the carbonate facies, but also because of these modifications change the bioerosion rates and the grain-size spectrum of the sediments being produced (Chazottes *et al.*, 1995, 2002, 2008). In addition, nutrient availability may obstruct coral recruitment (Smith & Buddemeier, 1992; Atkinson *et al.*, 1995). Different scenarios for variations in biotic assemblages related to changes in trophic levels and photosynthesis, leading to the preference of mixotrophic nutrition systems, are discussed by Pomar & Hallock (2008).

Salinity
Natural coral reef communities do well within a salinity range between 25‰ and 40‰ and can deal with long-term and short-term salinity variations (Coles & Jokiel, 1978; Muthiga & Szmant, 1987). For example, surface salinities on Great Bahama Bank vary between 37‰ and 42‰, while for the Tongue of the Ocean salinities range between 36‰ and 37‰, and for the Straits of Florida between 35.5‰ and 36.5‰ (Ginsburg *et al.*, 1958). The distribution of non-vertebrates and their biodiversity throughout environments with varying salinity levels, brackish to hypersaline, was discussed extensively by Heckel (1972). Lewis (2001) discussed that for salinities

of 40 to 60‰ algal photosynthesis decreased, and coral respiration increased. Values exceeding 40‰ may lead to swift decrease in taxa (Smith & Buddemeier, 1992). A lethal salinity threshold of over 45‰ was found for corals exposed for a longer period of time to such elevated salinity levels (Lewis, 2001). Also values below 20‰ may be lethal for coral growth in a short period of time (Smith & Buddemeier, 1992). Hence, periodical or frequent changes decreasing salinity below the lower tolerance level will severely affect local reef areas (Smith & Buddemeier, 1992). No maximum salinity thresholds were found influencing the calcification rates in *Mytilus* shells, while minimum salinity levels varied between 14.7‰ and 20‰ (Malone & Dodd, 1967).

Certain algal communities have a greater tolerance for high salinities, and hence may occur in large terminal lakes like the Great Salt Lake (Stephens, 1990; Harris *et al.*, 2013), hypersaline lakes on Eleuthera Island (Bahamas; Dupraz *et al.*, 2004, 2009) and sabkha environments (e.g. Kenig *et al.*, 1990; Duane & Al-Zamel, 1999; Bontognali *et al.*, 2010; Lokier *et al.*, 2013). For the Florida Keys coral reef system, Porter *et al.* (1999) discussed that raised salinities could reduce the negative effects of elevated temperature and concluded that temperature and salinity have contrasting outcomes on coral photosynthesis. In restricted saline environments like for the Miocene in south-east Spain, however, biotic diversity was significantly reduced with only *Porites* sp. surviving at the end (e.g. Riding *et al.*, 1991; Braga & Martín, 1996).

Substrate

The type of substrate plays an important role for specific biota like corals that need a hard surface for their larvae to settle. Certain suspension feeders prefer a hard substrate; echinoderms might graze on a hard substrate, but also feed on soft to mobile substrate. Hence, the type of substrate partially determines the type of biota that may occur. Heckel (1972) and Flügel (2010, pp. 605–606) described the substrate preference of modern animals and plants with: (i) colonial corals and certain clams (borers) having a preference for a hard substrate; (ii) hard to firm substrate occupied by solitary corals, red algae, green algae, sponges, bryozoans, oysters and barnacles; (iii) hard to soft substrate inhabited by foraminifera, blue-green algae and brachiopods, amongst others; and (iv) firm to soft and even moderate mobile substrate occupied by starfish, echinoids, some clams (burrowers) and ostracods. Gastropods cover the entire substrate range, hard to mobile, and the same holds for microbial induced carbonate precipitation (Heckel, 1972).

Carbonate saturation

Carbonate saturation is repeatedly discussed as another important factor influencing carbonate precipitation, accumulation and preservation (e.g. Pomar & Hallock, 2008). The water chemistry factor is proposed to be the critical environmental factor influencing biologically controlled and induced carbonate precipitation (Lowenstam, 1981; Mann, 1983), while environmental conditions like temperature control specific saturation levels needed for prolific carbonate production and distribution (e.g. Broecker & Takahashi, 1966; Opdyke & Wilkinson, 1990, 1993; Smith & Buddemeier, 1992; Gattuso *et al.*, 1998; Weiner & Dove, 2003; Riding & Liang, 2005; Pomar & Hallock, 2008; Michel *et al.*, 2019). Various studies discussed that for the present-day ocean latitudinal variations in the seawater carbonate saturation state agree with variations in water temperature (e.g. Riding & Liang, 2005; Jiang *et al.*, 2015), which is important as calcification in coral reef communities is tightly linked to the degree of aragonite saturation (Suzuki *et al.*, 1995; Gattuso *et al.*, 1998). Recent studies by Laugié *et al.* (2019), argued that this factor is less important in driving variations in modern carbonate production than has been repeatedly stressed in the literature.

Regional environmental controls

Besides the aforementioned ocean-wide factors regional constraints may influence the mode of carbonate precipitation and determine the type of carbonate factory that will develop (Table 1). As briefly discussed in the *Introduction*, surface and deep-water ocean currents influence the distribution of present-day benthic carbonate communities (e.g. James, 1997; Schlager, 2005).

Ocean currents

The absence of large-scale tropical reef development off the west coasts of South America and Africa are region-specific anomalies linked to ocean gyres introducing cold surface waters to low latitudes (e.g. Lees & Buller, 1972; Lees,

1975; Grigg, 1982; James, 1997; Schlager, 2005). At the same time, western boundary currents may carry warm waters to temperate latitudes expanding the tropical depositional range like for example the Gulf Stream bathing Bermuda (e.g. Crossland, 1988; Opdyke & Wilkinson, 1990). Other currents with waters of tropical origin extending the T-factory realm to higher latitudes are the Agulhas Current along the east African coast, the Leeuwin Current of western Australia bathing the Houtman Abrolhos islands, the Kuroshio Current reaching the Ryukyu Islands of Japan, the East Australia Current flowing along the eastern Australia coast and the south Equatorial Current in the South Pacific (e.g. Crossland, 1988). For example, the warm southerly-flowing Leeuwin Current bathing the coast of Western Australia resulted in the development of so-called high-latitude reefs that differ from a typical T-factory biotic assemblage with sediments that contain a mix of cool-water and tropical carbonate biota with coralline algae and molluscs, competing with corals (Crossland, 1988; Collins *et al.*, 1993, 2003).

Another example of large-scale ocean currents, directing the development of shallow-water carbonate sediment production systems occurs in the Galapagos Archipelago. There, the El Niño – Southern Oscillation (ENSO) and upwelling from the Equatorial Undercurrent determine the diversity and distribution patterns of shallow-water carbonate producers, which are benthic foraminifera in this case (Humphreys *et al.*, 2016, 2018; Reymond *et al.*, 2016).

Upwelling and non-upwelling systems

Ocean surface currents might also introduce local upwelling of cold nutrient-rich waters as observed for the coast of Mauritania, resulting in a turnover of the biotic assemblage towards a cool-water factory assemblage dominated by bivalves and foraminifera (Michel *et al.*, 2011; Klicpera *et al.*, 2015). The above-mentioned Galapagos Archipelago study (Humphreys *et al.*, 2016, 2018; Reymond *et al.*, 2016) and the Gulf of Panama studies discussed in the next paragraph (Reijmer *et al.*, 2012a) display a similar response to upwelling events. The Maldives platform of the Indian Ocean illustrates partial demise of its atolls caused by seasonal upwelling events associated with the onset and intensification of the Indian monsoon (e.g. Betzler *et al.*, 2013, 2018).

Ocean-atmospheric systems

Other changes in tropical carbonate factories, from a tropical factory (T-factory; Schlager, 2003) to a cool-water factory type (C-factory; Schlager, 2003), could be related to changes in the El Niño – Southern Oscillation (ENSO) climatic and oceanic events that result in variations in sea-surface temperature and nutrient content near the Galapagos Islands in the eastern tropical Pacific Ocean (Humphreys *et al.*, 2016, 2018; Reymond *et al.*, 2016).

Seasonal changes in trade wind patterns may also result in changes in the distribution of biota modifying the occurrence of a specific carbonate factory as discussed for the Gulf of Panama and the Gulf of Chiriquí (Reijmer *et al.*, 2012a). In the Gulf of Panama, the trade wind changes initiated seasonal upwelling patterns that resulted in the modification of the carbonate factory from a T-factory to a modified C-factory, while the adjacent Gulf of Chiriquí lacking seasonal upwelling displayed no changes in the T-factory sediment production.

Seasonal patterns in monsoonal and oceanographic processes allowed for the development of high latitude coral reefs in the Gulf of Aqaba (Mergner & Schuhmacher, 1974, 1981; Dullo *et al.*, 1996) and the carbonate ramp deposits in the Arabian/Persian Gulf (e.g. Purser, 1973; Crossland, 1988) while the current systems aided in optimizing the physico-chemical environmental setting for colonization of tropical biota. Laugié *et al.* (2019) discussed that the Arabian/Persian Gulf could be classified as special type of carbonate setting deviating from the T-factory system.

Atmospheric regimes

Seasonal variations like passing cold fronts play an important role in the quantity of sediments exported from the shallow-water areas of the Bahamas (Wilson & Roberts, 1992, 1995; Roth & Reijmer, 2004, 2005). The trade winds with a prevailing east to west direction drive the redistribution of carbonate sediments that originate within the shallow-water realm resulting in the preferential progradation of the carbonate sedimentary system and even the infill of an old seaway on the Bahamas as observed for the Great Bahama Bank (Eberli & Ginsburg, 1989).

The interaction between seasonal changes in trade winds and the mountain morphology of the adjacent landmass was observed in the tropical, low latitude Gulf of Panama and Gulf of

Chiriquí (Reijmer *et al.*, 2012a). In the Gulf of Panama, the changes in the trade wind and the absence of a mountain range blocking the northeast trade winds during the rainy season (May to November) initiate seasonal upwelling patterns resulting in the modification of the carbonate factory, as shown by a changeover from a tropical (T-factory; Schlager, 2003) to a modified cool-water assemblage (C-factory; Schlager, 2003). In the adjacent Gulf of Chiriquí, the Talamanca and Central Cordilleras reduce the effect of the seasonal changes of the trade wind and no seasonal upwelling occurs. Hence, no modification of the carbonate sediment production occurs (Reijmer *et al.*, 2012a).

Shallow-water dynamics
Tides and currents drive sediment production rates, for example coral reef development, settlement of biota, and regulate the associated sedimentation distribution patterns within the shallow-water realm of carbonate platforms, shelves and ramps, determining the infill of accommodation (e.g. Purkis & Harris, 2016; Weij *et al.*, 2019). A critical step in this process is the re-instalment of the wave and current patterns during the transition from a lowstand to a highstand in sea-level when the pre-existing shallow-water platform morphology is reflooded. The rapidity of this process ultimately will determine the hydrodynamic energy levels across a platform like Great Bahama Bank, which not only will determine the facies variations across the platform (Ginsburg *et al.*, 1958; Purdy, 1963a,b; Enos, 1974; Reijmer *et al.*, 2009; Harris *et al.*, 2015) but also accommodation infill patterns (e.g. Purkis & Harris, 2016; Weij *et al.*, 2019).

Currents may regulate the influx of nutrients within carbonate producing realms, and thus will impact coral/algal growth. The swell wave refraction at the edge of a flat-topped platform or the shallow-water realm of carbonate shelves and carbonate ramps may not only regulate reef development, but also control sediment transport as shown for the Houtman Abrolhos islands (Eastern Indian Ocean) influenced by the Leeuwin Current (Collins *et al.*, 1993, 2003).

Terrestrial sediment and water input
Another important local factor can be the influx of terrestrial sediments, for example clays and sands of various origins, influenced by: (i) the turbidity; and (ii) quantity and input location of the terrigenous sediments. Periodically such sediments may cover parts of the sediment substrate and the associated carbonate biotic assemblages, impacting overall carbonate sediment production. The studies of Perry (2003, 2005) unequivocally demonstrated this for the Mozambique Channel where the high turbidity level and mobile siliciclastic-dominated substrate tailored the carbonate factory to produce a site-specific mix of tropical (for example, corals) and temperate biota (for example, coralline algae, molluscs and a low diversity of benthic foraminifera).

In the mixed system of Safaga Bay (Red Sea, Egypt) the bottom morphology together with the hydrodynamic setting, controlled facies development during the glacial–interglacial transition. Coral reefs relocated on the topographic highs, while seagrass, coarse sand and mud-dominated facies with facies-specific biota developed in the coastal and deep-water areas (Piller & Pervesler, 1989; Piller & Mansour, 1990, 1994). The influx and distribution of siliciclastic material affected water turbidity and mainly restricted the coral reef depth distribution and hence the associated carbonate sediment production. Otherwise the siliciclastic sediment input and transport and carbonate reef development and associated sediment production were separated. However, the mobility and unstable nature of a sandy substrate limited the expansion of the coral reef carpet.

On a seismic-scale, carbonate and siliciclastic systems commonly are separated systems that develop in spatiotemporal settings related to sea-level fluctuations, transgressions and regressions, flooding or exposing shallow-water regions (Belize: Esker *et al.*, 1998; Ferro *et al.*, 1999; Great Barrier Reef: Dunbar & Dickens, 2003; Mut Basin, Turkey: Bassant *et al.*, 2005; Janson *et al.*, 2007; Gulf of Papua: Tcherepanov *et al.*, 2008a,b, 2010; Jorry *et al.*, 2010; Bonaparte Basin: Bourget *et al.*, 2014). Transport of siliciclastics is commonly restricted to channel systems that originate during sea-level lowstands and are reflooded during the following transgression. This separation allows carbonates to develop close to the siliciclastic fairways during transgressions and highstands in sea-level (e.g. McNeill *et al.*, 2000; Bauch *et al.*, 2011). Another source of terrestrial material might be windblown dust which may easily cross oceans (Stuut *et al.*, 2005; Lindhorst *et al.*, 2019). For the Bahamas, Swart *et al.* (2014) proposed that atmospheric dust acted as fertilizer, stimulating carbonate production in the shallow waters of the Great Bahama Bank.

Aforementioned factors influence the growth of skeletal systems and drive microbial precipitation, but also the formation of non-skeletal particles. The various strategies will result in different carbonate sedimentation patterns with different facies end-products at different times. Schlager (2000, 2003, 2005) and Reijmer (2016) distinguished four end-members of the carbonate sedimentation systems or so-called carbonate factories. The specific factories possess different sedimentation modes that reflect different growth strategies with different overall geometries, carbonate mineralogy and grain sizes.

FACTORIES

The term carbonate factory was used by the carbonate research group working in the SHELL carbonate sedimentology laboratory in Miami headed by Robert Ginsburg (including Paul Enos, Noel James, Ron Perkins and Eugene Shinn); although it is unclear who coined the term for the first time. The term 'carbonate factory' was introduced to define the narrow depth zone where tropical reefs and detrital carbonates are produced (e.g. Tucker & Wright, 1990).

In 2000 and 2003 Schlager defined the benthic carbonate factory system and proposed a three-fold subdivision with tropical (T-factory), cool-water (C-factory) and mud-mound (M-factory) benthic carbonate factories (Fig. 1); the planktic carbonate factory was discussed as a fourth system. The latter is traditionally dealt with in the context of palaeo-oceanography. The Schlager (2003) carbonate factory concept is based on the style of carbonate precipitation in aquatic realms: (i) abiotic; (ii) biotically induced; or (iii) biotically controlled (Lowenstam, 1981; Figs 1 and 2). In the latter category a distinction was made between sunlight-controlled organisms (phototrophic) and nutrient-controlled organisms (heterotrophic). Reijmer (2016) proposed adding the cold-water coral reef system as a fourth independent system; originally this carbonate production system was discussed as a part of the cool-water factory (Schlager, 2000, 2003). It was evaluated as a fourth type of carbonate factory because it has its own set of individualities, some of which do show some overlap with the other factories: it shares the type of dominant skeletal builder, scleractinian corals, with the T-factory, and the nutrient related and light-independent carbonate production mode with the C-factory type (Table 2). All factories either have a narrow range of biota with a similar style of carbonate precipitation (cool-water factory and cold-water-coral factory) or contain a specific combination of abiotic, biotically induced and biotically controlled precipitation modes such as the tropical and mud mound factories (Fig. 3).

The five main carbonate factories distinguished by Schlager (2000, 2003, 2005) and Reijmer (2016) are (Figs 4 and 5): (i) T-factory, in which the T relates to tropical or 'top-of-the-water-column'; (ii) CWC-factory; CWC stands for cold-water-coral; (iii) C-factory, in which the C is derived from cool-water or controlled precipitation; (iv) M-factory, with M representing microbial, micrite or mud-mound; and (v) the P-factory, in which the P relates to planktic carbonate production, for example, planktic foraminifera, coccoliths and pteropods.

Tropical factory (T-factory)

Present-day tropical factory (T-factory) sediments contain skeletal grains derived from abundant zooxanthellate corals, calcareous green algae, calcareous red algae, as well as benthic foraminifera and echinoderms; bryozoans and bivalves are rare to common (Flügel, 2010, p. 35). The non-skeletal fraction comprises ooids, aggregate grains, peloids and carbonate mud (Flügel, 2010, p. 35). Growth and sediment production in the T-factory mainly depends on light and water temperature. Bosscher & Schlager (1992, 1993) determined the light-dependent rate of reef growth and demonstrated that high carbonate production rates related to the growth rates and sediment productivity of biota living in the photic zone. The T-factory is more or less restricted to the tropical zone between 30°N and 30°S or the 18°C winter isotherm (Fig. 6; Tables 2 and 3). Open ocean surface currents related to ocean gyres transporting colder waters to lower latitudes, for example, the west coast of South America or west coast of Australia (Collins *et al.*, 2003; Twiggs & Collins, 2010), or upwelling areas, such as Mauritania along the west coast of Africa (Michel *et al.*, 2011; Klicpera *et al.*, 2015) or the Gulf of Panama (Reijmer *et al.*, 2012a), modify this pattern.

The carbonate platform morphology of the Bahamas for example with a rim, reef barrier, at the edge of the platform results from the light

Table 2. Comparison of properties typifying the traditional tropical shelf carbonate model (A) with those for non-tropical limestones as exemplified by (B) cold-water coral reef systems and (C) modern carbonate deposits of New Zealand. Data from Brookfield (1988), Nelson (1988), Freiwald *et al.* (2004), Freiwald & Murray (2005), Schlager (2005) and van der Land *et al.* (2011). LMC: low-magnesium calcite (<4 mol% MgCO$_3$); IMC: intermediate-magnesium calcite (between 4 and 12 mol% MgCO$_3$); HMC: high-magnesium calcite (>12 mol% MgCO$_3$).

Environmental or facies parameter	(A) Tropical shelf carbonate model	(B) Cold-water corals	(C) New Zealand modern shelf carbonates
Latitude	From 30°N to 30°S	All latitudes	From 33°S to 49°S
Depositional setting	Shallow rimmed shelves and platforms	Deep shelves, deep water, seaways	Deeper open shelves, ramps and platforms
Marine climate zone	Tropical to warm subtropical	Tropical to polar	Warm to cool temperate
Sea-water temperature (mean)	Above 23°C	Below 4 to 13°C	13 to 19°C
Sea-water temperature (minimum)	About 14°C	About 4°C	9 to 12°C
Sea-water salinity	Normal-hypersaline	Normal	Normal
CaCO$_3$ saturation at/in seabed	Highly supersaturated	Mildly supersaturated to locally under-saturated	Mildly supersaturated to?locally under-saturated
Water circulation	Restricted to open	Deep-water current-dominated shelves, slopes to seaways	Open, strongly storm-dominated and tide-dominated
Shelf gradient	<0.5 m/km	>0.5 m/km	0.25 to 2 m/km
Reef structures	Common (especially coral/coralgal)	Common (especially coral)	None (some oyster banks)
Sedimentation rates	10 to 1000+ cm/kyr	10 to 15 cm/kyr	1 to 15 cm/kyr, often relict
Carbonate content	>90%	30 to 100%	50 to 100%
Siliciclastic grains	Rare	Rare to abundant	Rare to abundant
Dolomite and evaporite minerals	Common to rare	Absent	Absent
Non-skeletal carbonate grains (e.g. ooids, pellets)	Common to abundant	Absent	Absent
Major skeletal grain types	Calcareous green algae, corals (hermatypic), benthic foraminifera, molluscs, coralline algae	Corals (ahermatypic), benthic and planktic foraminifera, sponges, bryozoans, molluscs, echinoderms, barnacles, brachiopods	Bryozoans, molluscs, mainly bivalves, mainly benthic foraminifera, echinoderms, barnacles, coralline algae, serpulids, brachiopods, corals (ahermatypic), sponges
Algal mats/stromatolites	Common	Absent	Absent (or not preserved)
Overall diagenetic regime	Constructive	Destructive	Destructive
Carbonate mud	Common to abundant	Common	Absent to rare, flushed and bypassed offshore
Main origins of carbonate mud	Disintegration calcareous green algae and inorganic precipitation	Nannofossils; terrigenous input	Physical abrasion, bioerosion and maceration of skeletons

Table 2.   (continued)

Environmental or facies parameter	(A) Tropical shelf carbonate model	(B) Cold-water corals	(C) New Zealand modern shelf carbonates
Primary sediment mineralogy	Aragonite > HMC > IMC > LMC	LMC + IMC > HMC ≥ Aragonite	LMC + IMC > HMC ≥ Aragonite
Main environment of alteration of metastable carbonate grains	Subaerial/meteoric	Submarine to shallow burial	Beginning submarine
Environment of major lithification	Submarine and subaerial/meteoric	Subsurface burial	Unlithified
Timing of cementation	Mainly early diagenetic	Early diagenetic	–
Major carbonate cements	Aragonite and HMC	Mainly LMC	–
Major sources of cements	Seawater and dissolution of aragonite grains	Dissolution of aragonitic skeletons	–
Carbonate petrography (after Dunham, 1962)	Mudstone, wackestone, packstone, grainstone, rudstone and boundstone	Grainstone, packstone and rudstone	Grainstone and rudstone
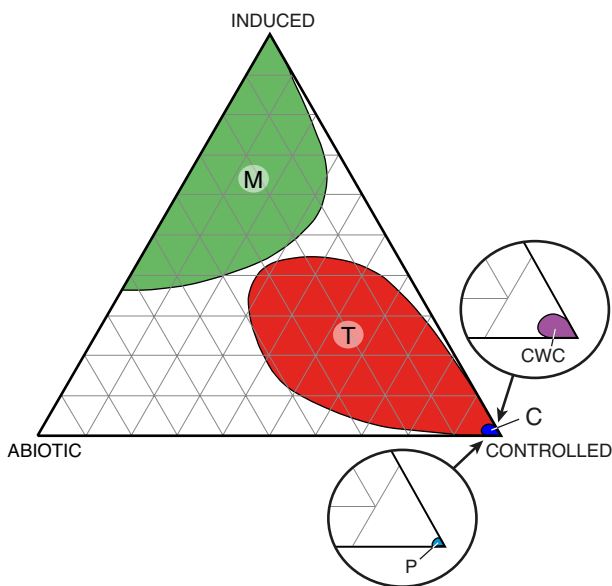
Fig. 3. Abiotic, biotically induced and biotically controlled sediments in carbonate factory deposits. The CWC-factory, C-factory and P-factory cover a nearly monospecific set of biotically controlled sediments. The M-factory and the T-factory are characterized by a combination of the three sediment types that partially overlap, but each possess factory specific sediment mixtures; the M-factory is dominated by abiotic and biotically induced sediments, and the T-factory by biotically controlled sediments. Modified from Schlager (2003, 2005).

and water-temperature controlled production mode (Figs 4, 6, 7 and 8). The barrier plays an important role in stabilizing the platform edge and separating the low energy, shallow-water lagoon and the highly dynamic open ocean environment. The reef barrier forms the upper part of the steep slopes surrounding the platform that vary in grain-size, but are mostly coarse-grained and cement fairly rapidly, 8 to 10 mm/100 yr; with aragonite being the dominant mineralogy (Grammer *et al.*, 1993, 1999). Subaerially exposed platform interior sediments express even faster cementation rates with freshwater vadose calcite cements developing within 10 years (Dravis, 1979, 1996). Grain-sizes may vary along the slopes with differences materializing between the windward and leeward sides of an isolated platform during glacial and interglacial times (Rendle-Bühring & Reijmer, 2005). Surface and deep-water currents subsequently modulate the grain-size distribution patterns of the exported sediments (Betzler *et al.*, 2014).

The modern-day T-factory usually shows a flat top and steep slopes as it is closely tied to the light-saturated zone (Figs 7 to 10). The entire system is very sensitive to relative changes in sea-level and a relatively small drop in sea-level already might eliminate most of the sediment production zone (e.g. Schlager *et al.*, 1994); 95% of the surface area between 0 m and 200 m
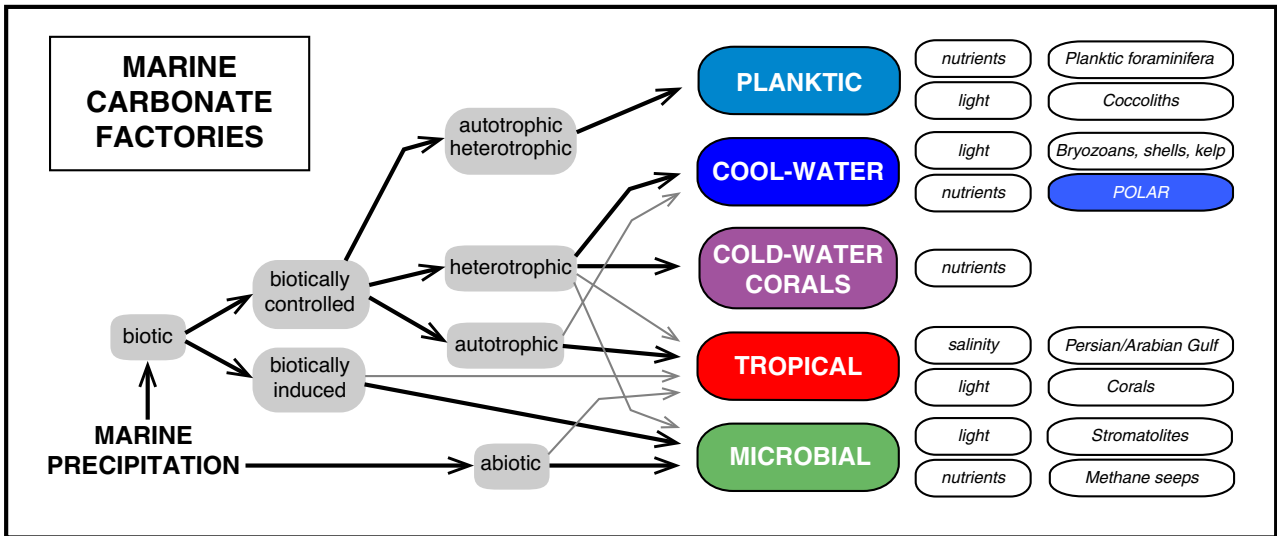
Fig. 4. Revised version of the carbonate factory classification scheme of Schlager (2003, 2005), for comparison see Fig. 1. The marine precipitation mode is subdivided into: (i) biotically controlled precipitation with an autotrophic tropical factory (T-factory), a heterotrophic cold-water-coral factory (CWC-factory), a heterotrophic cool-water factory (C-factory) and an auto/heterotrophic planktic factory (P-factory); and (ii) biotically induced precipitation dominating the microbial-factory (M-factory). All factories can be subdivided into light-dominated, nutrient-dominated, or salinity-dominated subclasses for which biota or depositional realms are given. The CWC-factory shares the corals with the T-factory and the heterotrophic carbonate production mode with the C-factory. Abiotic precipitates can be found within the T-factory and M-factory. The P-factory is an independent factory, biotically controlled precipitation with autotrophic and heterotrophic organisms. The polar factory is highlighted while it displays slightly different characteristics when compared to those of the main cool-water factory, see *Discussion* for more details. Thick arrows: main contribution; thin arrows: minor contribution.
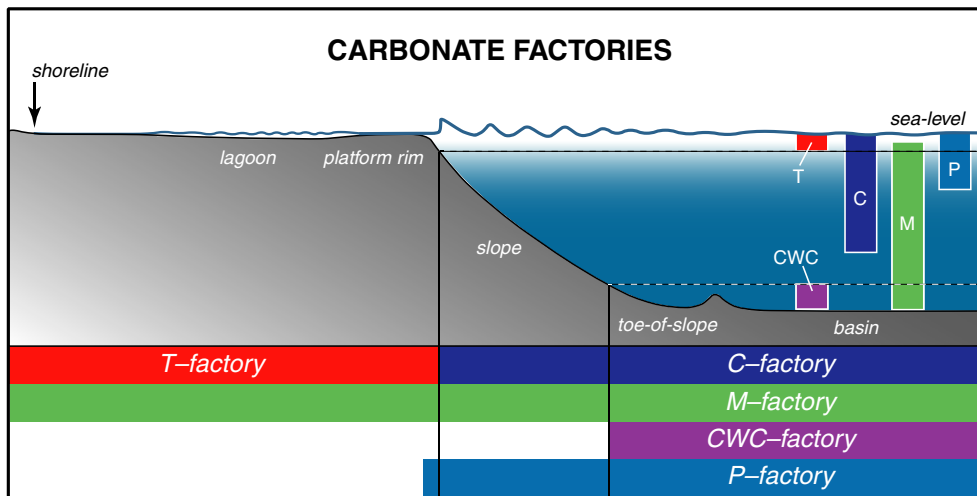
Fig. 5. Schematic overview of the carbonate factory distribution along a flat-topped carbonate platform and the depth-dependent production profiles within the marine realm. No water depth implied other than sea-level. Upper dashed line: base of the photic zone. Lower dashed line marks the toe-of-slope to basin transition.
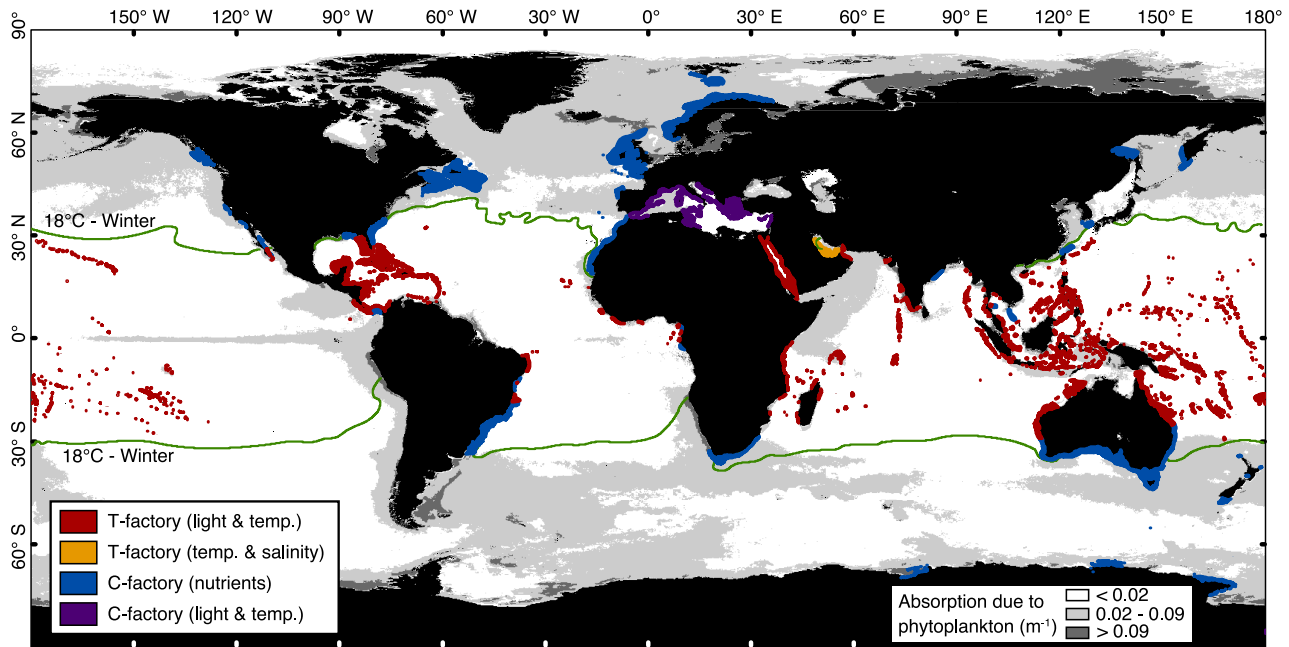
Fig. 6. Global distribution of modern shallow-water marine carbonate factories after Laugié *et al.* (2019). Green lines: 18°C isotherm for the coldest winter month. Subdivision of individual factories is based on Michel *et al.* (2018, 2019) and agrees with the factory classification proposed in this study. The geochemical factory defined by Laugié *et al.* (2019) for the Arabian/Persian Gulf is characterized by its restricted salinity range but is classified as part of the T-factory. Background oceanographic map is based on remote-sensing data of marine primary productivity; absorption classes due to phytoplankton in white, light grey and dark grey.

water depth at Great Bahama Bank and Little Bahama Bank is shallower than 20 m water depth (Fig. 8). Hence, with a limited drop in sea-level, a major part of the sediment production area will be lost. The photic zone and surface-area-dependent sediment production pattern with sea-level related sharp changes in sediment production is called highstand shedding (e.g. Droxler & Schlager, 1985; Reijmer *et al.*, 1988; Schlager *et al.*, 1994). Such sedimentation patterns were also described for numerous other full marine carbonate systems; for example, Pedro Bank (Caribbean; Glaser & Droxler, 1991, 1993; Andresen *et al.*, 2003), Red Sea (Emmermann *et al.*, 1999), Maldives (Fig. 9; e.g. Jorry *et al.*, 2010; Paul *et al.*, 2012), Southern Indian Ocean (Counts *et al.*, 2018) and the Great Barrier Reef (Fig. 10; e.g. Webster *et al.*, 2012).

Carbonate ramp systems are defined by gentle slopes, and frequently display the interaction between the light-saturated zone and sediment production. These sedimentation systems often display rhythmic sedimentation cycles with varying sediment composition in response to sea-level variations (e.g. Wright & Burchette, 1998; Triassic, Netherlands: Borkhataria *et al.*, 2005; Jurassic, Spain: Bádenas *et al.*, 2010;

Cretaceous, Oman: van Buchem *et al.*, 2002; Miocene, Bahamas: Betzler *et al.*, 1999, Reuning *et al.*, 2002; Recent, Persian/Arabian Gulf: Lokier *et al.*, 2018).

While this carbonate system exports abundant sediment from the shallow-water areas towards the adjacent slopes and the surrounding basins forming a halo of platform derived sediments around the production sites, the overall sedimentation pattern can be labelled as 'Spread' (Fig. 7).

Cold-water-coral factory (CWC-factory)

A summary of the occurrence of cold-water and deep-water coral banks along the north-western European margin, their environmental conditions and growth strategy was provided by Teichert (1958) referring to earlier studies along the Norwegian coast (e.g. Broch, 1922; Nordgaard, 1930), the continental slope of Ireland and France (e.g. Gravier, 1908; Joubin, 1922) and the Mediterranean (e.g. Pruvot, 1894, 1895; Table 3). These deep-water sedimentary systems are characterized by the occurrence of hermatypic corals (for example, *Lophelia* and *Madrepora*) and are marked by a very high biodiversity (Fig. 11; Freiwald & Roberts, 2005). The cold-water-coral

Table 3. Summary characteristics of benthic and pelagic carbonate factories.

Category	Factory				
	T-factory	CWC-factory	C-factory	M-factory	P-factory
Abbreviation	**T:** Tropical **T:** Top-water-column	**CWC:** Cold-Water coral reefs	**C:** Cool-water **C:** Controlled precipitation	**M:** Microbial **M:** Micrite **M:** Mud-mound	**P:** Planktic
Distribution	Tropical zone between 30°N and 30°S, with modification through surface currents related to ocean gyres and upwelling areas	Worldwide distribution	(i) Extends poleward from limit of tropical factory (at approx. 30°N/S) to polar latitudes; (ii) low latitudes below thermocline, deeper than warm surface waters; (iii) upwelling areas	Worldwide distribution	Worldwide distribution
Steering factors	Light and water temperature steer production profiles ensuring high production rates through biota living in the photic zone	Strongly depends on the steady influx of nutrients either through slope currents or pelagic input	Nutrients and relatively low temperatures steer the biologically controlled production of carbonate sediments	Microbial-mediated precipitation of mud. Most prominent features are microbial mats and organic EPS matrix steering different organo-mineralization processes	Light, water temperature, nutrients
Production profile	Photic zone, up to 140 m water depth (Pacific Ocean)	Low production rate, large production window, 40 m up to 2500 m water depth	Low-moderate production over a large depth window, 0 m to over 400 m	High production upper slope, below wave base to 500 m water depth, and methane seeps (deep sea)	Production in the upper part of the water column, down to 500 m water depth
Contributors – skeletal	Corals, large benthic foraminifera, bryozoans, calcisponges, red and green algae, numerous others	Corals, bivalves, brachiopods, ascidians, sponges, planktic foraminifera	Calcareous algae, bryozoans, molluscs, planktic and benthic foraminifera, echinoderms, barnacles, sponges, ascidians	Microbial products (muds, peloids), bryozoans, sponges, calcareous algae, foraminifera	Planktic foraminifera, coccoliths, pteropods (siliceous: diatoms, radiolaria)
Contributors – non-skeletal	Ooids, peloids	Minor peloids	Minor peloids	Microbial-mediated precipitation	Not present
Dominant mineralogy	Aragonite, HMC and minor LMC	Aragonite, LMC	Calcite (LMC and HMC), aragonite	HMC, some aragonite	Calcite, aragonite
Diagenetic potential	High	High	Low	High	Low

Table 3. (continued)

Category	Factory				
	T-factory	CWC-factory	C-factory	M-factory	P-factory
Depositional geometries	(i) Flat-topped platforms; (ii) carbonate ramps	(i) Mounds; (ii) ridges	(i) Cool-water: shaved shelf; (ii) polar: deep shelf	(i) Flat-topped platforms with deepened platform margin; (ii) mud mound systems	(i) Open-ocean seafloor; (ii) sand-waves (Cretaceous chalk deposits)
Slope morphology	Exponential concave	Steep framework dominated	Gaussian	Linear	Current (wave) dynamics related
Sediment export modes	Highstand shedding	Framework and catchment	Siliciclastic behaviour	Slope shedding	Pelagic production and deposition; can be seasonal
Sedimentation pattern	Spread: system exports abundant sediment from shallow-water areas towards the adjacent slopes and surrounding basins	Frame: system constructs coral framework, a coral mound, related to a certain position; nutrient-dependent	Move: changes in currents and waves, shift of the depositional sediment loci. Removal out of shallow-water areas; shaved shelf	Stick: ability of system to glue (through microbial activity) sediments at the platform margin and upper slope; capacity to build fast prograding systems	Production: system is totally dependent on sediment production (shells) within the water column; nutrient and light-dependent
Case studies – Present-day	Arabian Gulf, Bahamas, Florida Keys, Maldives, Great Barrier Reef, Southern Indian Ocean, Pacific	Hovland, Propeller mound, Rockall Plateau, Porcupine, Bahamas, Campos, Santos, etc.	Australian shelf, Norwegian shelf, Antarctica, Arctic	Shark Bay, upper slopes Great Bahama Bank, slope Tahiti (lake systems)	Worldwide oceans
Case studies – Fossil	Miocene South China Sea, Miocene Mediterranean, Great Bahama Bank, Maldives, Great Barrier Reef	Not known; for alternative interpretation see Hebbeln & Samankassou (2015)	Pleistocene Alaska, Plio-Pleistocene Rhodes (Greece) and Australia, Miocene France, Oligocene–Holocene south-east Australia, Permian Australia palaeoceanographic ODP and IODP legs	Emsian, Namurian, Jurassic Jbel Bou Dahar (Morocco), Triassic: Dolomites (Italy), Carboniferous Sra de Cuera (Spain), Devonian Canning Basin, etc.	World oceans, Cretaceous chalks, see

reef systems share the stony corals with the T-factory and originally were assigned to the C-factory because of their nutrient-dependent growth strategy (Schlager, 2005; Figs 5 and 7). The cold-water-coral factory (CWC-factory) can be found throughout a wide range of water depths below the photic zone across all oceans.

Their occurrence is linked to site specific sets of environmental variables, for example, temperature, salinity, seawater density, dissolved oxygen and nutrient supply, but also currents reducing sediment input (Tables 2 and 3; e.g. Rüggeberg *et al.*, 2011; Wienberg & Titschack, 2017). The growth strategy of the coral mounds,

as they are frequently called, is linked to ocean circulation processes and distinct water masses supplying nutrients that vary in accordance with climatic variations. The currents are not only important for the supply of food, but also play a role in the distribution of eggs, sperm and larvae, colonizing new areas or re-colonizing areas after glacial–interglacial changes in water mass distribution and current orientation (e.g. Henriet *et al.*, 2014; Hebbeln & Samankassou, 2015). New discoveries are added frequently and now cover a wide range of localities throughout the: (i) North and South Atlantic for an overview (Freiwald *et al.*, 2004; Freiwald & Roberts, 2005; Mienis *et al.*, 2014), Norway (Freiwald *et al.*, 1997; Fig. 11A to E), Ireland (Mienis *et al.*, 2009a,b; van der Land *et al.*, 2014; Fig. 11F), Gulf of Cadiz (Wienberg *et al.*, 2009), Mediterranean (Freiwald *et al.*, 2009), Morocco (Foubert *et al.*, 2008; Hebbeln *et al.*, 2019), Mauritania (Wienberg *et al.*, 2018), Namibia (Hanz *et al.*, 2019), north-west Atlantic (Mienis *et al.*, 2014), Florida (Grasmueck *et al.*, 2006; Correa *et al.*, 2012; Mulder *et al.*, 2012; Lüdmann *et al.*, 2016), Gulf of Mexico (Mienis *et al.*, 2012; Hebbeln *et al.*, 2014), Brazil (Viana *et al.*, 1998; Pires *et al.*, 2014), Uruguay (Carranza *et al.*, 2012) and Argentina (Muñoz *et al.*, 2012); (ii) the Indian Ocean (Maldives; Reolid *et al.*, 2017) and Australia (Coral Sea; Beaman *et al.*, 2016); and (iii) the Pacific (Hawaii; Long & Baco, 2014; British Columbia; Neves *et al.*, 2014; Alaska; Etnoyer & Morgan, 2005; Stone, 2006). The position and growth history of the coral mounds may vary through time depending on their response to climate changes and associated variations in ocean circulation and water mass distribution. The cold-water coral colonies are able to build sturdy frameworks consisting of living corals and coral rubble, with abundant associated biota, and sediments (muds to silts) infilling the coral framework. Early diagenetic alteration modifying the primary composition of the carbonate mound sediments results in lithification and further stabilization of the mounds (e.g. van der Land *et al.*, 2011). Based on aforementioned characteristics the sedimentation pattern can be described as 'Frame' (Fig. 7).

Cool-water factory (C-factory)

The cool-water factory (C-factory) is characterized by biologically controlled production of carbonate sediments in areas with sufficient nutrients and relatively low temperatures (Figs 5 and 7). In surface waters, the C-factory operates at higher latitudes than the T-factory, northward of 30°N and southward of 30°S or to the north or south of the 18°C winter isotherm (Tables 2 and 3; Fig. 6). The Great Australian Bight is a well-known example (e.g. James *et al.*, 1994, 1999; James & Bone, 2011; Fig. 12). In addition, the heterotrophic biota of the C-factory and the dominance of suspension-feeding biota link this factory to zones with a high marine productivity, upwelling areas and low-temperature waters below the thermocline.

In the shallow-water realms the transition zone between the T-factory and the C-factory at 25 to 30°N and 25 to 30°S (Fig. 6) is characterized by an oligotrophic–mesotrophic–eutrophic, warm-temperate system with red algal and seagrass derived biota (Table 4; Betzler *et al.*, 1997a; Halfar *et al.*, 2000, 2004; Michel *et al.*, 2018). A clear transition between the T-factory and C-factory can be found in the Gulf of California, with a latitudinal extent from 23° to 30°N. Here, coral-dominated shallow-water T-factory carbonates in the south, are replaced by a warm-temperate system with red algal-dominated subtidal to inner-shelf carbonates moving up north, and a C-factory with molluscan bryozoan-rich inner to outer shelf carbonates in the northernmost part of the gulf (Halfar *et al.*, 2004, 2006b). Large red algal-dominated systems are also known from the North Atlantic (along Norway, Ireland, Scotland, north-eastern Canada; e.g. Leonard *et al.*, 1981; Henrich *et al.*, 1992, 1995); eastern Caribbean (see Foster, 2001; and references therein); the Mediterranean (Bosence, 1985; Fornos *et al.*, 1992; Fornos & Ahr, 1997); the Brazilian shelf (Abrolhos continental shelf; e.g. Amado-Filho *et al.*, 2012; Brasileiro *et al.*, 2018); the Gulf of California (Halfar *et al.*, 2000, 2004, 2006b); Japan (Matsuda, 1989; Tsuji, 1993; Matsuda & Iryu, 2011); Australia (e.g. James *et al.*, 1994, 1999; James & Bone, 2011; Fig. 12); New Zealand (e.g. Nelson, 1988); and the Red Sea (Piller & Rasser, 1996).

Large-scale T-factory and C-factory systems can coexist as described for the north-western shelf of Australia (Carnarvon Basin; Anell & Wallace, 2020). In the Miocene this depositional system comprises a non-rimmed C-factory shelf in deeper waters together with a T-factory platform with steep slopes and a pronounced margin positioned closer to the continent.

In contrast to the T-factory with its production profile covering the upper part of the water column, the C-factory production profile displays

Marine Carbonate Factories
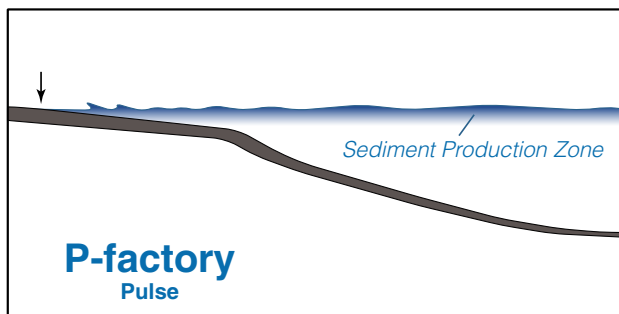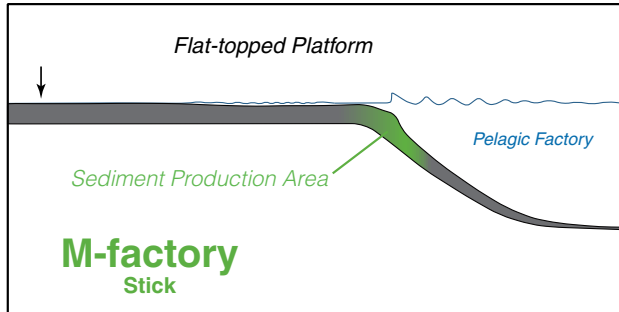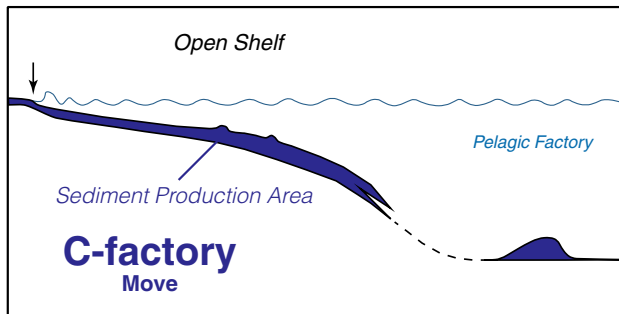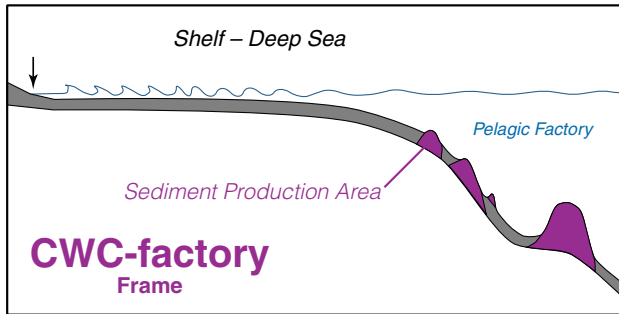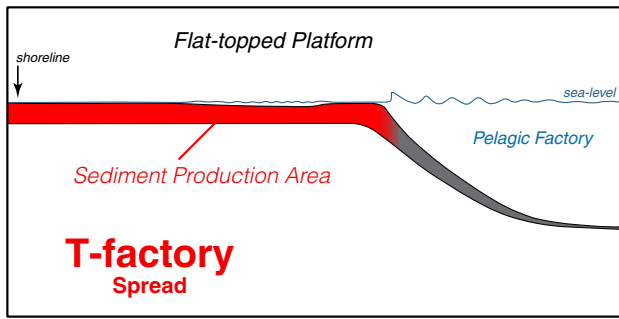
Production profiles

Sediment production

© 2021 The Author. *Sedimentology* © 2021 International Association of Sedimentologists, *Sedimentology*, **68**, 1729–1796
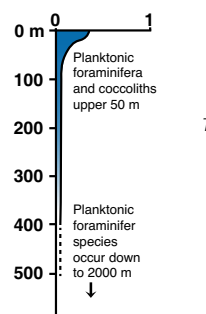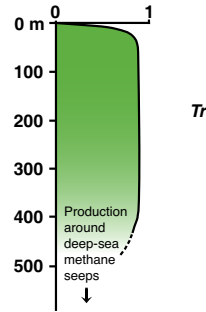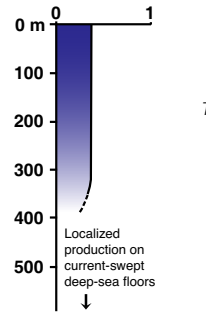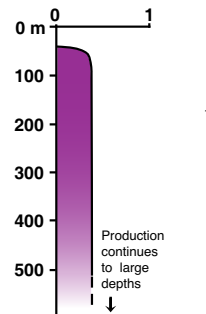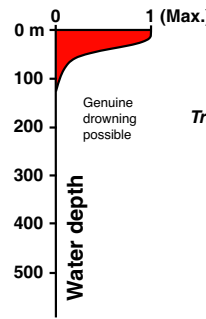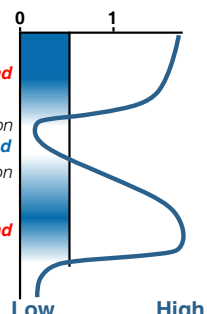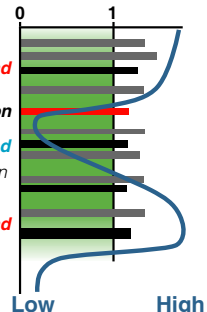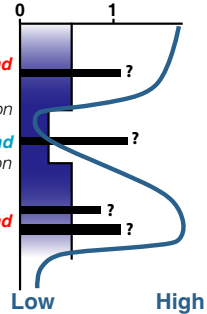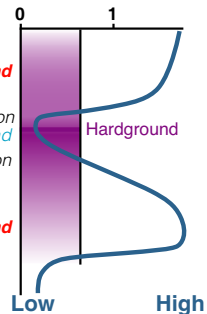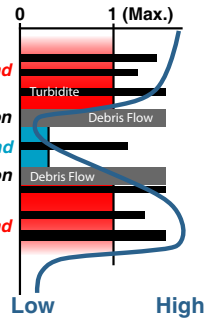
Fig. 7. Individual characteristics for carbonate factories are given covering the platform profiles, individual production windows and sediment export variations. The T-factory discloses sharp variations in sediment production and export between sea-level lowstands and highstands, because of the light-dependent sediment production window interacting with the flat-topped platform geometry. Transgression and regression are sharp transitions. The CWC-factory displays subtle variations in sediment production related to nutrient input variations during changes in sea-level. Hardground might mark transgression interval, sea-level lowstand to highstand transition. The C-factory illustrates an open shelf system, a wide sediment production window and restricted sediment production during sea-level lowstands and extensive but thinner highstand deposits. Transgression and regression deposits have different 3D dimensions at the shelf edge, see Fig. 19. The M-factory, only the flat-topped platform is shown, exhibits a wide production window and fairly continuous sediment export. Transgression might display a marked surface (Della Porta *et al.*, 2002, 2004). The P-factory represents open-ocean carbonate sediment contribution, main sediment production within the photic zone. The terms 'Spread', 'Frame', 'Move', 'Stick' and 'Pulse' are general terms describing the sediment production and export pattern for the individual carbonate factories.

moderate production rates over a wider water-depth range (Figs 5 and 7). Production is not limited to shallow-waters for the suspension feeding biota that dominate this system (Schlager, 2003). However, the seagrass and kelp dominated part of the system occupies facies realms situated within the photic zone (e.g. James & Bone, 2011; Michel *et al.*, 2018).

Another characteristic of this factory is the open sedimentary system lacking shallow-water barriers as found in the other factories. The poor cementation of the warm-temperate carbonates facilitates the transport of the coarse-grained bioclasts (e.g. Nelson, 1988; Halfar *et al.*, 2006a). The low cementation rates in the cool-temperate realm (Tables 2 and 3) combined with the absence of a shallow-water barrier results in a sedimentation regime in which waves and currents control sediment transport and redistribution. Hence, the sediment distribution along the shallow neritic shelf is characterized as a 'shaved shelf' (James *et al.*, 1994); a vigorous hydrodynamic environment where sediments produced on the rocky substrate are routinely swept away. The sediments on parts of the shelf of the Great Australian Bight are a mix of relict sediments formed during Marine Isotope Stage (MIS) 3 and MIS 4 and recent carbonate sands (James & Bone, 2011, p. 35). The warm-temperate Mediterranean open-shelf setting also exhibits a relation between water depth, wave base and carbonate facies development. Shallow-water grass meadows with large benthic foraminifera, red algae, bryozoans and green algae to rhodolith-rich bioclastic sediment just below storm-wave base are found there (Carannante *et al.*, 1988; Fornos *et al.*, 1992; Fornos & Ahr, 1997; Fig. 12).

As for other carbonate factories the present-day C-factory displays further diversification (Table 4) when moving towards higher latitudes with a decrease in faunal diversity of the carbonates (e.g. Leonard *et al.*, 1981; Henrich *et al.*, 1992, 1995). The Brazilian open shelf is another area on which C-factory transitions from warm-temperate with branching red algae, *Halimeda* and *Amphistegina* sp. to cool-temperate with molluscs, echinoderms, barnacles and bryozoans (Carannante *et al.*, 1988) can be found.

As changes in currents and waves result in a shift of the sediment depocentres and the sediments are fairly mobile, the overall sedimentation pattern can be labelled as 'Move'. The sedimentary system agrees in multiple ways in its response to sea-level changes with sedimentation patterns observed in siliciclastic systems.

Microbial factory (M-factory)

Microbial activity, for example, bacteria, cyanobacteria and bio-mediated precipitation of mud characterize the mud-mound/microbial factory (M-factory; Schlager, 2000, 2003). The most prominent features of this factory are the microbial mats and microbial textures, which originate from in-place carbonate precipitation through biologically induced and influenced mineralization in association with microbes from various key groups, and biofilm extracellular polymeric substances (EPS). The ability to follow different carbonate precipitation strategies within different environments is also expressed in the different morphologies, from individual mounds to flat-topped platforms, and different environments, non-marine or marine, shallow to deep, in which the M-factory can flourish (Figs 5 and 7); for more details see Dupraz *et al.* (2009) and Della Porta (2015).

The production profile of this factory displays fairly steady production rates (Fig. 7), which can reach tropical levels (Kenter *et al.*, 2005), within a wide range of environments and water
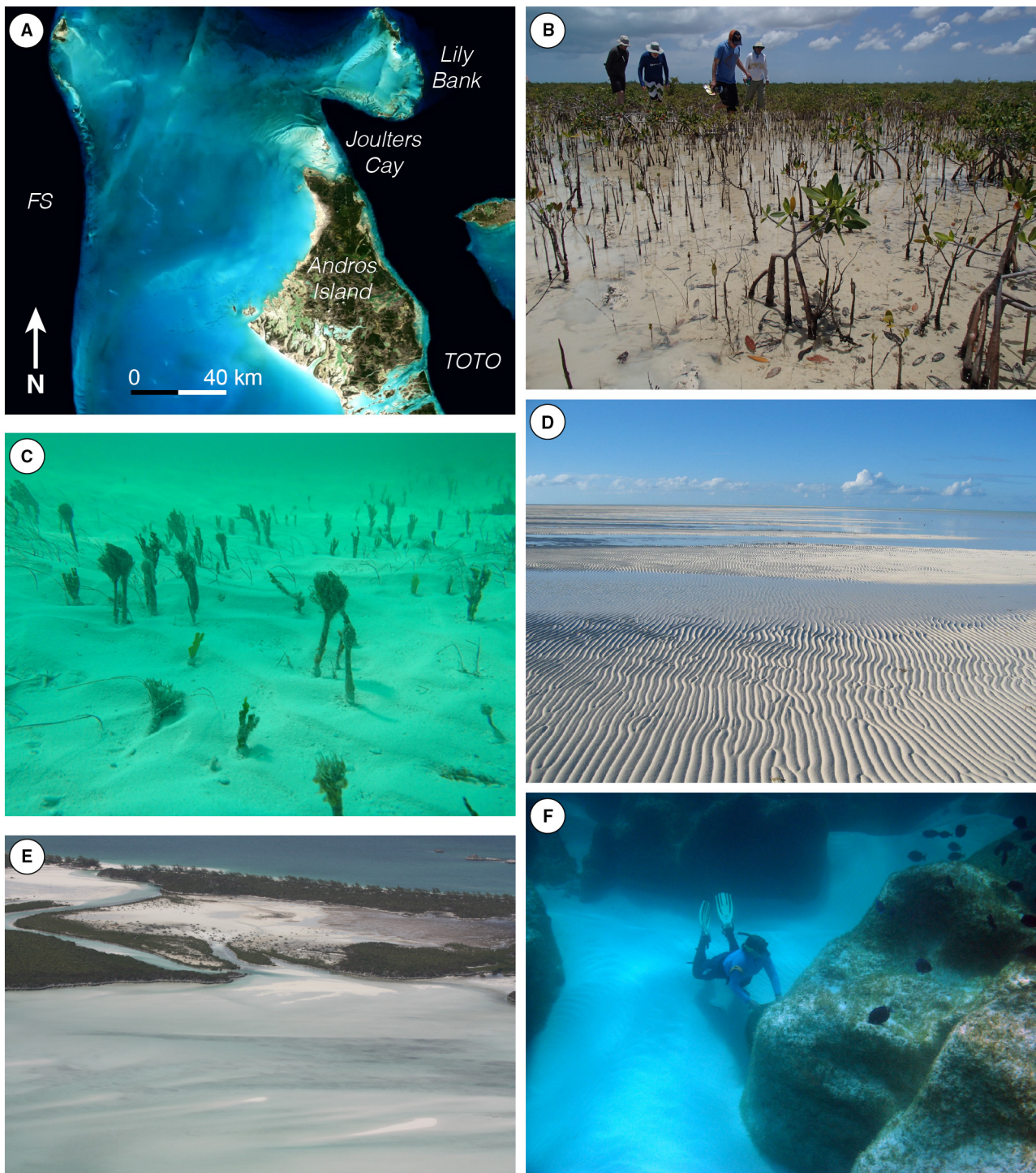
Fig. 8. T-factory 1: The Bahamas. (A) Satellite image of the north-western part of Great Bahama Bank (GBB). FS: Florida Straits; TOTO: Tongue of the Ocean. (B) Mangrove tidal flat, west of Andros Island. Persons for scale (*ca* 1.8 m tall). (C) *Penicillus* sp. and *Halimeda* sp. colonies and seagrass in shallow-water sands, Lily Bank. Note the wave and current ripples and the currents bending the top of the algal colonies to the left. Image view front *ca* 70 cm across. (D) Ooid tidal flats at Joulters Cay. Height of ripples *ca* 10 cm. (E) Shroud Cay (Exumas, Bahamas) with mangroves, barrier island and tidal channel. North-east view towards Exuma Sound, *ca* 2 km across. (F) Large stromatolite colonies (scuba diver for scale) in channel south of Little Hall's Pond. Photograph sources: (A) ESRI World Imagery; (B) and (C) Gene Rankey (University of Kansas, Lawrence, USA); (D) and (E) Gregor Eberli (RSMAS, Miami, USA); (F) Kelly Jackson (RSMAS, Miami, USA).
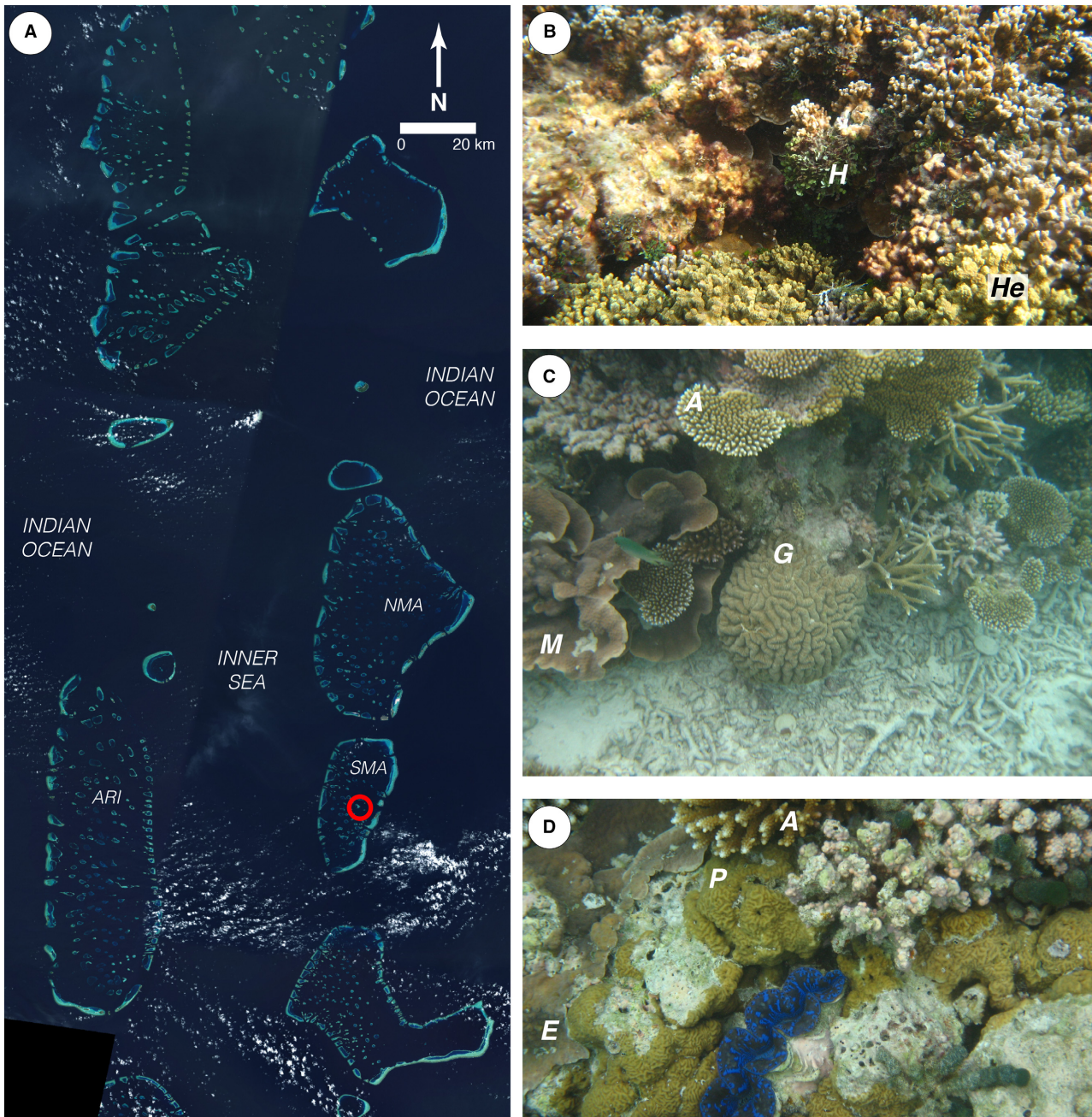
Fig. 9. T-factory 2: The Maldives. (A) WorldWind satellite image of the northern Maldives. Red circle marks position of reef biota shown in (B) to (D); patch reef positioned in the lagoon of South Malé Atoll (SMA). NMA: North Male Atoll, ARI: Ari Atoll; (B) to (D) Patch reef impressions South Malé Atoll; (B) 'H': *Halimeda* sp.; 'He': *Hydnophora exesa* (all colonies visible). Picture width *ca* 80 cm; (C) at the top: 'A': *Acropora cytherea*, as are all the other visible table-shaped colonies; 'G' in the middle: *Gyrosmilia interrupta*; 'M' on the left: *Montipora* sp. Diameter of skeletal coral debris at the base (*Acropora* sp. sticks) does not exceed 2 cm. (D) 'E' on the left: *Echinopora lamellose*; 'P' in the middle: probably *Porites rus.*; 'A' at the top: *Acropora nasuta*. Open Tridacna shell (purple) measures *ca* 10 cm. Photograph sources: (B) to (D) Christian Betzler (Universität Hamburg, Germany). Coral determinations: Bernard Riegl (Nova Southeastern University, Dania, USA).

depths (Table 3; Fig. 5). The production profile shows high production rates down to 500 m water depth or even deeper, for example, around methane seeps (Fig. 7) (e.g. Peckmann *et al.*, 2001, 2003; Goedert *et al.*, 2003; Liebetrau *et al.*, 2014). Production in the shallow-water
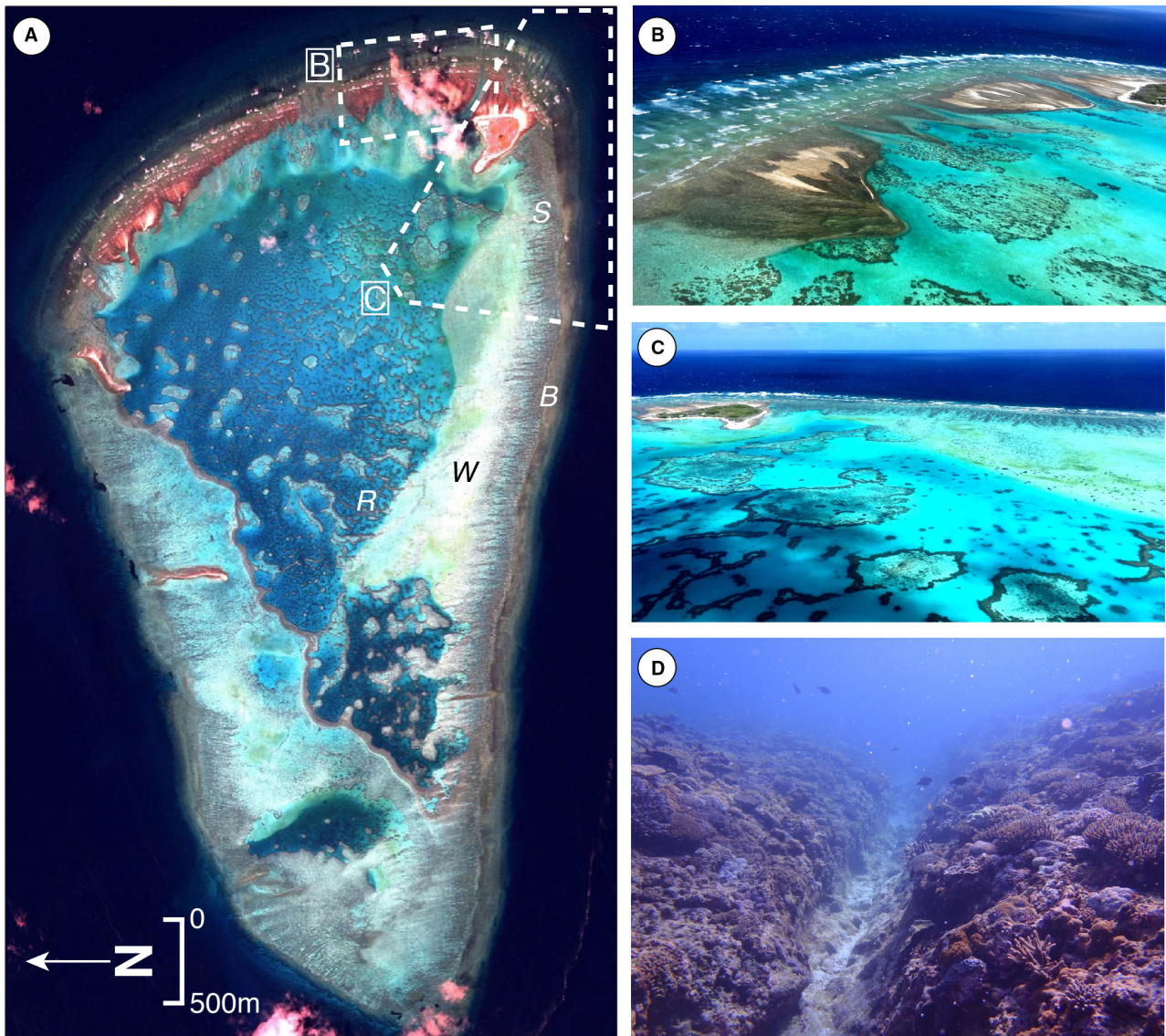
Fig. 10. T-factory 3: Great Barrier Reef, One Tree Island. (A) 2009 World View 2 satellite image of One Tree Island, Great Barrier Reef. Dashed quadrants mark overviews provided in (B) and (C). Brown edge: barrier reef ('*B*') with spur and groove systems ('*S*'); White/light green: wash-over fans ('*W*'); Dark blue: lagoon with reticulate patch reefs ('*R*'). (B) Overview edge, One Tree Island with reef edge marked by the breaking waves (left), succeeded by a shallow reef barrier, some shoals, wash-over fans, and a lagoon with small patch reefs (right); view marked in (A). (C) Overview from the lagoon towards the reef edge. Note the reticulate reef distribution in the lagoon; view marked in (A). (D) Spur and groove system marking the edge of the platform. For detailed information on this system the reader is referred to Duce *et al.* (2016, 2020). Width of groove *ca* 1 m. Photograph sources: Geocoastal Research Group, University of Sydney, Australia.

areas is affected by the waves due to the sensitivity of the biota to these physical processes. This is most likely also the reason why the sediment production area within the flat-topped platform systems is situated on the upper slope, just below the wave base as known from Carboniferous, Jurassic and Triassic carbonate platforms (Fig. 13; Scheibner & Reijmer, 1999; Keim & Schlager, 2001; Kenter *et al.*, 2005; Merino-Tomé *et al.*, 2012; Della Porta *et al.*, 2014).

Another characteristic of this factory is the formation of mound build-ups, for example, the Carboniferous of Belgium (e.g. Lees & Miller, 1995), the Devonian of Algeria (Wendt *et al.*, 1997) and Morocco (Fig. 13C to F; e.g. Brachert *et al.*, 1992). Large flat-topped platforms are also

frequent and include, for example; the Carboniferous of Kazakhstan (e.g. Kenter *et al.*, 2005; Collins *et al.*, 2014), the Triassic of the Dolomites (e.g. Bosellini, 1984; Brandner *et al.*, 1991; Keim & Schlager, 1999, 2001) and the Jurassic of Morocco (Fig. 13A; e.g. Kenter & Campbell, 1991; Scheibner & Reijmer, 1999; Blomeier & Reijmer, 2002; Verwer *et al.*, 2009; Merino-Tomé *et al.*, 2012; Della Porta *et al.*, 2014).

In present-day reef environments of Tahiti, microbialites infill the primary pore space between the coralgal framework (Séard *et al.*, 2011), producing a mixed T-factory and M-factory deposit. Microbial binding was also described as one of the factors stabilizing steep carbonate slopes (e.g. Kenter, 1990; Keim & Schlager, 1999, 2001; Adams & Kenter, 2014); recent described examples are the modern slope of Great Bahama Bank (GBB; Reolid *et al.*, 2017) and the upper Miocene in the Sorbas Basin in south-east Spain (Reolid *et al.*, 2014). Microbial activity is an important factor in stabilizing the platform margin of the GBB T-factory enabling platform progradation (Busson *et al.*, 2019). Hence, the term 'Stick' describes the overall sedimentation pattern very well, because of the ability of the system to glue (through microbial activity) sediments and build sturdy systems (Fig. 7).

Relative changes in sea-level do not have a large impact on the production rates of this system, because for flat-topped M-factory carbonate platforms the main sediment production is positioned on the upper slope (Figs 7 and 14). Zhou & Pratt (2019a,b) discussed that peloidal sediment production of Upper Devonian mud mounds takes place within the photic zone between storm-weather and fair-weather wave base. With sediment production extending over a wide water-depth range (Fig. 7), the slope-derived sediment production remains fairly constant through time, irrespective of sea-level changes. This sedimentation pattern has been characterized as slope shedding (Fig. 14; Kenter *et al.*, 2005).

Planktic factory (P-factory)

The last carbonate factory comprises carbonate sediment production in the open ocean realm through planktic foraminifera, coccolithophores, pteropods and other pelagic (non-)carbonate organisms (Table 3; Figs 5 and 7). The term 'planktic' is used in this manuscript instead of 'planktonic' following the linguistic argumentation discussed by Emiliani (1952, 1991).

Foraminifera with a benthic life mode, agglutinated forms, are known from the Cambrian, and from the Late Triassic or Jurassic they entered the planktic realm (e.g. Grigyalis & Gorbachik, 1980; Kucera, 2007). At present, planktic foraminifera show a wide-ranging latitudinal and temperature zone distribution. The majority occur in the surface or near-surface waters of the open ocean. Those populating the photic zone commonly possess a symbiotic relationship with photosynthesizing algae, which is useful for those species living in warm oligotrophic waters with ample light (Kucera, 2007). Planktic foraminifera can be omnivores or selective carnivores (Hemleben *et al.*, 1989). They display periodic pulses of primary productivity, linked to seasonal variations in sea-surface temperature.

The calcification of coccolithophores is driven by photosynthesis limiting their occurrence to the photic zone (e.g. De Vargas *et al.*, 2007). They occur in a range of trophic modes, from autotrophic, to heterotrophic and mixotrophic (e.g. Müller, 2019). They are known to occur from the Late Triassic forward and have become an important part of the oceanic phytoplankton system since then (Bown *et al.*, 2004). At present their diversity patterns vary and correlate well with climate tendencies; warmer climates show a higher diversity (Bown *et al.*, 2004). Production rates vary on seasonal scales, with surface nutrients and water stratification being important parameters (e.g. Poulton *et al.*, 2014). They are especially known from the white cliffs bordering the Channel separating southern England from northern France and from the southern English coast (Fig. 15).

Another well-known group of marine zooplankton are pteropods, which are a group of heterobranch, gastropod molluscs. Pteropods originated in the Late Cretaceous and are the pelagic source of aragonite in deep-sea sediments (Milliman, 1974, p. 105; Haq & Boersma, 1978, p. 151).

All three carbonate producers described above are an important part of the full-marine sediments found in the vicinity of carbonate platforms, the so-called peri-platform oozes (Schlager & James, 1978), a mix between platform derived sediments and open-ocean input. The production rates for the coccolithophores and the foraminifera vary with the seasons thereby registering these variations in their skeletons. One could call this carbonate
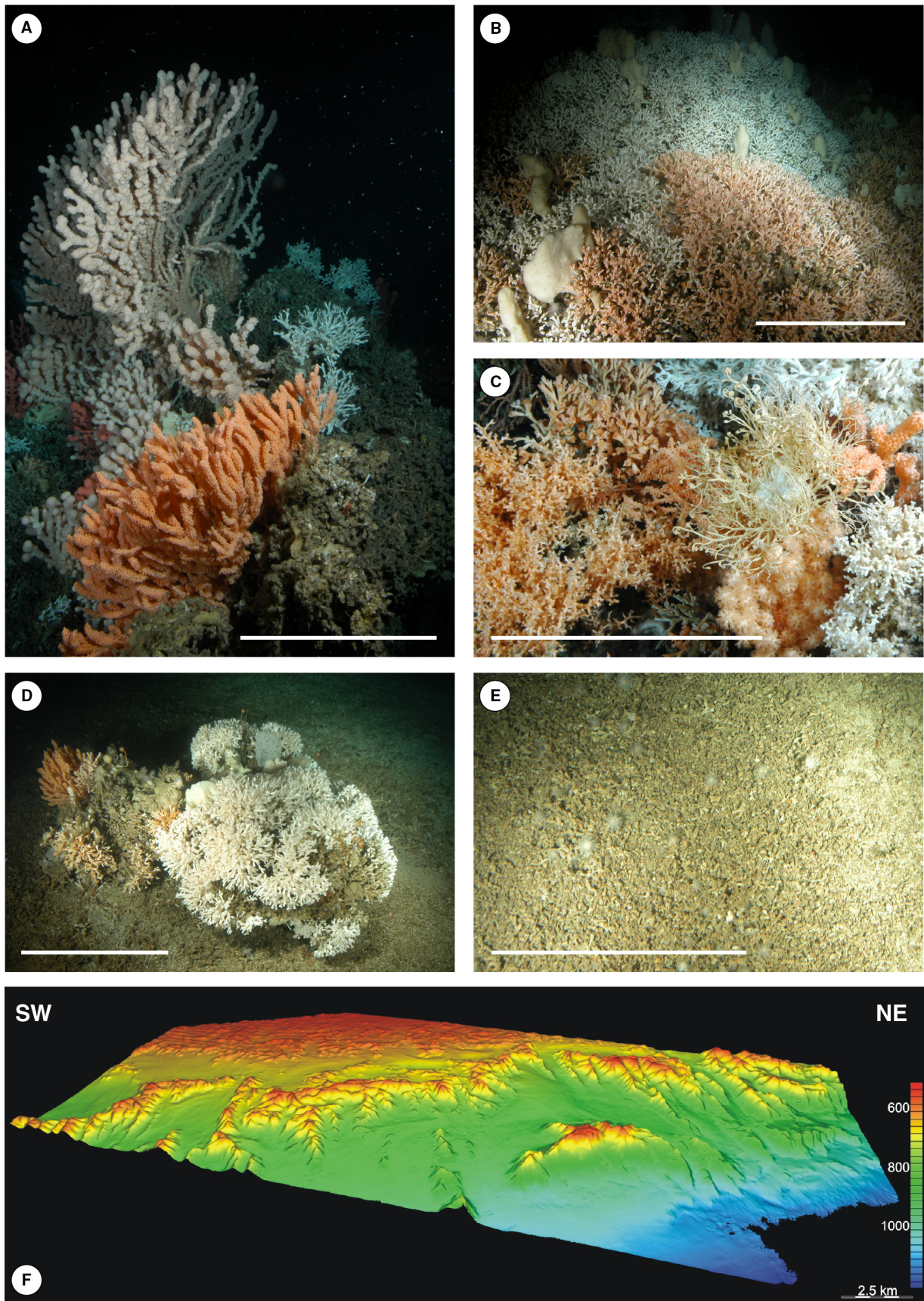
Fig. 11. CWC-factory: Norway, North Atlantic Ocean. (A) Sula Reef, Norway (64°N): illustrated are from top to bottom *Paragorgia arborea* (left), *Lophelia pertusa* (right), *Primnoa resedaeformis* on dead *Lophelia* coral framework. Scale bar *ca* 50 cm. (B) Stjernsund, Norway (64°N): *Lophelia* reef (both colour varieties) with sponges (*Mycale* sp.). Scale bar *ca* 50 cm. (C) Røst Reef, Norway (67.5°N): illustrated are white *Lophelia pertusa* (upper right), orange *Lophelia pertusa*(top centre), white *Madrepora oculate* (lower right), orange *Madrepora oculate* (centre left), *Primnoa resedaeformis* (below *Gorgonocephalus,* between white and orange *Madrepora*), *Paragorgia arborea* (between white *Lophelia* and white *Madrepora*, right of *Gorgonocephalus*). Scale bar *ca* 50 cm. (D) Single coral patch at Stjernsund, Norway (70°N): Living white (right) and orange (left) *Lophelia* corals with dead coral framework below or left on coral rubble field at Stjernsund. Additional fauna attached, for example, *Primnoae*, *Paragorgia*, hydrocorals and sponges. Scale bar *ca* 50 cm. (E) Coral rubble facies at Stjernsund, Norway (70°N): Submersible JAGO-Team GEOMAR Kiel: Coral rubble facies from the flank of Stjernsund. Scale bar *ca* 50 cm. (F) Multibeam map *R/VPelagia* (2006) of Rockall Bank (North Atlantic Ocean, 55°N to 60°N), with active growing CWC mounds. Water depth scale on the right. Photograph sources: (A) to (E): © JAGO Team, GEOMAR, Kiel, Germany – (A): 2008; (B), (D), (E): 2005; (C): 2007; (F) courtesy of G. Duineveld, M. Bergman and F. Mienis (Royal NIOZ, Netherlands).

sediment production system the P-factory, in which the P stands for planktic or 'Pulse' related to the seasonal production of biota (Fig. 7).

PRODUCTION PROFILES

The different carbonate factories each have their individual production profiles (Figs 5 and 7). These either reflect the water depth in which the individual factory reaches its optimum growth and sediment production, for example the T-factory, or environmental processes determining the types and amounts of sediment produced (Table 3).

T-factory

The dominant control, light, means that the production profile declines sharply with depth (Fig. 7; Bosscher & Schlager, 1992). Light penetration fluctuates throughout the oceans with maximum depths varying between *ca* 45 m for the Great Barrier Reef, Bahamas and Barbados to name a few, to nearly 100 m for Belize and Jamaica and 140 m for Pacific atolls (Schlager, 2005, p. 16). The interaction between the surface area within the zone with light penetration controls, to a large extent, the quantity and type of sediment production; see the section on *Sediment export*. The growth rates of the corals making up the reefs are strongly tied to the light parameter (Enos, 1991; Bosscher & Schlager, 1993; Dullo, 2005; Gischler & Hudson, 2019).

CWC-factory

The CWC-factory strongly depends on the steady influx of nutrients either through deep-water currents or pelagic input (e.g. Freiwald & Roberts, 2005). The sediment production profile shown in Fig. 7 displays low rates compared to the other factories, but with a larger depth range. The CWC-factories along the Irish margin (e.g. van Weering *et al.*, 2003; Mienis *et al.*, 2006; van der Land *et al.*, 2014) as well as the communities in the Mediterranean demonstrate variations in their occurrence related to glacial and interglacial time intervals (Fink *et al.*, 2012; Hebbeln *et al.*, 2019).

C-factory

In the C-factory, production rates lean heavily on the availability of nutrients (Schlager, 2005, p. 24; James & Bone, 2011). The maximum rates in the production profile are lower when compared to the T-factory but cover a wider depth range (Fig. 7). Relative changes in sea-level have a minor effect on the overall production rates of the C-factory but do result in significant re-sedimentation of sediments produced in shallow-water during these changes, as illustrated for the Great Australian Bight (Saxena & Betzler, 2003).

M-factory

The M-factory is characterized by fairly stable and relatively high sediment production and export rates irrespective of sea-level changes (Fig. 7), as the main sediment production sites on the flat-topped M-factory platforms are situated at the upper slope with a preference for the nutrient-rich waters of the thermocline (Keim & Schlager, 1999, 2001; Kenter *et al.*, 2005; Schlager, 2005). Minor differences might occur during phases of progradation and aggradation (Della Porta *et al.*, 2004). This enables these platforms to prograde over large distances; the
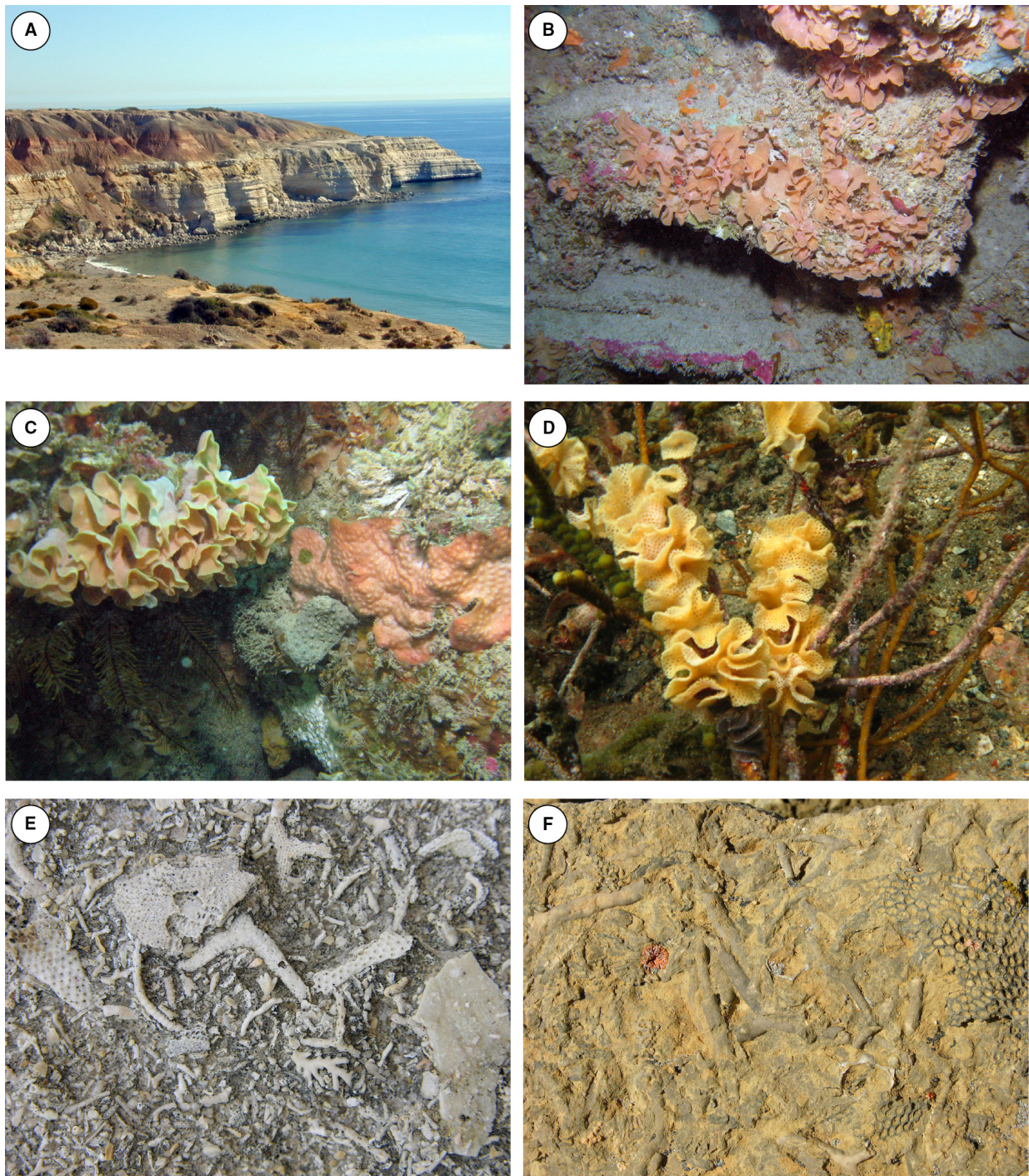
Fig. 12. C-factory: South Australia and Canada. (A) Field view of Upper Eocene cool-water limestones (white) overlain by Plio-Pleistocene siliciclastics (dark); cliffs *ca* 40 m high; Blanche Point, South Australia. (B) Prolific growth of fenestrate bryozoans and scattered coralline algae, 18 m water depth, southern Victoria, Australia, image width *ca* 25 cm. (C) Fenestrate bryozoans growing on macroalgae (branching brown biota) at upper left, with pink sponges at right and small encrusting grey bryozoan below, 12 m water depth, southern Victoria, Australia, width = 20 cm. (D) Close view of fenestrate bryozoan on gorgonian, 12 m water depth, southern Victoria, Australia, image view = 10 cm across. (E) Bedding plane view of bryozoan grainstone-rudstone, Oligocene, Pt. Willunga Formation, Pt. Willunga, South Australia, image = 10 cm across. (F) Bedding plane view of robust branching (centre) and fenestrate (right) bryozoans, Assistance Formation, Middle Permian, Ellesmere Island, northern Canada; image view *ca* 20 cm. Photograph source: Noel P. James (Queen's University, Kingston, Canada).

Table 4. Latitudinal distribution and seawater temperature characteristics of modern non-tropical and tropical carbonates (after Flügel, 2010, table 2.9, p. 34).

Flügel (2004, 2010)	Flügel (2004, 2010)	Latitudinal range	Seawater temperature	Subdivision	Latitudinal range	Seawater temperature	Present-day occurrence
NON–TROPICAL CARBONATES (Cool–water carbonates)	POLAR CARBONATES	>50° N and S	COLD WATER <5 to 10°C (mean) -1.5 to 16°C (range)	Polar	>60° N and S to 70° N and S	>5°C	Beyond the Arctic Circle: Central Greenland Sea, Barents Sea, Ross Sea, Antarctica, Arctic eastern Canada, northern Norway, western Canadian Shelf
				Subpolar	>50° to <60° N and S	5 to 10°C	North-western Europe
	TEMPERATE CARBONATES	30° to 50° (60°) N and S	COOL WATER *ca* 10 to 18°C (mean) >10 to 25°C (range)	Cool-temperate	30° to 50° N and S	5 to 10°C	Southern Australia, Tasmania, New Zealand
				Warm-temperate	25° to >30° N 25° to 30° S	10 to 18°C	Mediterranean Sea off North Africa, south-western Australia
TROPICAL CARBONATES	TROPICAL CARBONATES	30°N to 30°S	WARM WATER 18 to >22°C (mean) >18 to 30°C (range)	Subtropical	–	18 to 22°C	Bahama, Florida, Bermuda, Persian Gulf, Shark Bay
				Tropical	–	>22°C	Great Barrier Reef, Indian Ocean, Pacific Ocean

Rosengarten mountain chain (Dolomites, Italy) is a well-exposed example displaying this feature (Fig. 16; Maurer, 2000). Other case studies include the Canning Basin in Australia (e.g. Playford, 1980; Playton & Kerans, 2015a,b) and the Guadalupe Mountains in the USA (Tinker, 1998; Playton & Kerans, 2018).

P-factory

The production of the P-factory depends on seasonal changes during which surface nutrient availability (nitrate, phosphate and silicate) varies together with water stratification, influencing nutrient positioning throughout the seasons (e.g. Poulton *et al.*, 2014). For planktic foraminifera, the seasons, water masses and water depths are important parameters regulating species abundance and associated sediment production of shells that can sink to the sea bottom (e.g. Schiebel & Hemleben, 2005). Planktic foraminifera thrive in the uppermost tens of metres of the water column, and may, depending on the reproduction cycle, move down to 400 m water depth; certain species are known to occur down to 2000 m water depth (Schiebel &
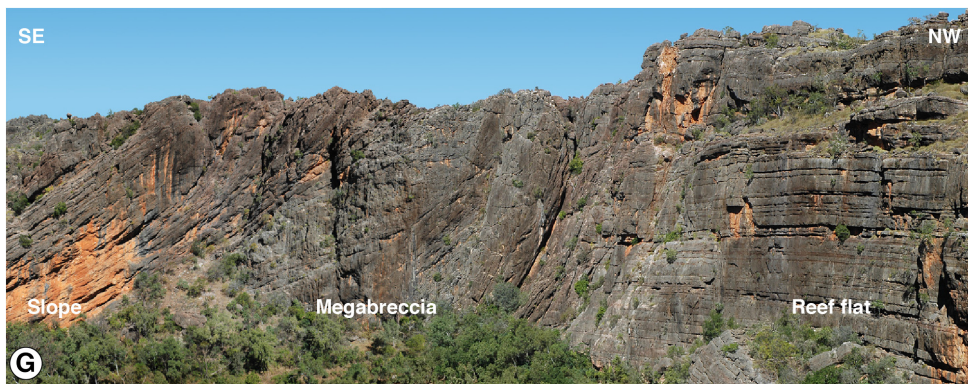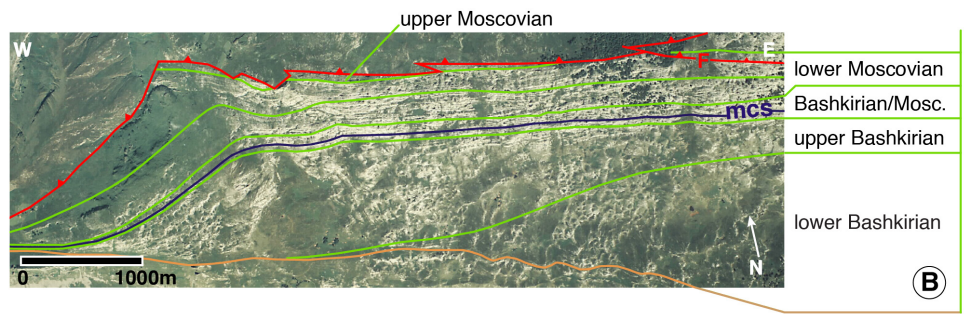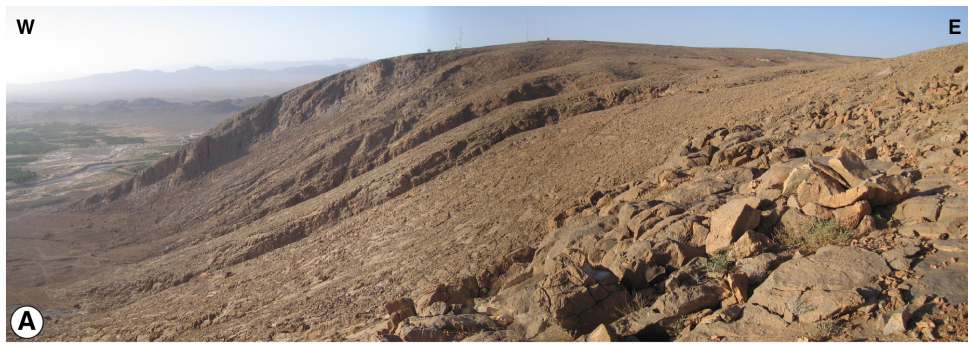
Fig. 13. M-factory: Morocco, Spain and Australia. (A) Panoramic overview of the western slope and platform margin of a Lower Jurassic high-relief M-factory carbonate-factory platform (Jbel Bou Dahar, central High Atlas, Morocco). Modified from Merino-Tomé *et al.* (2017). Shown from east to west: nearly horizontal platform top, basinward-dipping outer platform (100 to 200 m wide), platform break, and steeply dipping slope deposits (left side). Stratal surfaces can be traced from the platform interior basinward along the platform break and slope. (B) Aerial photograph of the Carboniferous high-relief, flat-topped M-factory carbonate platform of the Sierra de Cuera (Cantabrian Zone, northern Spain). Right side of photograph: platform deposit. Left side of photograph: steep slope with linear clinoforms. Green lines: chronostratigraphic boundaries. Purple line (MCS): main stratal correlation surface connecting inner platform (right) with toe-of-slope deposits (left). Red lines: faults. Modified from Della Porta *et al.* (2002). (C) Series of Lower Devonian (Emsian) carbonate mud-mound build-ups of the Kess-Kess Formation at Hamar Laghdad, Eastern Anti-Atlas (Morocco). Cars for scale. For a detailed description of the sedimentary sequence see Brachert *et al.* (1992) and Aitken *et al.* (2002). (D) Single Lower Devonian (Emsian) carbonate mud-mound build-up of the Kess-Kess Formation at Hamar Laghdad, Eastern Anti-Atlas (Morocco). Red arrow marks person at top of mud-mound for scale. For a detailed description of the sedimentary sequence see Brachert *et al.* (1992) and Aitken *et al.* (2002). (E) and (F) Details of biota within a mud mound build-up of the Kess-Kess Formation with stromatactis cavities (E), and tabulate corals (thamnoporids, favositids and auloporids) embedded in bioclastic wackestones. Pencil for scale. (G) Late Devonian carbonate platform margin to slope transition, Windjana Gorge (Canning Basin, Western Australia). Slope (left): debris-dominated foreslopes. Megabreccia: rudstone–grainstone, blocks and backfilled megabreccia. Reef flat (right): reef flat deposits exposing thickets of stromatoporoids, bafflestone to floatstone fabrics, that interfinger seaward with reef deposits and landward with backreef deposits. After Playford *et al.* (2009) and Playton & Kerans (2015a,b).

Hemleben, 2005, fig. 2). The distribution and production of calcareous nannoplankton (coccoliths) relates to zones with high organic productivity combined with quality and intensity of light, water temperature and latitudinal variations (e.g. Haq & Boersma, 1978, pp. 80–87; Flügel, 2010, pp. 404–405). The bulk of the calcareous nannoplankton live in the upper 100 to 150 m of the world's oceans, but with highest concentrations in the photic zone (Haq & Boersma, 1978, pp. 80–87). Pteropods have a limited tolerance to changes in salinity and water temperature, and thrive in warm, tropical zones in the uppermost 500 m of the water column (Haq & Boersma, 1978, pp. 152–153).

MINERALOGY AND GRAIN SIZES

The individual factories not only have different sediment production windows and sediment export modes, but the sediments produced also differ in their dominant carbonate mineralogy, i.e. aragonite, high-magnesium calcite (HMC) or low-magnesium calcite (LMC). The grain-size spectrum also differs, i.e. the variation in grain sizes produced and exported (Table 3).

T-factory

This factory displays a large variety in skeletal grains and associated grain sizes. This variation relates to the wide spectrum of biota, which includes zooxanthellate corals, calcareous green and red algae, benthic foraminifera, echinoderms, bryozoans and bivalves (Flügel, 2010, p. 35; Figs 8 to 10). In addition, non-skeletal components, such as ooids, peloids and aggregate grains, dominate in certain parts of the sedimentary system (Fig. 8). The same holds for the carbonate mud (e.g. Reijmer *et al.*, 2009; Swart *et al.*, 2009; Harris *et al.*, 2015). Rendle-Bühring & Reijmer (2005) discussed that variations in grain sizes in carbonate slope to basin sediments related to changes in carbonate platform productivity and export in response to eustatic changes in sea-level (Fig. 17). In the Santaren Channel on the leeward margin of Great Bahama Bank, fine-grained sediments dominated during interglacial intervals while coarse-grained sediments prevailed during glacial periods. The sand–mud ratio is fairly consistent at the windward margin in Exuma Sound (Fig. 17), but when all thin gravity deposits are included a slightly reversed trend was found with coarser grained sediments during interglacial periods and finer grained deposits in glacial times (Rendle-Bühring & Reijmer, 2005).

The mineralogy of modern T-factory sediments is dominated by aragonite followed by HMC and LMC (Schlager, 2005, p. 23; Tables 2 and 3; Fig. 18). The sediments on Great Bahama Bank contain between 77.7% and 100% aragonite with a mean of 93.3% (Reijmer *et al.*, 2009; Swart *et al.*, 2009). High-magnesium calcite (HMC) content varies between 0% and 22.3%
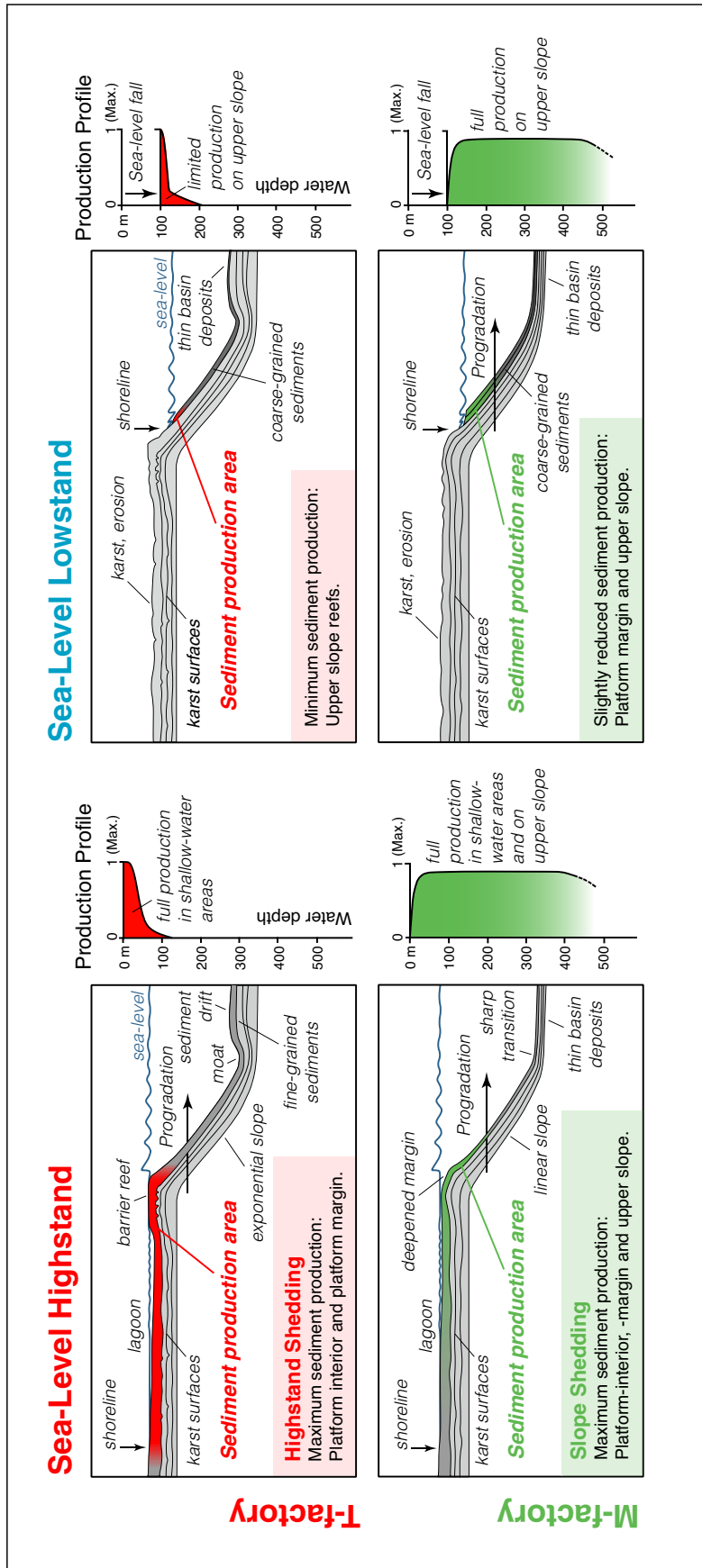
Fig. 14. Upper panels: T-factory systems show large production areas (marked in red; left upper panel) situated in the photic zone during sea-level highstands (see left production profile) resulting in high sediment production and export rates. Sharply reduced production and export due to the severe reduction in the size of the sediment production area positioned within the photic zone during sea-level lowstands (right upper panel). Production profile displays photic zone and slope angle interaction with a reduction in the size of the sediment production area during sea-level lowstands (far right). This sediment export pattern is called highstand shedding (Droxler & Schlager, 1985). Production area characteristics indicated in lower left corner of all platform graphs. Platform margin sediment export is dominated by sand-sized grains while the platform top sediments are more mud-dominated. See studies by Rendle *et al.* (2000), Rendle-Bühring & Reijmer (2005) and Reijmer & Andresen (2007) for more information on grain-size export variations of T-factory sediments. Lower panels: The main sediment production area of M-factory systems is positioned on the upper slope, and hence highstand and lowstand sediment production and export modes do not differ significantly. Production profiles nearly remain the same for highstands and lowstands in sea-level. This fairly continuous sediment export pattern is called slope shedding (Kenter *et al.*, 2005). The M-factory is sand and rubble dominated as shown by the straight steep slopes (Kenter, 1990; Schlager & Reijmer, 2009; Adams & Kenter, 2014). Some compositional differences between highstand and lowstand sediments do exist, see Reijmer (1998) and Della Porta *et al.* (2002, 2004) for more information.

Fig. 15. P-factory: United Kingdom. Cliff at Birling Gap near Eastbourne (South England) exposing Santonian – Lower Campanian P-factory 'Chalk' strata looking northward. Note the black chert bands and nodules. Person for scale, *ca* 1.8 m tall. Photograph source: Florian Smit (University of Copenhagen, Denmark).

(mean = 6.5%), and low-magnesium calcite (LMC) from 0 to 3.9% (mean = 0.2%; Reijmer *et al.*, 2009).

CWC-factory

The mounds of the CWC-factory show an alternation of coral-dominated intervals and lithified intervals (e.g. Mienis *et al.*, 2009a; van der Land *et al.*, 2010). Thin-section point counting revealed that the coral-dominated intervals contain up to 82% coralline material with minor sponge needles, echinoderms, brachiopods and gastropods, embedded in a fine-grained matrix (van der Land *et al.*, 2010). The sediments in the lithified intervals consist of coralline material (2%), coccoliths (68%) and planktic foraminifera (29%; van der Land *et al.*, 2010).

In the coral-dominated intervals, 40% of the components have an aragonitic mineralogy, 51% have a LMC mineralogy and less than 2% have a HMC mineralogy (van der Land *et al.*, 2010; Tables 2 and 3; Fig. 18). Other mineralogies comprise biogenic silica with less than 0 to 5% and terrestrial-derived silica with 6%. In the

lithified intervals only 1 to 5% are aragonitic components, 1 to 5% are HMC fossils and 3% of the material is terrestrial-derived silica. The sediment is dominated by fossils with an LMC mineralogy (94%).

C-factory

The C-factory displays a variety of grains across the entire grain-size spectrum (James & Bone, 2011, p. 47). The grains include calcareous algae, bryozoans, molluscs (scaphopods, bivalves and gastropods) and foraminifera (free and encrusting, large and small, benthic and pelagic; Tables 2 and 3; Fig. 12). The Holocene sediments on the shaved shelf along southern Australia show strong hydrodynamic partitioning with low energy semi-protected gulfs and a high-energy open shelf in the zone of wave abrasion (James & Bone, 2011, p. 210). In the high-energy zone the recent sediments consist of a mix of Holocene bio-fragments, relict carbonate particles of Pleistocene origin and siliciclastic grains (James & Bone, 2011, p. 85). The semi-protected areas, seagrass beds or sub-wave-
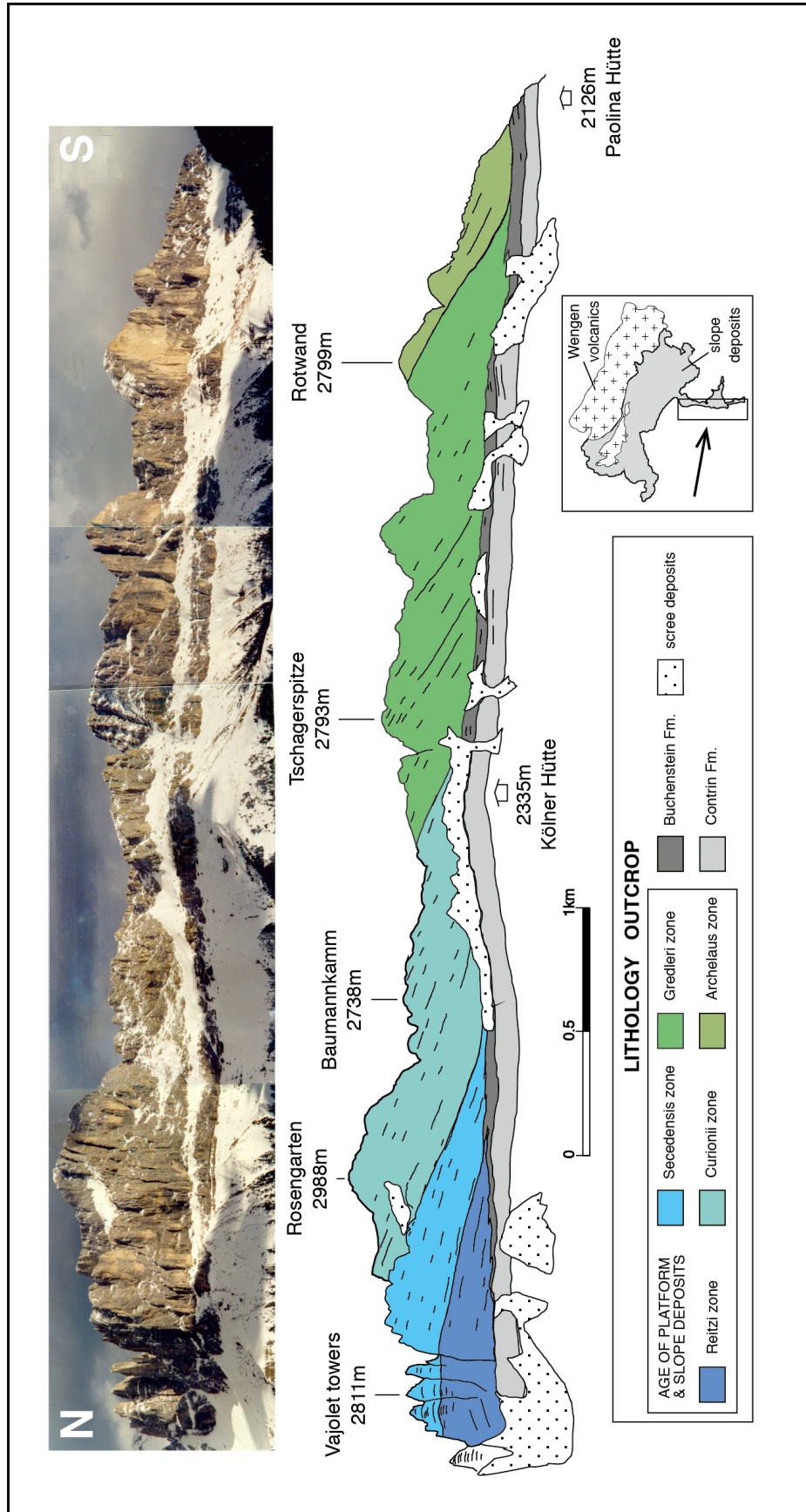
Fig. 16. Photo-panorama and interpretation of slope (Schlern Dolomite Formation) and basin deposits (Buchenstein Formation) at Rosengarten/Catinaccio (Dolomites, Italy). Indicated are various stages of platform progradation for successive ammonite zones. Dating based on radiometric ages and conodont biostratigraphy. Small inset lower right marks geological sketch of Schlern/Rosengarten platform with position photo-panorama indicated. Overview displays fairly continuous, sea-level-independent, progradation of the M-factory system. Modified from Maurer (2000).
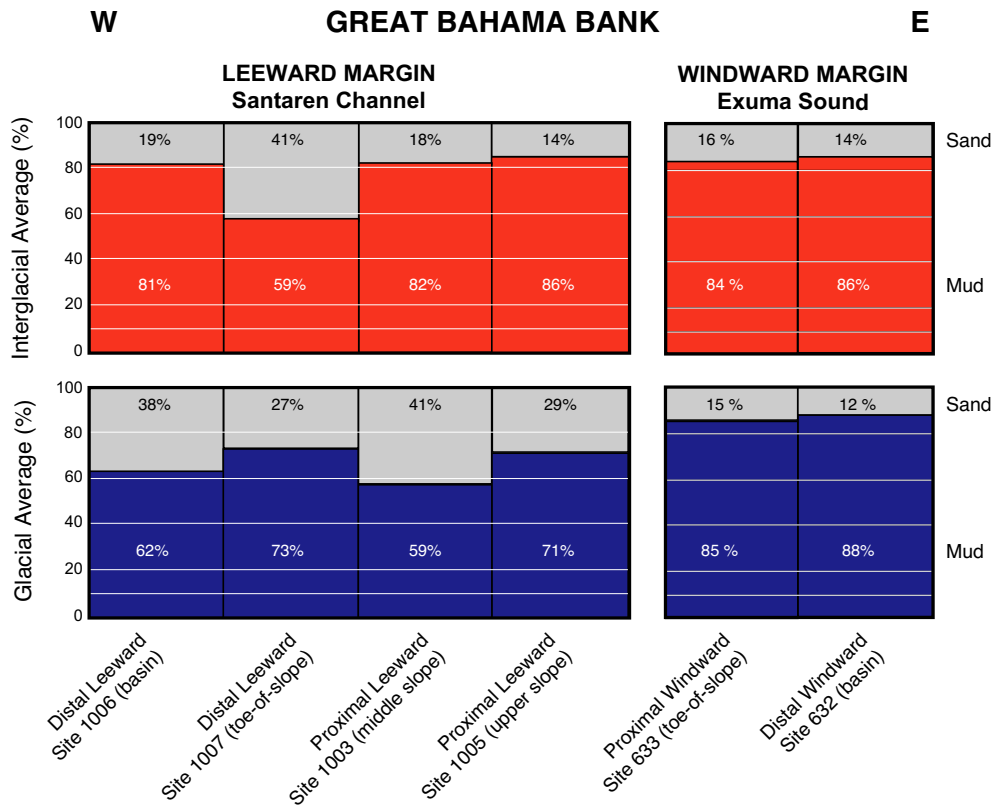
Fig. 17. Comparison of average sand–mud ratios for both interglacials and glacials for: (i) ODP sites 1005 (upper slope), 1003 (middle slope) 1007 (toe-of-slope) and 1006 (basin) positioned on the leeward slope of Great Bahama Bank in the Santaren Channel; and (ii) ODP Sites 633 (toe-of-slope) and 632 (basin) positioned on the windward side in Exuma Sound. Averages cover Pleistocene to Holocene (Marine Isotope Stages 1–21). On the leeward side interglacial intervals tend to be mud-rich while glacial intervals are coarser grained. Windward sites show comparable interglacial and glacial sand–mud ratios. Modified from Rendle-Bühring & Reijmer (2005).

base locales, contain more muddy facies, including poorly sorted muds and sandy muds with molluscs, coralline algae and benthic fora-minifera. Sediments on the shelf-margin slope comprise an alternation of grainy, aragonitic and HMC-rich sediments with tunicate spicules, relict bioclasts and bryozoan detritus, and micritic LMC-rich sediments with large amounts of sponge spicules (Saxena & Betzler, 2003; Fig. 19).

The surface sediments of the C-factory possess up to 50% aragonite, 40% intermediate-Mg cal-cite (IMC; between 4 mol% and 12 mol% $MgCO_3$) and HMC (>12 mol% $MgCO_3$) and up to 10% LMC (Tables 1 and 3; Fig. 18). However, carbonate dissolution due to oxic to anoxic microbial degradation of sedimentary organic matter results in the almost complete loss of aragonite in the upper sub-seafloor sediments (James & Bone, 2011, p. 192).

M-factory

In the M-factory, sediment export largely depends on sediment production in the upper slope – platform margin realm (Fig. 7). For the Triassic basin sediment of the Northern Calcare-ous Alps, Reijmer *et al.* (1991, 1994) noted that sub-Milankovitch scale variations in mud clast input to the toe-of-slope and basin agreed with periodic climate changes as registered in the inner platform sediments (Lofer cyclothems; Schwarzacher & Haas, 1986; Berger, 1989). This link demonstrated that M-factory sediment export to the slopes is dominated by a continu-ous supply of crusts and peloidal mud clasts (Reijmer *et al.*, 1991, 1994; Schlager & Reijmer, 2009; Keim & Schlager, 2001). Recent studies on the Permian Capitan slopes discussed that the peloidal mud-clast dominated sediments derived from the upper slope form individual breccia
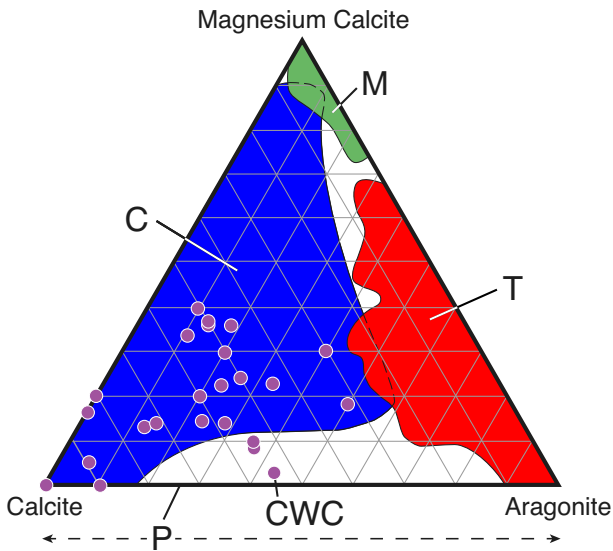
Fig. 18. Mineralogical composition of the T-factory, C-factory, M-factory, CWC-factory and P-factory. Modified from Schlager (2005). C-factory and T-factory based on Bathurst (1971), Milliman (1974) and Morse & Mackenzie (1990). M-factory based on Neuweiler (1995) and Russo *et al.* (1997). CWC-factory, purple dots, based on van der Land *et al.* (2010) and Titschack *et al.* (2016). P-factory variation along the calcite–aragonite baseline is based on Milliman (1974) and Berger (1978).

sets shaping the individual clinothems (Playton & Kerans, 2018). Similar patterns were also observed for the Carboniferous Sierra de Cuera (Fig. 13; e.g. Della Porta *et al.*, 2004) and the Jurassic Jbel Bou Dahar slopes (Kenter & Campbell, 1991; Scheibner & Reijmer, 1999; Blomeier & Reijmer, 2002; Merino-Tomé *et al.*, 2012; Della Porta *et al.*, 2014).

The mineralogy of the M-factory is dominated by HMC (Russo *et al.*, 1997; Neuweiler *et al.*, 1999; Schlager, 2005; Fig. 18). Other carbonate mineralogies are also present but in minor quantities (Table 3).

P-factory

In the P-factory grain-size is dominated by the production of coccoliths, planktic foraminifera, pteropods, etc., in the photic zone. The grain-size of the calcareous biota varies between 10 to 100 μm in diameter for the coccospheres and 2 to 20 μm for the coccolith plates (e.g. Bown *et al.*, 2004), a maximum diameter of 600 μm for planktic foraminifera (Milliman, 1974) and up to 1 to 2 cm as maximum shell

length for pteropods (Scholle & Ulmer-Scholle, 2003). The radiolarians vary between 100 μm to more than 2 mm (Scholle & Ulmer-Scholle, 2003).

The mineralogy of the carbonate P-factory is dominated by LMC of the coccoliths and planktic foraminifera (Fig. 18; Milliman, 1974). Pteropods are the main aragonite suppliers (Milliman, 1974; Berger, 1978). Other important components are formed by radiolaria and diatoms, which are non-carbonates with an amorphous (opaline) silica skeleton (Haq & Boersma, 1978, p. 203; Table 3).

PLATFORM MORPHOLOGIES

The different styles of carbonate platform development are related to production profiles and thus the sensitivity of the system as a whole to environmental changes (Fig. 7). These differences are very well expressed in the response of the T-factory, C-factory and M-factory to relative changes in sea-level, which will be discussed later in the manuscript (Table 3).

Large-scale morphologies

T-factory systems display varying morphologies ranging from carbonate ramps with gentle slopes with a maximum angle of repose of 1° (Read, 1985) to flat-topped rimmed platforms (Figs 8 to 10). The slope profile of the present-day Arabian/Persian Gulf is described as the example of a homoclinal carbonate ramp. The other carbonate ramp type is the distally steepened ramp where the change in slope angle occurs at far distance from the high-energy shoals of the shallow ramp (Read, 1985). Other morphological profiles included rimmed shelves, isolated platforms and atolls. The modelling study of Williams *et al.* (2011) discussed multiple types of platform geometries occurring through geological history, reflecting variations in sediment production, sediment (re-)distribution, subsidence, sea-level fluctuations, antecedent topography and environmental shaping factors. In the fossil record the T-factory setting may have been different when compared to today's distribution, as shown by the Jurassic and Cretaceous carbonate platforms of the Middle East exhibiting a very characteristic morphological feature with platforms enclosing organic-rich intrashelf basins (e.g. Murris, 1980; Droste, 1990; van Buchem
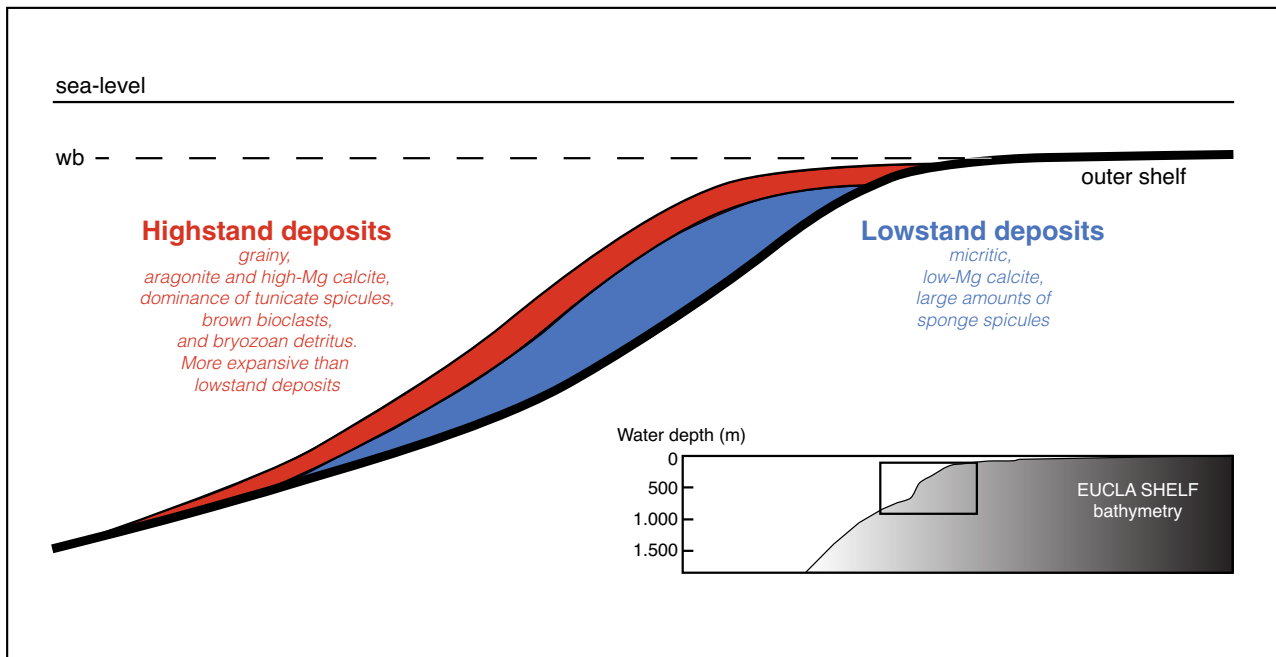
Fig. 19. Development of C-factory shelf slope sequences along the Eucla shelf slope, bathymetry provided in lower right box, in response to eustatic sea-level variations. Wave abrasion impacts the inner to middle shelf during sea-level highstands and the outer shelf during sea-level lowstands. Lowstand deposits (in blue) are lens-shaped while highstand deposits (in red) develop an extensive wedge at the shelf edge. Major compositional variations indicated. wb: wave base. Modified from Saxena & Betzler (2003).

et al., 2002; Buchem et al., 2010; Razin et al., 2010).

The cold-water corals of the CWC-factory create their own morphology and are limited by the nutrient distribution window (Kenyon et al., 2003), and the interplay of current speed winnowing fines and, at the same time, allowing larvae to settle on available substrates (e.g. Kenyon et al., 2003; Duineveld et al., 2007). Mounds may reach heights of up to 157 m, with a mean of 71.7 m, as illustrated by the Magellan mound province, Porcupine Basin, west of Ireland (Huvenne et al., 2007) or Rockall Plateau (Fig. 11F; Duineveld et al., 2007). Large clusters of CWC mounds were found off the coast of Norway, Ireland (Fig. 11), the Bahamas, Mexico, Morocco, Mauritania, Angola and Namibia (see Hebbeln & Samankassou, 2015, for an overview; Wienberg et al., 2018; Hebbeln et al., 2019; Hanz et al., 2019).

The morphologies of C-factory environments enclose non-rimmed ramps, open shelves and large offshore banks (James, 1997). Because no barriers are present, waves and currents can enter the system without any restrictions (Fig. 12). Hence, the sedimentary environment is subdued due to forceful hydrodynamic processes that control the sediment distribution in the shallow-water areas resulting in a shaved shelf environment (James et al., 1994). C-factory sediments in general are poorly cemented and hence prone to re-sedimentation processes, as discussed by Puga-Bernabéu et al. (2014) for the temperate sediments of south-east Spain that contain shell beds, sediment gravity flows and deposits with hummocky and swaley cross-stratification related to unconfined flow processes linking grain-size to the hydrodynamic energy of the depositional environment.

At present the sediment binding capacity of the M-factory biota is known from relatively small-scale deposits like the upper slope of the Bahamas and Tahiti (Séard et al., 2011; Reolid et al., 2017). In the fossil record, however, the sediment binding capability is expressed in two morphological end-members characterizing this factory being: (i) the classical mud mounds, known for example from Ireland and Belgium (e.g. Lees, 1964; Boulvain, 2001), Algeria (Wendt et al., 1997) and Morocco (Brachert et al., 1992); and (ii) the flat-topped steep-sided platforms, known from the Dolomites (Italy; e.g. Bosellini, 1984, 1989), Sierra de Cuera (Spain; e.g. Bahamonde et al., 1997, 2004; Della Porta et al.,
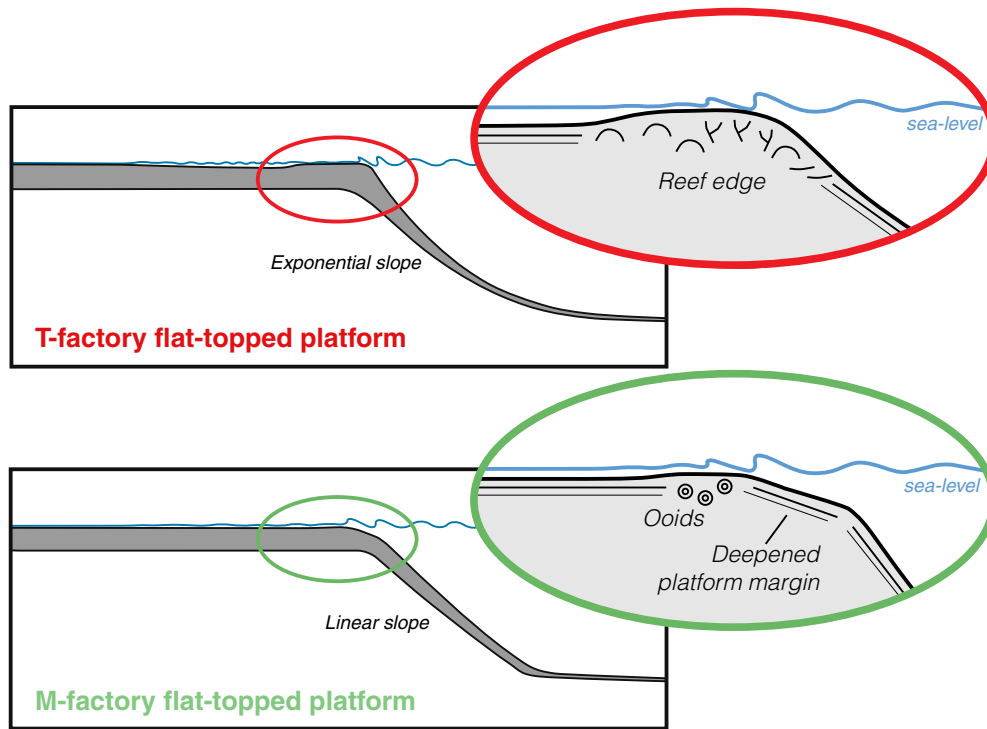
Fig. 20. Comparison between platform margin morphology of the T-factory with a reef rimmed flat-topped platform with a flat lagoon and steep exponential slope, and the M-factory with a flat lagoon, and a deepened margin with 8° to 10° basinward dipping beds (also termed fall-in beds; Kerans & Harris, 1993; Della Porta *et al.,* 2014) marking the transition to the sediment-production sites on the steep upper linear slope. See Fig. 21 for an example from the Sella platform, Dolomites, Italy.

2003), Jbel Bou Dahar (Morocco; Kenter & Campbell, 1991; Verwer *et al.*, 2009), the Guadalupe Mountains (USA; e.g. Playton & Kerans, 2018) and the Canning Basin (Australia; e.g. Playford, 1980; Frost & Kerans, 2009; Fig. 13). The mud mounds tend to display a variety of morphologies as discussed for the Dinantian Waulsortian mud mounds by Lees & Miller (1995) and incline to develop a flat top when reaching into the zone of intensive wave action (Schlager, 2005).

Contourite drifts, mass-transport deposits and sand waves are some of the morphological expressions that can be related to P-factory sediments. These carbonate sediment features are well-known from Cretaceous chalk (e.g. Surlyk & Lykke-Andersen, 2007; Gale *et al.*, 2015; Fig. 15) where they possess a strict P-factory composition but are also known from the present-day Bahamas (Chabaud *et al.*, 2016; Eberli & Betzler, 2019; Mulder *et al.*, 2019) and Maldives (e.g. Betzler *et al.*, 2017; Lüdmann *et al.*, 2018a,b), which both consist of a mix of P-factory and T-factory derived sediments.

Platform margins

Platform margins of flat-topped carbonate platforms differ depending on the carbonate factory. The margins of flat-topped, T-factory carbonate platforms often develop a distinct rim formed by reefs and islands, the classical reef-rimmed margin (Table 3; Figs 8 to 10 and 20). M-factory systems not only form single steep-sided carbonate mud mounds, but also are known for their steep-sided, flat-topped platforms with a non-rimmed edge. However, the margin profile covering the transition of the platform interior towards the slope at the platform edge differs from the T-factory margin profile with a deepened margin, also described as 'fall-in beds' (Figs 20 and 21; Kerans & Harris, 1993; Tinker, 1998). These are slightly inclined beds at the edge of the platform that connect the (sub-)horizontal platform lagoon sediments, and the steeply inclined slope deposits. They have an angle of repose varying between 5° and 10° as described for the platform margin profiles of the Jbel Bou Dahar
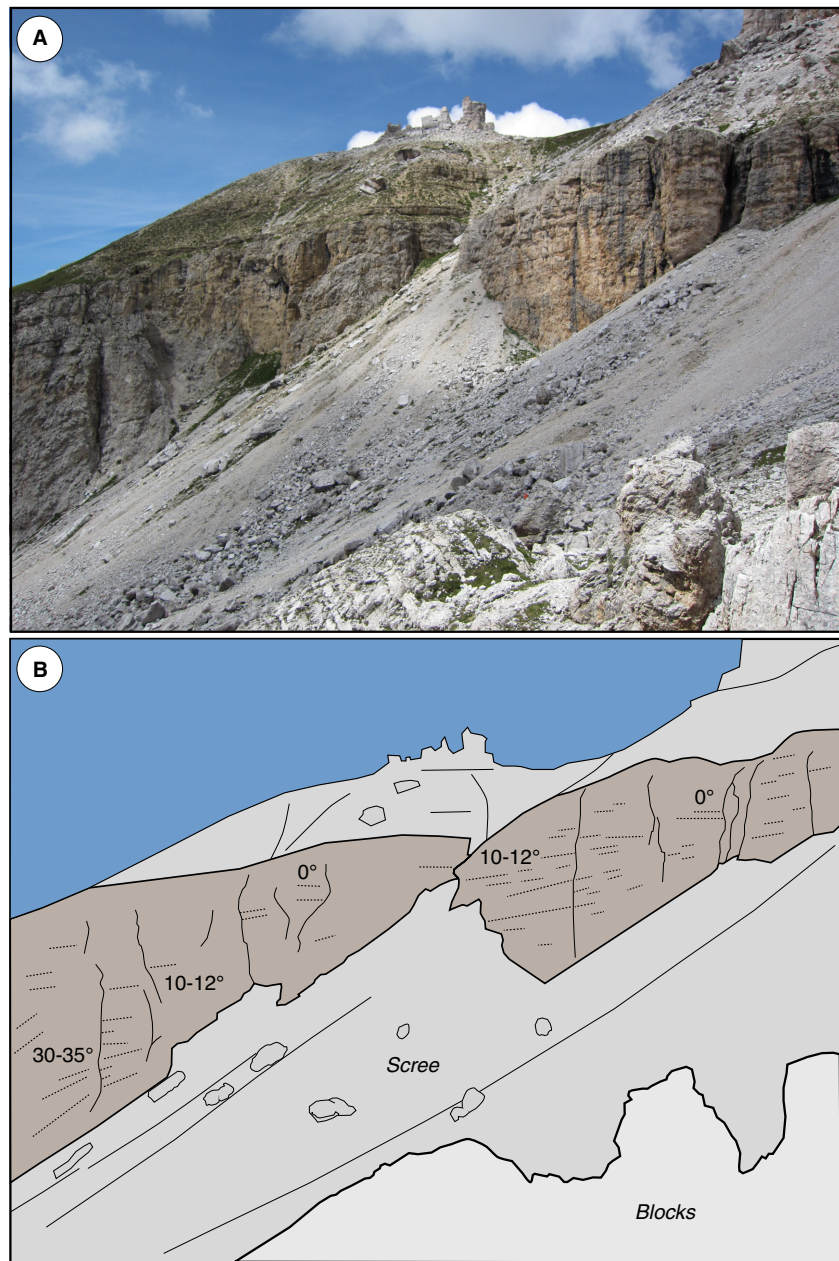
Fig. 21. Overview of the bedding geometry at Piccolo Pordoi (Sella Platform, Dolomites, Italy). (A) Outcrop photograph of M-factory platform margin. (B) Line drawing marking the nearly horizontal platform top-set beds on the right (north), the deepened margin (8° to 10° dip) in the centre and the 25° to 35° linear steep slopes of the clinoforms on the left (south). For a detailed sediment analysis of these deposits see Keim & Schlager (2001). Platform top-set bed interval (0° succession right side of photograph) measures *ca* 10 m. Interval thins to a few metres towards the south (left side of photograph).

(Fig. 13A; Scheibner & Reijmer, 1999), the Sella carbonate platform by Keim & Schlager (2001; Fig. 21) and the Sierra de la Cuera (Fig. 13B; Della Porta *et al.*, 2003).

CWC-factory systems build provinces of individual coral mounds along the continental margins of the Atlantic Ocean (Fig. 11), Mediterranean Sea and the Gulf of Mexico as well as the Indian and Pacific oceans (e.g. Hebbeln *et al.*, 2019, and references therein). The individual mounds have: (i) varying shapes, that usually are current related and can vary from circular to arcuate, and irregular with single or multiple peaks; (ii) different heights, between several metres and over 300 m; and (iii) possess changeable lengths, up to several hundreds of metres (e.g. Freiwald *et al.*, 2004; Mienis *et al.*, 2007; Roberts *et al.*, 2009). They mainly occur in water depths between 200 m and 1000 m (Hebbeln & Samankassou, 2015; Hebbeln *et al.*, 2019; Fig. 11).

C-factory systems do not tend to build barrier systems in shallow waters, but may form sedimentary structures, for example, current and wave ripples, sand bars and sand spits or beaches (Fig. 22; south-east Spain; e.g. Villalobos &
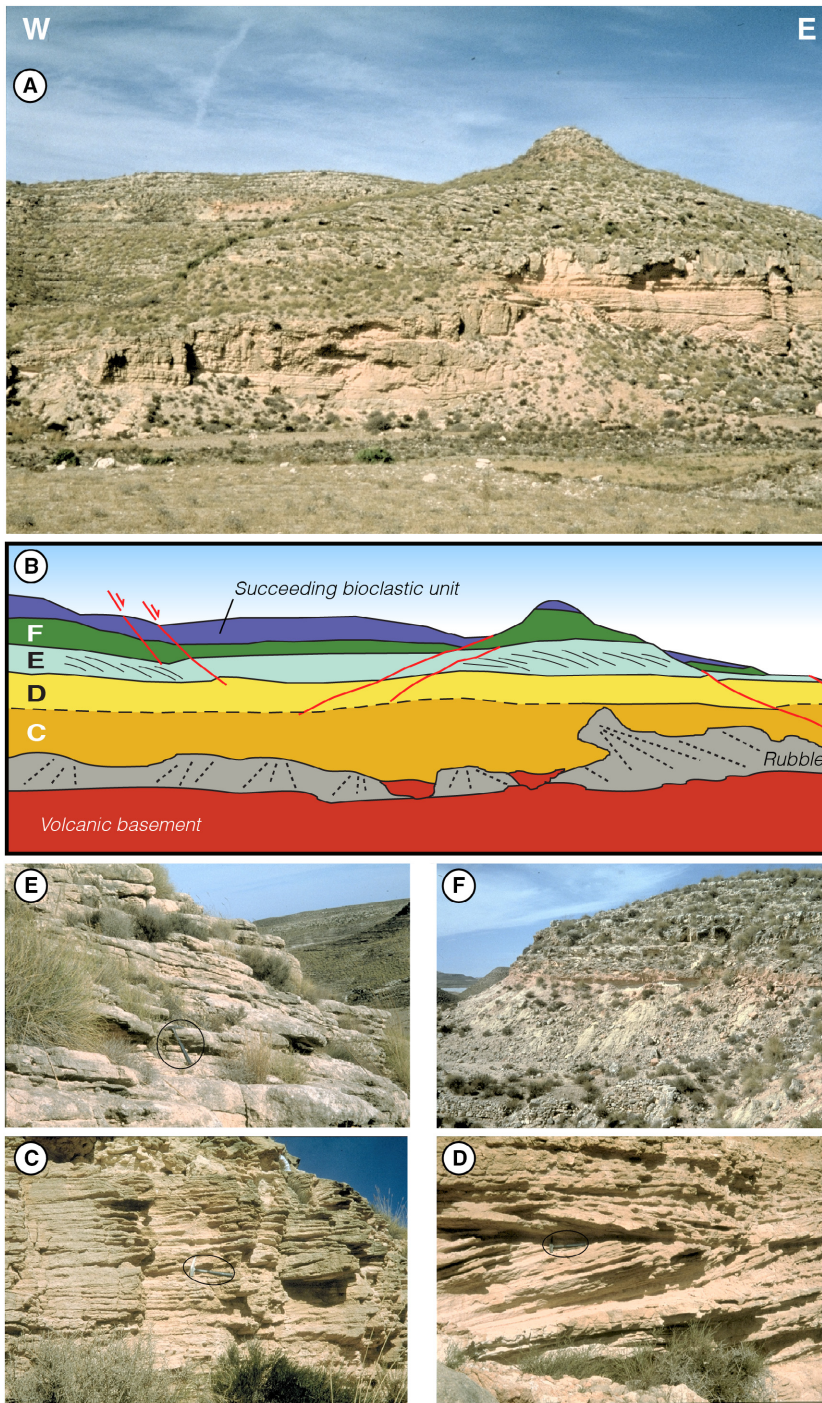
Fig. 22. C-factory at Cañada Méndez, Agua Amarga, south-east Spain. (A) Overview and (B) interpretation of the Cañada Méndez (Agua Amarga) outcrop. Height hill right-hand side picture *ca* 100 m. Letters 'C' to 'F' on the left side of (B) refer to units highlighted in (C) to (F). Modified from Villalobos & Braga (2003). (C) Lower unit resting unconformably on volcanic sands. Layers with cross-stratification are separated by thin continuous low-angle surfaces. Deposits are interpreted as storm-generated fans that accumulated on the protected side of a high or submarine volcanic ridge located to the south of the outcrop. Black circle: Hammer (33 cm) for scale. (D) The succeeding unit contains abundant trough cross-stratification. The sediments are interpreted as marine dunes migrating parallel to the coast. Black ellipsoid marks hammer (33 cm) for scale. (E) The third unit contains a succession marked by low-angle parallel lamination corresponding to beach sediments. Black ellipsoid: 33 cm hammer for scale. (F) The upper unit, height cliff *ca* 10 m, comprises fine sands with high-angle lamination interpreted as coastal aeolian dunes, and poorly-developed, unconsolidated muds, partially red coloured, with rhizoliths that are interpreted as coastal lagoon deposits. Photographs and figure by Juan C. Braga and José M. Martín (University of Granada) in Villalobos & Braga (2003). See also Betzler *et al.* (1997b) for a detailed description of the facies.

Braga, 2003; Puga-Bernabéu *et al.*, 2014). All aforementioned sedimentary structures reflect the loose sands character of this sedimentary system (south-east Spain; Betzler *et al.*, 1997b; Braga *et al.*, 2006; New Zealand; Anastas *et al.*, 1997). They were also found as submarine canyon fills (Fig. 26; Oligocene–Holocene, Gippsland Basin, south-east Australia; Wallace *et al.*, 2002; Mitchell *et al.*, 2007), or within a tide-influenced incised valley (Miocene, Provence, France; James *et al.*, 2014).

P-factories do not tend to form any barrier systems, but their sediments may form various deep-water sedimentary structures, such as mounded and sheeted drifts, valleys, moats, channels and sediment waves. These

sedimentary structures are omnipresent in the Cretaceous nannofossil oozes in the North Sea Basin (e.g. Surlyk & Lykke-Andersen, 2007; Gale *et al.*, 2015; Buls *et al.*, 2017).

Platform slopes

The angle of repose of carbonate slopes varies depending on the carbonate factory delivering the sediment and the processes operating on the slopes (Table 3). Comparing carbonate slope deposits and large-scale continental scree deposits (Kirkby, 1987) evidenced that the internal friction of the sediments (Kenter & Schlager, 1989), the angularity and sorting of the grains and clasts influenced the angle of repose (Kenter, 1990). The percentage of mud in the matrix and the interaction with microbial processes were two additional factors; with the amount of mud decreasing the angle of repose and the microbial processes leading to an increase (Kenter, 1990; Reolid *et al.*, 2014, 2017). Compared to their siliciclastic counterparts, mud-dominated carbonate slopes reach higher angles of repose because of higher internal cohesion (Kenter, 1990). Other factors increasing the sediment strength can be early diagenetic processes that might act locally or regionally and lead to development of steeper slopes in carbonate environments. Cementation rates within carbonate depositional systems can be very rapid, not only on the platform top in response to freshwater induced, diagenetic processes (Dravis, 1979, 1996) but also on the slopes where partial syn-depositional marine cementation of carbonate sands developed within eight months at a water-depth of 60 m (Grammer *et al.*, 1993, 1999).

Angles of repose surpassing 30° frequently characterize the upper slopes of carbonate slope systems; angles may even reach 45° (Kenter, 1990). Low-angle systems with slope angles below 5° characterize the toe-of-slope to basin domains. The carbonate ramp system of the present-day Arabian/Persian Gulf displays a carbonate facies distribution along such a low angle slope (Purser, 1973). In siliciclastic systems slope angles exceeding 5° are considered to be unstable and susceptible to re-sedimentation processes. The differences in slope angles of carbonate and siliciclastic systems become important when evaluating sediment deposition and re-deposition processes as well as the sediment transport processes in response to relative sea-level changes. These changes will determine the small-scale and large-scale sequence stratigraphic systems tracts in both systems.

Adams & Kenter (2014; Fig. 23) specified that similar slope morphologies existed in siliciclastic and carbonate sedimentary systems that developed in similar settings. Siliciclastic slopes tend to be less inclined than carbonate slopes, while the latter have a higher stabilization potential through early cementation and microbial binding. Adams & Kenter (2014) distinguished between slopes with a sigmoidal, concave or planar curvature (Fig. 23). Carbonate systems with a sigmoidal slope curvature (Gaussian mathematical expression) develop at shelf-breaks in response to base-level fluctuations. Cool-water carbonate systems such as known from the Great Australian Bight display these slope curvatures at the depositional centres at the outer shelf edge (Feary & James, 1998; James *et al.*, 2004). Concave slopes link to an exponential function and are known from T-factory systems like the western slope of Great Bahama Bank (Fig. 24; Eberli & Ginsburg, 1987, 1989) and to some extent reflect the interplay between sediment input at the platform edges and downslope sediment transport. Planar or linear slopes are very characteristic for M-factory systems with their microbial boundstone-dominated, deep and oligophotic sediment production sites producing linear slopes composed of rubble, boulders and sand (Figs 13 and 21; e.g. Keim & Schlager, 2001).

Slopes in T-factory systems are shaped by: (i) the grain-size distribution, and thus related to the sediment export spectrum of the carbonate platform; (ii) cementation processes; (iii) slope adjustment processes; and (iv) currents; but also (v) unique slope faunas. Hence, T-factory slope systems reflect a combination of sediment production by the reef system on the platform edge and slope, and the input of sediments originating in the platform interior. The slopes of this factory tend to have an exponential (concave) shape (Fig. 23; Adams & Kenter, 2014) with an in general fining of sediments downslope combined with a decrease in slope angle (Rendle *et al.*, 2000; Rendle & Reijmer, 2002). Leeward–windward variations do exist in the sand to mud ratios along the slope for glacial–interglacial time intervals (Rendle-Bühring & Reijmer, 2005; Reijmer & Andresen, 2007). However, recent studies illustrated that contour currents winnowing the fine sediments, reshape the grain-size distribution along the platform margin to basin transect with coarse-grained sediments occurring at the toe-of-slope instead of fine muddy sediments (Betzler *et al.*, 2014).
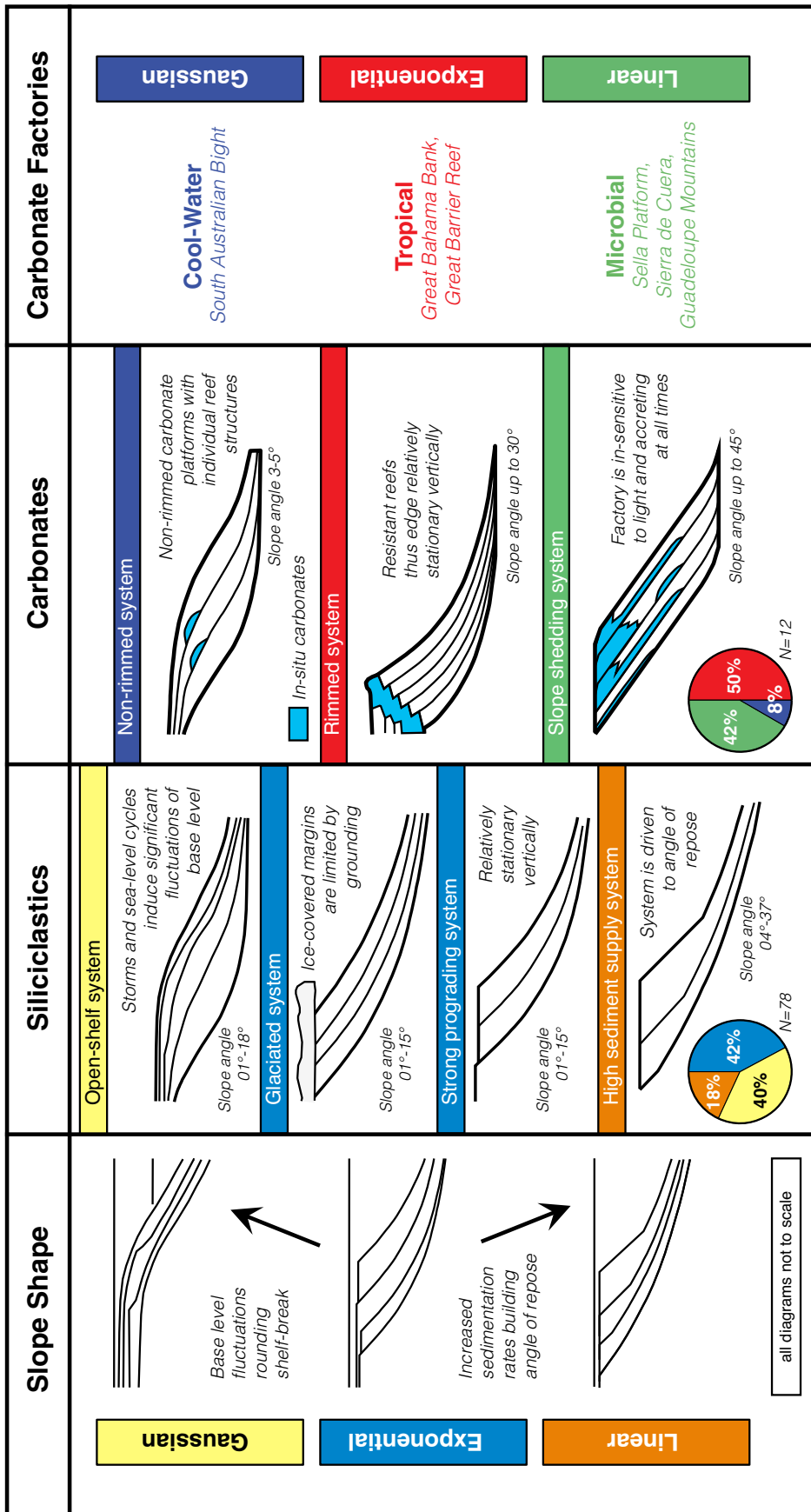
Fig. 23. Subdivision of siliciclastic and carbonate slope systems into three groups based on their slope profile: Linear, Exponential or Gaussian. Siliciclastic (left) and carbonate (right) sedimentary systems comprise all three types of shelf-break geometry and slope curvature developing within different sedimentary settings. Cartoons accompanied by a short description of the sedimentary systems and variation in slope angles. Pie diagrams show relative proportions of Gaussian, Exponential and Linear profiles within siliciclastic and carbonate systems. T-factories, C-factories and M-factories display different shelf-break to slope curvature systems. Modified from Adams & Kenter (2014).
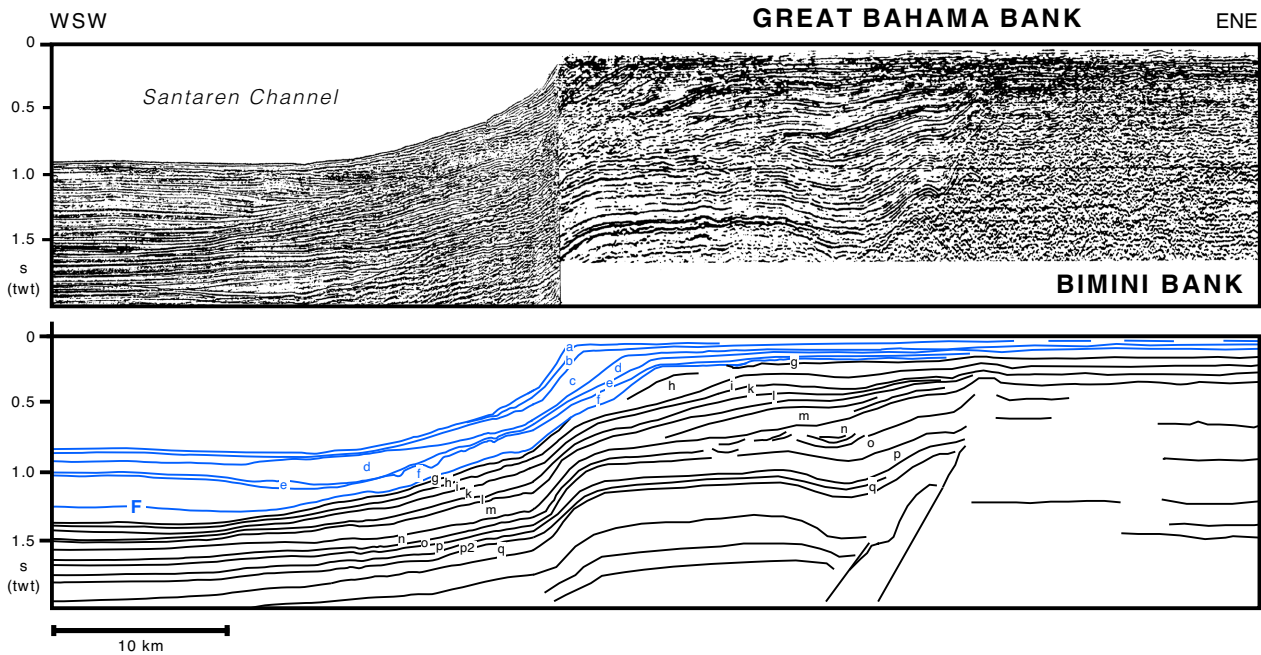
Fig. 24. Upper panel: composite seismic profile covering Santaren Channel (WSW) and Great Bahama Bank (ENE; Eberli *et al.*, 1997). Lower panel: interpretation seismic profile. Depositional sequences indicated by letters. Sequence boundary 'F' at the base of sequence 'f' marks the transition from a carbonate ramp (black lines) to the present-day flat-topped carbonate system (blue lines). Note the increase in thickness depositional sequences in the slope to basin transect during the flat-topped phase illustrating highstand shedding at work. Modified from Betzler *et al.* (1999).

The upper part of the T-factory slope may be stabilized by microbial processes (Reolid *et al.*, 2017) or early cementation processes (Grammer *et al.*, 1993, 1999). Similar processes were also observed at the platform margins of Tahiti (Séard *et al.*, 2011). These slopes commonly become over-steepened resulting in large-scale destabilization processes, with margin collapse and slope failures (Jo *et al.*, 2015; Principaud *et al.*, 2015; Schnyder *et al.*, 2016; Le Goff *et al.*, 2020). Other processes seen are the infill of primary cavities of a T-factory system by an M-factory system, microbialites in this case, resulting in a very stable combination of coralgal communities and two types of microbial systems (Séard *et al.*, 2011); the so-called 'reefal microbialites' that formed with a slight time delay within the coralgal communities in shallow-water environments, and the 'slope microbialites' that developed in deeper waters at a later time (Séard *et al.*, 2011).

CWC-factory slope declivities depend on the reef-building capacity of the corals. Coral mound belts display elongated morphologies with varying lengths but narrow widths (e.g.

Hebbeln *et al.*, 2019; Fig. 11F). The systems may reach very high angles of repose related to the coral rubble making up the slopes (e.g. Mienis *et al.*, 2006; Hebbeln *et al.*, 2019) and early stabilization by hard/firmgrounds and/or semi-lithified sands (de Haas *et al.*, 2009). Slope angles vary from 20°/30° to up to 80° (see De Mol *et al.*, 2002 for an extensive overview; de Haas *et al.*, 2009).

Slopes in C-factory systems have a Gaussian shape (Fig. 23; Adams & Kenter, 2014) as demonstrated for the slopes of the highstand and lowstand sedimentary wedges at the outer shelf edge of the South Australian Bight sedimentary system (Feary & James, 1998; Saxena & Betzler, 2003; James *et al.*, 2004). Saxena & Betzler (2003) discussed the development of these sedimentary wedges in response to sea-level fluctuations with extensive shelf margin wedges developing during sea-level highstands and reduced wedges deposited during sea-level lowstands (Fig. 19).

M-factory slopes tend to develop higher slope angles while microbial processes and rapid cementation processes stabilize the upper parts

of the slope (Keim & Schlager, 2001; Della Porta *et al.*, 2003; Playton *et al.*, 2010; van der Kooij *et al.*, 2010). These systems are very coarse-grained sedimentary slope systems with a linear shape (Figs 13, 16, 21 and 23; Adams & Kenter, 2014); as illustrated by clinoforms known from various carbonate platforms in the Dolomites (Bosellini, 1989; Kenter, 1990). For the Sella platform (Triassic, Italy), Keim & Schlager (2001) estimated the sediment composition for the margin to upper slope to consist of 68% automicrite, 22% pure detrital sediments and 10% strongly altered grains; the lower slope contained 63% detrital sediments, 10% automicrite and 27% extensively dolomitized grains (Fig. 21). For the slopes of the M-factory platform of the Carboniferous Sierra del Cuera, Della Porta *et al.* (2003) discussed similar percentages with boundstones varying from 99.5% on the upper slope to 10% at the lower slope, and breccias ranging from 0.4% at the upper slope to 80%; reaching even 92% during aggradation phases. Hence, these slope sediments are dominated by automicritic carbonate sand and rubble (Keim & Schlager, 2001) and the origin of the muds on these slopes differs from those in the T-factory while the microbial activity produces muds, but in a sand grain size (Della Porta *et al.*, 2003; Schlager & Reijmer, 2009). These coarse-grained slopes are able to maintain high slope angles of up to 35°; or even 45° within the upper slopes where microbial binding prevails. The M-factory slopes also tend to develop complex slope stacking patterns in which boundstone accretion, local instability and failure, and resulting slope breccia deposition dominate (Brandner & Keim, 2011; Playton & Kerans, 2018). Slope shedding *sensu* Kenter *et al.* (2005) prevails, with a deep-oligophotic production realm determining the development and progradation of these steep, debris-dominated slope systems (Keim & Schlager, 2001; Della Porta *et al.*, 2003; Kenter & Schlager, 2009). These systems operate independent of allocyclic, high-frequency changes in accommodation (Playton & Kerans, 2018). Variations in the sediment composition and stratal patterns occur during progradation and aggradation of M-factory platforms (Della Porta *et al.*, 2004), but also on a smaller scale with repeated shifts from debris to silt-dominated and grain-dominated deposits (Playton & Kerans, 2015a; Playton & Kerans, 2015b).

P-factory slopes link to sedimentary structures like contourite drifts and mass-transport deposits. They therefore depend on the overall sand grain-size and mud content of the deposits following slope stability rules related to these sediment characteristics (e.g. Kenter & Schlager, 1989; Kenter, 1990).

SEDIMENT EXPORT

The sediment export systems of the different factories vary significantly and depend on the sediment-production processes for each factory dependent and the factory-dependent morphology (Fig. 7; Table 3). The interaction of the morphology with changes in relative sea-level and associated changes in the marine and atmospheric environment determine the sediment production processes through time. Sediment production and export reflect the growth strategy of the carbonate secreting systems, and are reflected in the overall sediment spectrum, for example, carbonate mineralogy, variations in grain-sizes and cementation processes. Hence, the benthic carbonate factories exhibit factory-dependent sediment production and export modes.

T-factory

Significant fluctuations in sediment export characterize the T-factory and these systems reach their maximum production and export rates when large production areas are positioned in the photic zone (Droxler & Schlager, 1985; Schlager *et al.*, 1994). When these production realms are exposed, during sea-level lowstands, a severe reduction occurs in the amount and type of sediments that can be produced and exported to the surrounding slopes and basins. As highlighted before, this sharp contrast in sediment production and export is known as highstand shedding (Figs 7 and 15; Droxler & Schlager, 1985; Schlager *et al.*, 1994). The vast amount of sediments that can be exported by T-factories also stands out in seismic data with well-developed sediment wedges covering the slope and basin as known from Great Bahama Bank (Fig. 24; Eberli *et al.*, 1997; Betzler *et al.*, 1999).

Not only variations in the amount of sediments exist but also differentiation in the grain-size spectrum when comparing sediment deposition during sea-level lowstands and highstands. These systems demonstrate a predominance of sands during sea-level lowstands and muds during sea-level highstands (Rendle-Bühring &

Reijmer, 2005; Reijmer & Andresen, 2007). However, some variations do exist between the windward and leeward side of the platform with grain-size patterns slightly out of phase (Rendle-Bühring & Reijmer, 2005). Other windward–leeward variations in sediment export are shown by the progradation and aggradation patterns on Great Bahama Bank closing one of the intraplatform seaways (Eberli & Ginsburg, 1987, 1989). While T-factories export abundant sediment from shallow-water areas towards their surroundings, which may be up to 50 km as discussed for Pedro Bank (Caribbean) by Andresen *et al.* (2003) or even over 50 km (south-west Indian Ocean; Counts *et al.*, 2019; Jorry *et al.*, 2020), one could describe the overall sedimentation pattern as 'Spread' (Reijmer, 2016; Fig. 7).

CWC-factory

The CWC-factory is a sedimentary system that has the ability to construct several tens to hundreds of metres high sedimentary structures at varying water depths below the storm-wave base. These systems consist of a living coral framework producing coarse rubble, together with a large variety of other biota, but also act as a sediment baffler enabling fast mound/ridge accumulation (Fig. 11; Dorschel *et al.*, 2007; Huvenne *et al.*, 2009; Fink *et al.*, 2013). While frame-building corals forming mounds predominate in this system, the sediment production term 'Frame' is proposed for this factory (Reijmer, 2016). Sediment export is limited in this system and only affects the direct surroundings of the production sites (Fig. 7). These sedimentary systems may form large-scale clusters of mounds with various shapes and heights (Fig. 11; e.g. Mienis *et al.*, 2007; Fink *et al.*, 2013; Hebbeln *et al.*, 2019). Vertical mound accretion rates of 220 cm/kyr were reported from the giant coral mounds off Ireland (Frank *et al.*, 2009).

C-factory

The C-factory shows a different sediment distribution model in which waves and currents predominate, the so-called *shaved shelf* model (James *et al.*, 1994), with sediment deposition below wave base and enhanced sediment dispersal to deeper waters. The overall sedimentation pattern was labelled as 'Move' because changes in currents and waves control the position of the sediment depositional loci (Reijmer, 2016). The sedimentary response of the C-factory to sea-level changes resembles that observed in siliciclastic-dominated sedimentary systems (Figs 7 and 26). The infill of incised valleys by these sediments (Fig. 26; Wallace *et al.*, 2002; Mitchell *et al.*, 2007), and their occurrence within a tide-influenced incised valley (Miocene, Provence, France; James *et al.*, 2014) exemplify this type of 'siliciclastic' sediment behaviour. The deposition of sediment wedges at the outer shelf edge resulting from waves and currents transporting sediments produced in the shallow-water realm also demonstrate the 'Move' aspect of the entire sedimentary system (Saxena & Betzler, 2003). Other examples of a siliciclastic type of sediment behaviour are described for the Agua Amarga basin (south-east Spain; Fig. 22) where cool-water carbonates develop beach deposits, storm barriers and wash-over fans (Betzler *et al.*, 1997b; Villalobos & Braga, 2003).

M-factory

The M-factory, with its dominance of sediments of microbial origin, is a system with abundant early cementation (van der Kooij *et al.*, 2010) combined with a dominance of coarse-grained sediments, sands and large blocks (e.g. Kenter *et al.*, 2005; Schlager & Reijmer, 2009; Brandner & Keim, 2011; Della Porta *et al.*, 2014; Playton & Kerans, 2018). Hence, this factory has the possibility to build steep slopes while it produces coarse-grained sediments, but also displays a high sediment stabilization potential (Kenter, 1990; Adams & Kenter, 2014). The sediment production term 'Stick' relates to the dominance of microbial activity and associated diagenetic processes in this system resulting in a fairly continuous sediment production through time and lower sediment export towards the surrounding basins (Fig. 7; Reijmer, 2016). The fairly continuous production of sediments within the main sediment production site at the upper slope of the platform was named slope shedding (Fig. 14; Kenter *et al.*, 2005). The contrast between the sticky sediment production and the reduced sediment export is very well expressed in the Dolomites when comparing, for example, the massive Sella build-up and the limited number of debris flows and calciturbidites marking the basin deposits outcropping on the Passo Pordoi, the Gardena Pass (Bosellini & Neri, 1991; Brandner & Keim, 2011) and Stuores Wiesen (Preto, 2012). As discussed above, sediment export of the M-factory is a continuous flow of sediment grains irrespective of sea-level fluctuations. This

input process was highlighted by variations in sediment composition within a vast series of Late Triassic gravity-flow deposits (Northern Calcareous Alps, Austria; Reijmer *et al.*, 1991, 1994), where the individual sediment layers demonstrate the uninterrupted presence of grains derived from upper slope to platform margin realms. These include various micro-problematica (*Tubiphytes* sp., *Lithocodium* sp. and *Bacinella* sp.) and benthic foraminifera. Hence these gravity-flow deposits do not show drastic variations in sediment composition as known from T-factory gravity-flow deposits that relate to sea-level variations flooding and exposing the sediment production realms (e.g. Haak & Schlager, 1989; Reijmer *et al.*, 2012b, 2015).

P-factory

The P-factory demonstrates seasonal variations in sediment production, that is to say the abundance of shells and/or skeletons produced. The sediment production term 'Pulse' thus was assigned to this factory (Fig. 7). The variations in abundance depend on the oceanic realm, the availability of nutrients, the water temperatures and the chemistry of the ambient seawater (e.g. Hemleben *et al.*, 1989; Schiebel & Hemleben, 2005). Hence sediment export to a large extent equals sediment production, but actual sediment deposition then depends, at least for the aragonite and calcite skeletons, on the depth of the ocean where the skeletons are deposited. It must be mentioned that coccoliths and planktic foraminifera developed in the Mesozoic, and pteropods established themselves in the Cenozoic (e.g. Flügel, 2010).

DISCUSSION

Classifying carbonate systems into carbonate factories permits the characterization of sediment production and export of a wide variety of carbonate producers through geological history. This classification system addresses the entire system and not the individual sediment producer, and thus seizes variations in environmental factors implementing changes of the individual systems.

Occurrences

The separation between the systems is not as rigid as one tends to think since all factories obey the principle that certain environmental factors need to be in place before they can develop. The diverse set of environmental factors that control factory development/type may vary spatially and temporally within the benthic oceanic realm (Fig. 5). The Great Bahama Bank slopes are a good example of this, because they show a very diverse benthic T-factory dominating the shallow waters, while downslope the influence of the M-factory comes into play with microbes stabilizing the upper parts of the slope (Reolid *et al.*, 2017). Moving further downslope C-factory elements appear (Schlager, 2005, p. 24), and in the adjacent Santaren Channel, CWC-factory systems are present (e.g. Correa *et al.*, 2012).

A similar mix of factories was found on the slopes of Tahiti where the T-factory dominates in the shallow-water realm, but when moving downslope M-factory elements start to infill the pore space of the T-factory sedimentary system. This combination results in an interesting mix of factory elements in which the M-factory microbes tend to stabilize the steep slopes of the T-factory (Séard *et al.*, 2011). Other examples of oceanographic parameters directing the development of carbonate factories is discussed for the Galapagos Islands (Humphreys *et al.*, 2016, 2018; Reymond *et al.*, 2016), the coast of Mauritania (Michel *et al.*, 2011) and Gulf of Panama (Reijmer *et al.*, 2012a), and various other examples (for a partial overview see Westphal *et al.*, 2010). In these systems local upwelling introduces a C-factory comparable system in tropical regions.

Subdivisions

Michel *et al.* (2019) and Laugié *et al.* (2019) proposed an alternative subdivision of the T-factory and C-factory based on the evaluation of the major sea-surface oceanographic parameters directing the development of the neritic carbonate factories being temperature, salinity and primary productivity (Fig. 6). These authors distinguish: (i) a marine biochemical factory as encountered in the Arabian/Persian Gulf, a depositional system with very specific environmental locales, high temperatures and high salinity, in an extensive carbonate ramp setting. This carbonate factory is classified as part of the T-factory in the factory systems used in this manuscript. It needs to be noted that it is the only carbonate ramp system in the present-day oceans, which might be the reason why it differs

from other typical T-factories; (ii) a photozoan factory – this factory agrees with the classical T-factory system; (iii) the photo-C factory, and (iv) the heterozoan factory. The photo-C factory describes the warm-temperate carbonate system (Betzler *et al.*, 1997a) in which light is an important controlling factor as known from the Mediterranean Sea and the western Great Australian Bight. The heterozoan factory represents the classical C-factory as known from south Australia and the Atlantic coast of Europe. A further subdivision of the C-factory was made based on: (i) the energy source for metabolic activities enabling carbonate production; and (ii) the hydrodynamics and physiography of the depositional system governing sediment accumulation (Michel *et al.*, 2018). Michel *et al.* (2019) discussed that individual palaeogeographic settings and processes working at a local-to-global scale, for example, climate, currents, organic matter cycle, topography, eustasy, and tectonics steered the development of the individual carbonate depositional systems (Tucker & Wright, 1990; Markello *et al.*, 2008; James & Jones, 2015). Hence, the Michel *et al.* (2018, 2019) subdivision is a useful addition as it highlights possible diversifications within each factory depending on the dominance of location-specific environmental factors. Modelling experiments for the Cretaceous (Pohl *et al.*, 2019, 2020) using the aforementioned subdivision together with a coupled ocean-atmosphere general circulation model and palaeo-bathymetry estimates, which were partially based on literature data, produced detailed carbonate factory distribution maps at a global scale for this time period.

A further possible subdivision of the present-day C-factory sediments reflects the diversification in benthic communities depending on the latitudinal position (Table 4; e.g. Leonard *et al.*, 1981; Henrich *et al.*, 1992, 1995), combined with different sediment behaviour in response to sea-level fluctuations. Faunal diversity decreases towards the higher latitudes (Leonard *et al.*, 1981). Low-diversity benthic communities are known from the Vesterisbanken (south-western Greenland Basin, 73°30′N/9°10′W; Henrich *et al.*, 1992, 1995), between 130 m and 400 m water depth with small sponge–bryozoan–serpulid mounds and hedges, molluscs, echinoderms, abundant planktic and benthic foraminifera, as well as crinoids in the deepest locales. On the Ross Sea shelf (Antarctica) stylasterine hydrocorals, barnacles or

bryozoans occur (Frank *et al.*, 2014, 2020), together with less abundant molluscs, echinoids, planktic and benthic foraminifera, sponge spicules and diatoms. In the latter sedimentary system, polar carbonate production mostly occurred on the shelf not covered by marine sea ice during glacial periods of lowered sea-level (Frank *et al.*, 2014, 2020), and preferably in areas away from the zone where meltwater-derived mud plumes from the glacier entered the marine realm (James *et al.*, 2009; Frank *et al.*, 2020).

Permian cold-water systems from Australia (Fig. 25; Table 4; Rao, 1981; James *et al.*, 2009; Frank *et al.*, 2012), the Sverdrup Basin in Canada (e.g. Beauchamp & Desrochers, 1997; Beauchamp *et al.*, 2009) and the Pleistocene of Alaska (James *et al.*, 2009) all show the above highlighted, low-diversity benthic communities adapted to the harsh cold-water environmental conditions. All in all, the cold/polar carbonate systems differ from the cool-water factory system with their low-diversity carbonate sediment producers, and in their response to sea-level fluctuations and the ultimate morphology of the system, but they can be interpreted as an end-member of the cool-water factory (Fig. 25; Table 4).

In the production–depth profiles of carbonate factories (Figs 2 and 7), Schlager (2005) highlighted the M-factory carbonate production around methane seeps. However, it needs to be mentioned that C-factory elements also might be associated with those seep carbonates (e.g. Peckmann *et al.*, 2001, 2003; Goedert *et al.*, 2003; Liebetrau *et al.*, 2014).

Factories and sequence stratigraphy

The carbonate factory system aids in differentiating between the sequence stratigraphic response of marine benthic carbonate sedimentary systems to relative variations in sea-level. All systems will display a different response related to factory-inherent characteristics. While T-factories will produce sharply contrasting sedimentation patterns in response to relative sea-level fluctuations (Figs 7 and 14), M-factories may display fairly continuous sediment production and export (Figs 7 and 16), while C-factories are characterized by sediment, wave and current dominated sequence development (Figs 7 and 19). CWC-factories and P-factories will reflect a more oceanographically controlled response (Fig. 7).
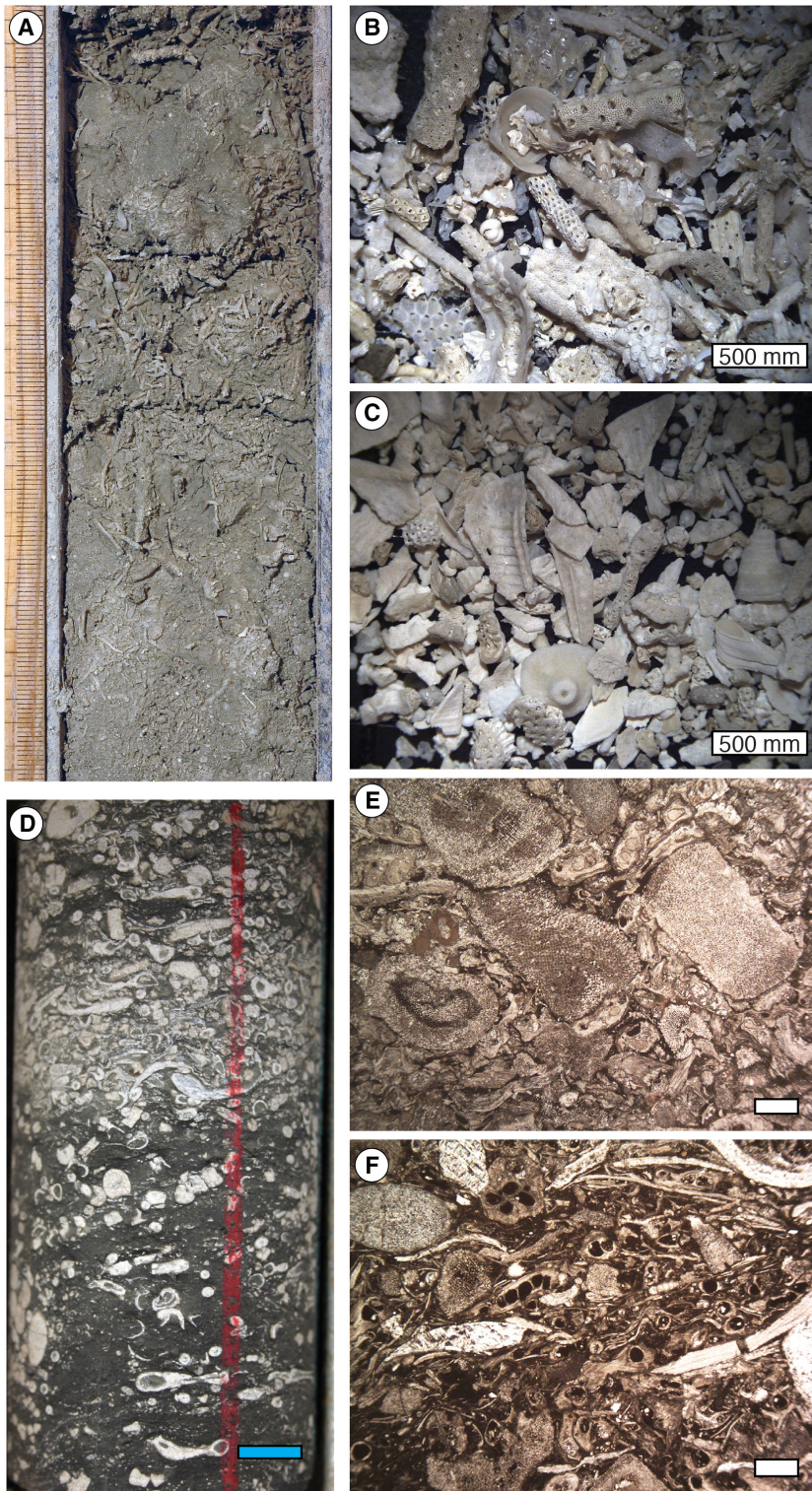
Fig. 25. Polar factory (C-factory subdivision, see Fig. 4 and *Discussion* for more details): Antarctica, Australia. (A) Northern Victoria Land shelf, Ross Sea Embayment, Antarctica: core photograph (Core ELT32-44) of bryozoan-rich facies with variations in bryozoan density on a 5 to 10 cm scale. Scale in millimetres (Frank *et al.*, 2014). (B) and (C) Photographs of skeletal separates (Frank *et al.*, 2020). (B) Fragmented minimally abraded bryozoan gravel. Piston core ELT32-44, 550 m water depth, northern Victoria Land shelf, 48 to 50 cm core depth interval. (C) Abraded barnacle gravel. Piston core ELT52-09, *ca* 500 m water depth on the western flank of Mawson Bank, 353 to 355 cm core depth. (D) Permian, Carnarvon Basin, Western Australia: core photograph of coarse crinoid-bryozoan grainstone in Gascoyne 1 well (Frank *et al.*, 2012). Scale bar = 1 cm. (E) and (F) Thin-section photomicrographs in plane polarized light. (Frank *et al.*, 2012). Scale bars = 500 µm. (E) Crinoid–bryozoan grainstone (Gascoyne 1 well). Grains are in stylo-contact. Phosphate and glauconite in intraparticle pore space. (F) Argillaceous packstone rich in crinoids, bryozoans and brachiopod debris (Burna 1 well). Photograph sources: Frank *et al.* (2012, 2014, 2020).

T-factory

T-factory systems are characterized by sediment volume partitioning during highstand and lowstand systems tracts, each sequence displaying individual sedimentation patterns and characteristics. Highstand systems tracts are associated with flooding of the usually extensive shallow-water realms with sufficient light penetration.

These highstand photic zone realms differ from the vastly reduced extent of the environments situated in the photic zone during sea-level lowstand systems tracts (Figs 7 and 8). These significant fluctuations in sediment production and changes in sediment storage opportunities, combined with the differences in types of sediments produced, result in large-scale variations of the locations at which sediment are deposited along the platform to basin transect (Fig. 24). It must be noted that at present the contrast between highstand and lowstand sedimentation patterns of T-factory carbonate platforms is highly diverged as the Earth is in an ice-age dominated time interval with exceptionally short-term, high magnitude sea-level fluctuations. Hence, general observations are discussed in the following paragraph that do apply at present, but a more varied picture of the effect of sea-level changes on T-factory systems, however, existed when going back in time.

Platform sedimentation depends on the amplitude of sea-level variation that may flood or expose the shallow-water realm of flat-topped carbonate platforms, for example the Bahamas or Great Barrier Reef, or may reflood large areas on carbonate ramps, such as the present-day Arabian/Persian Gulf. For flat-topped platforms certain fluctuations may not reach the edge of the platform and may not reflood the extensive shallow-water areas for extensive periods of time, as discussed for cores from the top of Great Bahama Bank by Kievman (1998). The sedimentary record on that platform exemplifies that a series of fluctuations in sea-level were represented by only one exposure surface (Kievman, 1998). Hence, the platform sequence will display a series of missed beats (Goldhammer et al., 1990; Drummond & Wilkinson, 1996). This carbonate factory expresses the direct link between the carbonate system platform morphology and the so-called reflooding window (Jorry et al., 2010) or production window (Paul et al., 2012) determining sediment production and export in T-factory systems (Figs 7, 9 and 24). The sediments exported are modulated on the slopes showing reversing grain-size trends and opposing grain-size sediment export patterns between leeward and windward sides, but no differences in the overall volumes (Fig. 17; Rendle-Bühring & Reijmer, 2005).

During highstand systems tracts, sediments can be stored on the platform top, with a complete infill of accommodation at the platform edge and partial infill of the shallow-water areas on the platform itself (Figs 8 to 10; e.g. Weij et al., 2019). Currents, waves and tides ultimately determine the sedimentation loci. The majority of the sediments, however, are exported to the slope and basin, by the process referred to as highstand shedding (Fig. 14; e.g. Droxler & Schlager, 1985; Reijmer et al., 1988; Schlager et al., 1994: Lantzsch et al., 2007; Webster et al., 2012; Betzler et al., 2014; Principaud et al., 2017; Jorry et al., 2020). Sediment wedges may develop on the platform slope (Wilber et al., 1990; Roth & Reijmer, 2004, 2005) and may be intensively reshaped by contour currents (Betzler et al., 2014; Fig. 24). At the same time drift deposits may develop at specific locations within the sedimentary basins (Rendle & Reijmer, 2002; Lüdmann et al., 2018a,b; Wunsch et al., 2018; Eberli & Betzler, 2019; Mulder et al., 2019; Paulat et al., 2019).

At present, the shoreline on the western side of Andros Island (Bahamas) is retreating landward (Rankey, 2002; Maloof & Grotzinger, 2012) while at the same time the western slope of Great Bahama Bank is prograding westward and steepening. Presently, it also contains thick Holocene sediment wedges at selected sites (Wilber et al., 1990; Roth & Reijmer, 2004, 2005). Hence, the development of highstand deposits may be highly variable across the entire T-factory sedimentation system, and the analysis of shoreline shifts (e.g. Catuneanu, 2020a) will not resolve the sequence stratigraphic development of the entire system in carbonate-dominated environments (Borgomano et al., 2020). In fact, the infill of accommodation space across flat-topped carbonate platforms will be less straightforward (Strasser, 2015) than assumed in many studies of fossil carbonate platforms (e.g. Goldhammer et al., 1990, 1991; Preto et al., 2001). Variations in unfilled accommodation characterize present-day flat-topped carbonate platforms (Reijmer et al., 2009; Swart et al., 2009; Harris et al., 2015; Purkis & Harris, 2016; Weij et al., 2019) introducing much uncertainty in the interpretation of the amplitude of sea-level changes related to these cycles. It needs to be mentioned that this pattern in part may be a function of the present-day icehouse setting with exceptional high magnitude, short-term sea-level fluctuations.

During the lowstand systems tracts, the major part of the shallow-water sediment production areas situated within the photic zone during sea-level highstands will be exposed (Fig. 14; e.g. Schlager et al., 1994). Erosion, dissolution

and cementation processes may dominate on top of the carbonate platform edifice, resulting in extensive karst and the formation of exposure surfaces. The systems tracts developing on the platform may be marked by a series of missed beats if the amplitude of subsequent sea-level change is too low to reflood the shallow-water platform as discussed for the Bahamas by Kievman (1998). At the same time a stack of low-stand wedges, dominated by production on the upper part of the carbonate platform slopes, will develop within the slope to basin environment (Betzler *et al.*, 2016). Winnowing by currents may reshape the deposits moving sediments to current protected areas.

The development of transgressive and falling stage systems tracts in T-factory systems depends on the interaction of the morphology of the depositional system, and the surface area available within the photic zone during these transitions (Jorry *et al.*, 2010; Paul *et al.*, 2012) and hence their extent may be limited. The transgressive and falling stage systems tracts may be marked by debris flows (Spence & Tucker, 1997; Reijmer *et al.*, 2012b, 2015). Oversteepening of the platform margin during high-stand systems tract and forced regressive systems tract may also be marked by mass-transport deposits (Jo *et al.*, 2015; Principaud *et al.*, 2015; Webster *et al.*, 2016; Wunsch *et al.*, 2017, 2018; Le Goff *et al.*, 2019), although these deposits at times can have a seismogenic origin (Floquet & Hennuy, 2003; Hennuy, 2003; Reijmer *et al.*, 2015; Puga-Bernabéu *et al.*, 2017).

CWC-factory
The sedimentary successions of cold-water coral systems usually display a succession of coral fragments embedded in a matrix of hemipelagic sediments alternating with intervals with reduced sedimentation or erosion (Fink *et al.,* 2013). Mounds at the south-west Rockall Trough (Fig. 11F) consist of a Holocene coral-dominated interval overlying lithified intervals lacking coral fragments containing coccoliths covered by calcite cements (van der Land *et al., 2010, 2014).

In general, mound growth and mound accumulation rates of this factory demonstrate pulsed growth associated with variations in the environmental setting that rely on changes in ocean circulation induced by climate variations (e.g. Kano *et al.,* 2007; Rüggeberg *et al.,* 2007; Eisele *et al.,* 2008; De Haas *et al.,* 2009; Mienis *et al.,* 2009a,b; van der Land *et al.,* 2013). Hence,

the sequence stratigraphic development of individual mounds and mound provinces exhibits stacked systems tracts linked to these pulses in mound growth (Fig. 7). Whether the fluctuations in accumulation rates are in concert with inter-glacial or glacial time intervals depends on global variations in ocean circulation. High productivity cycles may occur during the last glacial–interglacial transition (Fink *et al.,* 2013), the last glacial and succeeding deglaciation period (Wienberg *et al.,* 2018) or the last 11 000 years (van der Land *et al.,* 2014). According to Wienberg *et al.* (2018) vertical and/or lateral modifications of water masses moving the CWC-factory in and out of oxygen-depleted waters may control mound development. Other CWC-factories are controlled by variations in particle supply (e.g. Duineveld *et al.,* 2007), and even may shift in water depth, from shallow to deep, when moving in time from the Last Glacial Maximum at 11.5 ka BP to the present-day following changes in water density (de Mol *et al.,* 2011).

Transgressive and falling stage systems tracts within the CWC-factory system agree with the switch from one growth succession to the succeeding one (Fig. 7). It is the adaptation of the system to new oceanographic circumstances that will determine the possibilities of the CWC-factory to either: (i) continue its growth; or (ii) a transposition of the system to another water depth or location (e.g. Foubert *et al.,* 2008; Wienberg *et al.,* 2009; Fink et al., 2013); or (iii) a temporary stop in sediment production that will marked by a hardground (e.g. van der Land et al., 2010).

All in all, the sequence stratigraphic development of CWC-factory systems carry a strong environmental signal, for example, changes in global ocean circulation patterns and associated water-mass distribution, which both are linked, with a variable timewise response, to eustatic processes. At the same time the CWC-factory systems are less sensitive to variations in accommodation related to sea-level fluctuations.

C-factory
Nelson (1988) already stated that non-tropical shelf carbonates differ from their tropical counterparts in their structural, lithological, faunal, floral, mineralogical and diagenetic character. Betzler *et al.* (1997b) unequivocally demonstrated that the sequence stratigraphic concepts applied in T-factory systems cannot be used to evaluate the sedimentation patterns observed in

C-factory systems. The C-factory sedimentary systems, based on the types of sediments produced (for example, grains and mineralogy) and the lack of early cementation, tend to demonstrate a siliciclastic type of sediment behaviour (Figs 7, 19 and 22). On a mixed siliciclastic–cool-water carbonate shelf, this different behaviour might even result in a cyclic deposition of lowstand carbonates and highstand siliciclastics (Brachert *et al.,* 2003), which contrasts with T-factory sedimentation patterns (for example, highstand shedding; Schlager *et al.,* 1994).

The main contrast between transgressive and highstand and lowstand systems tracts in C-factory carbonate systems originates from currents and waves sweeping the shallow-water sediment production areas, remobilizing the sediments produced on the shelf (Figs 7 and 19). During highstand systems tracts waves and currents transport the major part of the sediments to the shelf-margin edge creating a shaved shelf (James, 1997) with shelf-margin wedges (Fig. 19; Saxena & Betzler, 2003; James & Bone, 2011, p. 207). This sediment transport process may result in a complex sediment volume partitioning across the shelf to basin transect. The thickness of the transgressive and highstand systems tracts is fairly constant across the slope (Fig. 19). They are coarse-grained and are dominated by metastable carbonate mineralogies (Saxena & Betzler, 2003). The lowstand systems tracts vary in thickness, are lens-shaped and become thinner towards the outer and upper slope (Saxena & Betzler, 2003). At the Eucla Shelf these deposits are fine-grained with high amounts of sponge spicules and micrite (Saxena & Betzler, 2003). The sediments along the Great Australian Bight comprise a mix of: (i) relict (*ca* 70 to 25 ka); (ii) stranded (18 to 10.4 ka); and (iii) Holocene (<10.4 ka) sediment particles (James & Bone, 2011, pp. 34–44) deposited at various depths along the shelf reflecting the interaction between biogenic sediment production, accommodation on the shelf and wave abrasion depth. In Bass Canyon (south-east Australia), one of the largest submarine canyon systems located within a cool-water carbonate environment (Mitchell et al., 2007), the C-factory dominated system displays variations in sedimentation rates across the slope and within the canyon. These rates are the highest during regressive systems tracts (slope: 82 to 100 mm/ka; canyon: 26 mm/ka) when sediments are removed from the shelf. They are moderate during the highstand systems tracts (33 to 58 mm/ka) as waves and currents

transport the sediments to the shelf edge forming extensive shelf wedges (Saxena & Betzler, 2003). During the lowstand and transgressive systems tracts they are the lowest (slope: 6 to 14 mm/ka; canyon: 8 to 10 mm/ka). The high sediment transport capacity in response to waves, current and lowering of wave base is also shown by the infill of incised valleys by C-factory sediments during transgression and highstands in sea-level (Fig. 26; Wallace *et al.,* 2002). The aforementioned sedimentation patterns clearly resemble those known from siliciclastic sedimentary systems (e.g. Carvajal & Steel, 2009).

Pedley & Grasso (2002) discussed that the systems tracts development along cool-water carbonate ramps differs from those observed for T-factory and open-ocean C-factory sedimentary systems. The sedimentation realm of the Mediterranean Pleistocene is characterized by a ramp-type coastal morphology, a shallow fair-weather wave base combined with the absence of strong bottom currents. This configuration resulted in the deposition of C-factory sediments on the ramp slope during the transgressive and highstand systems tract. During the falling stage systems tract, the sediments produced wedges at the shelf edge, while during the lowstand systems tract break-of-slope fans developed.

In summary, the individual systems tracts of C-factory sedimentary systems are marked by sediment volume partitioning depending on the water depth, morphology and topography of the basin, as well as the hydraulic regime (e.g. Gläser & Betzler, 2002). In general, the sedimentation patterns on the shelf and at the shelf margin within C-factory dominated sedimentation systems will depend on the width of the shelf, the C-factory biogenic production rates in combination with the amplitude of eustatic sea-level variations, and the associated variations in the wave abrasion depth. This pattern is similar to what has been observed and modelled for siliciclastic shelves (e.g. Zhang *et al.,* 2017, 2019), where sedimentation on shelves depends on the width of the shelf, and variations in accommodation and sediment supply. Hence, the sequence stratigraphic architecture of C-factory systems demonstrates great similarities to those proposed for siliciclastic shelves and deep-water systems.

M-factory
Microbially induced precipitation plus cementation not only stabilizes the steep margin and
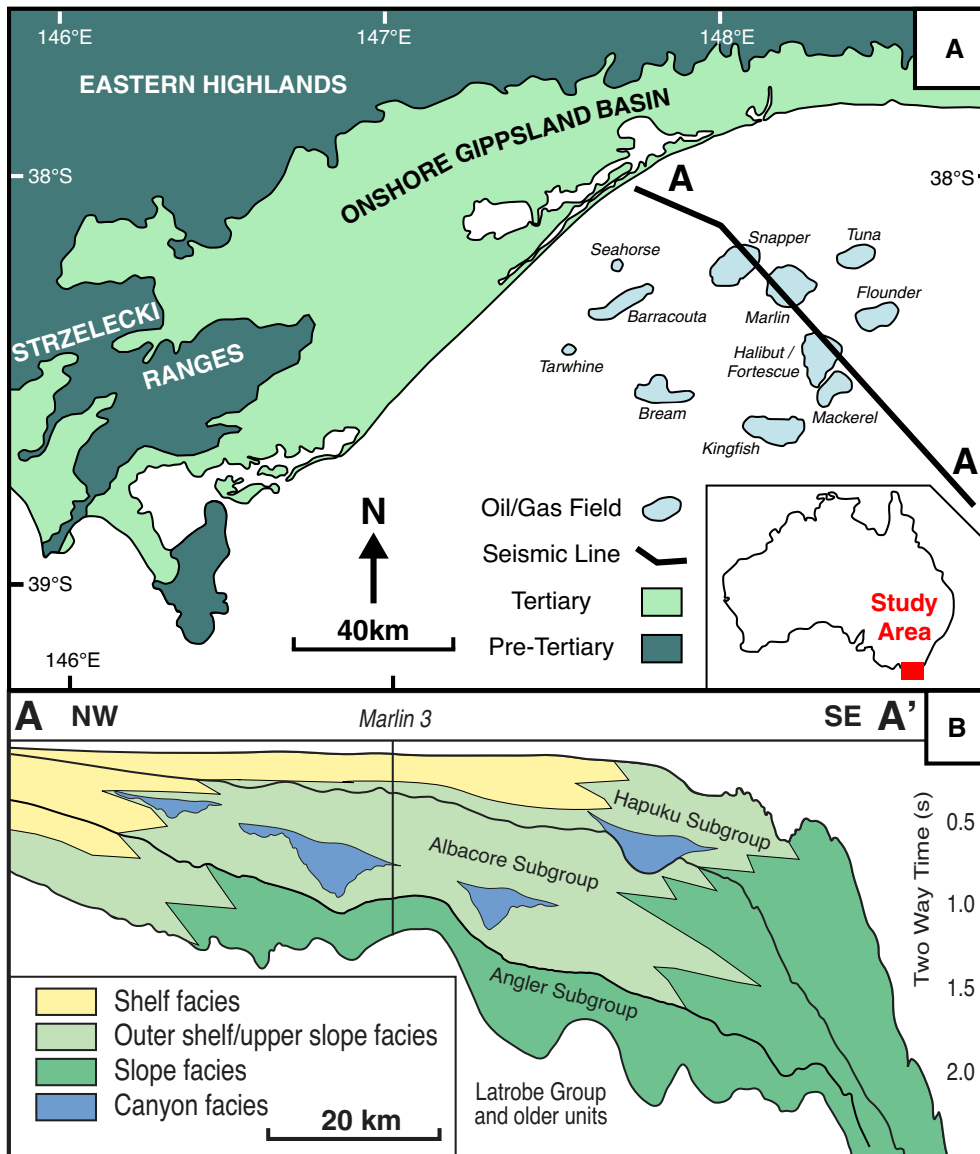
Fig. 26. (A) Gippsland Basin map with location of seismic profile shown in (B), and major oil and gas fields. (B) Interpreted seismic profile through the shelf, that can be subdivided into the shelf, outer shelf/upper slope, and slope facies of the Angler, Albacore and Hapuku subgroups forming the Seaspray Group. Canyon facies (in blue) mark incised valleys infilled by C-factory sediments demonstrating the siliciclastic-type behaviour of these sediments. Modified from Wallace *et al.* (2002).

upper slope but also produces surplus sediment that forms clinoforms in the middle to lower slope (Fig. 21; e.g. Biddle, 1981; Flügel, 1982, 2002; Bosellini, 1984; Brandner *et al.,* 1991; Keim & Schlager, 1999, 2001; Emmerich *et al.,* 2005a,b). These processes producing steep-sided carbonate platforms are known from the Devonian (Fig. 13; Playford, 1980; Playford *et al.* 1989; Playton & Kerans, 2015a,b), Carboniferous (Bahamonde *et al.,* 2000, 2004; Della Porta *et al.,* 2002, 2003; Collins *et al.,* 2014), Permian

(Beauchamp & Desrochers, 1997; Blendinger *et al.,* 1997; Beauchamp *et al.,* 2014; Playton & Kerans, 2018), Triassic (Bosellini & Rossi, 1974; Gaetani *et al.,* 1981; Kenter, 1990; Harris, 1993, 1994; Blendinger, 1994; Stefani *et al.,* 2010) and Jurassic (Crevello, 1990; Kenter & Campbell, 1991; Blomeier & Reijmer, 2002; Verwer *et al.,* 2009; Merino-Tomé *et al.,* 2012; Della Porta *et al.,* 2014).

The clinoforms of prograding systems display a complex stacking pattern of small-scale slope

breccia lobes forming at the toe-of-slope. These lobes gradually backfill upslope and by doing so produce a topography on which the upper slope boundstone, the automicrite-cement facies, can prograde (Playton & Kerans, 2018). Similar breccia lobes were also found infilling platform margin collapse features in Triassic (Gaetani *et al.,* 1981; Emmerich, 2001; Emmerich *et al.,* 2005a, b) and Jurassic (Scheibner & Reijmer, 1999) upper slope environments.

Aggradation, progradation and retrogradation of M-factory platforms depends on the productivity of the upper slope automicrite-cement facies and the sediment volume needed to be infilled along the margin to lower slope transect (Bosellini, 1984; Reijmer, 1998; Maurer, 2000). The sediment production process is more or less decoupled from variations in accommodation enabling sediment deposition on the platform top (Harris, 1993, 1994; Emmerich, 2004; Playton & Kerans, 2018).

The Triassic Rosengarten platform of the northern Dolomites is one of the most spectacular examples illustrating the interplay between sediment production and subsidence of an M-factory platform system (Fig. 16). This M-factory platform system showed an aggradation rate of 200 m/Ma (Maurer, 2000) or 780 to 850 m/Ma as proposed by the modelling experiments of Emmerich *et al.* (2005b). The progradation rate may be up to 2700 m/Ma (Maurer, 2000). The latter evidences the high sediment production potential of M-factory sedimentary systems during times with low subsidence rates. Other platforms in the Dolomites like the Latemar or Sella displayed different aggradation/progradation rates in response to their individual subsidence histories (e.g. Keim & Schlager, 2001; Emmerich *et al.,* 2005b). Platform margin destabilization was observed at the Latemar (Emmerich, 2001) and the Cipit boulders (Biddle, 1981) found at the toe-of-slope of the Sella platform document platform margin oversteepening and redeposition processes (e.g. Brandner *et al.,* 1991; Russo *et al.,* 1997). Sediment composition of the toe-of-slope sediments likewise varied depending on the progradation or retrogradation status of the platform (Reijmer, 1998). The slope progradation rates of 400 to 1000 m/Ma, and accumulation rates of up to 605 + 35 m/Myr, of the Carboniferous Sierra de Cuera M-factory platform fall in a similar range to those proposed for the aforementioned Triassic platforms (Della Porta *et al.,* 2003, 2004). At the Sierra de Cuera carbonate platform, aggradation and

progradation were also controlled by microbial boundstone growth, associated with local oversteepening, destabilization and failure resulting in slope breccia deposition (Bahamonde *et al.,* 1997, 2000, 2004; Della Porta *et al.,* 2003, 2004). A similar depositional process was discussed for the Permian foreslope architectures of the Capitan Formation (Playton & Kerans, 2018) that were marked by boundstone accretion combined with local slope instability and failure, and resultant slope breccia deposition. Progradation in these systems was not determined by sea-level fluctuations (Playton & Kerans, 2018), but was mainly governed by autogenic processes related to the deep oligophotic microbial margins that functioned fairly autonomous of allocyclic, high-frequency accommodation changes. Hence, changes in shallow-water accommodation did not link to progradation, aggradation and retrogradation patterns of the M-factory flat-topped platform itself while slope shedding (Kenter *et al.,* 2005) is a continuous process. At the M-factory flat-topped carbonate platform of the Sierra de Cuera, Spain (Fig. 13B; Della Porta et al., 2003; van der Kooij et al., 2010), however, a rapid rise in sea-level and associated sharp increase in accommodation, resulted in the deposition of red-stained micrite layers. These layers marked changes in oceanographic and environmental parameters associated with the transgressive systems tracts.

The sedimentation patterns described above stress the need for a careful evaluation of sediment production and export patterns active in M-factory sedimentary systems when assessing the response of these systems to eustatic sea-level changes. This approach contrasts sharply with the interpretation of deep-water settings near active M-factory platforms like the Sella (Dolomites, Italy) as detailed in Catuneanu (2020) in which the T-factory highstand shedding model is used as a sediment production and export mechanism. This approach ignores the large-scale and small-scale sediment production differences of T-factory and M-factory systems (see Fig. 14), and thus leads to erroneous sequence stratigraphic interpretations.

P-factory

Sequence stratigraphy in full pelagic realms greatly depends on interpreting the variations in biological sediment production within the water column. A wide series of geochemical proxies have been used to assess the skeletal compositional variations of the planktic biota and

demonstrated the strong link between oceanographic changes and climate variations in the (sub-)Milankovitch frequency bands. A plethora of publications have discussed these ties for numerous geological time intervals; see for example various scientific expedition proceedings of the Ocean Drilling Program, International Ocean Drilling Program and Integrated Ocean Drilling Program (http://www-odp.tamu.edu/publications). The planktic depositional record also documented large-scale tectonic processes, such as: (i) the closure of the Central American Seaway (e.g. Haug & Tiedemann, 1998; Reijmer *et al.,* 2002) and the south-east Asian gateway (e.g. Holbourn *et al.*, 2011); and (ii) the expression of the Campanian inversion in the North Sea Basin affecting the North Sea Chalk system (e.g. van Buchem *et al.,* 2018).

SUMMARY SEQUENCE STRATIGRAPHY IN CARBONATE FACTORY SYSTEMS

To summarize, the sequence stratigraphic patterns found for the M-factory differ significantly from those of the C-factories and T-factories displaying a strong slope shedding pattern (Kenter *et al.,* 2005) instead of the highstand shedding configuration of T-factories (Figs 14 and 24; Droxler & Schlager, 1985; Schlager *et al.,* 1994) and the siliciclastic operational mode of C-factories (Figs 7, 19, 22 and 26). Hence, the sequence stratigraphic interpretation of carbonate systems first needs a careful evaluation of the biota involved independent of the assessment of the stratal stacking patterns, bounding surfaces and shoreline trajectories because they will be different for each carbonate factory. The variations of the individual carbonate factories in response to tectonic and climate related variations will lead to variations in sedimentation patterns and sequence development of the individual systems. Hence, modelling of the individual systems combined with detailed seismic, core, log and outcrop analysis will be the way to assess the variations in the controlling mechanism for the individual depositional systems, as illustrated in many studies (e.g. Bosence *et al.,* 1994; Warrlich *et al.,* 2002, 2005; Cuevas Castell *et al.,* 2007; Burgess & Prince, 2015; Busson *et al.,* 2019 and Borgomano *et al.,* 2020). This approach contrasts with the sequence stratigraphic workflow proposed by Catuneanu (2020a,b), who stated that methodology and

modelling should be separated while uncalibrated modelling could demonstrate any scenario. However, a carbonate-factory dependent modelling approach can highlight the impact of variations in sediment supply versus accommodation while for carbonate factory systems variations in sediment production and export in response to eustatic sea-level variations and tectonic processes are factory-dependent. Therefore, the sediment supply – accommodation approach discussed in a vast series of studies (e.g. Catuneanu, 2006, 2019; Catuneanu *et al.,* 2011; Catuneanu & Zecchin, 2013) mainly addressed siliciclastic-dominated or mixed sedimentary systems but overlooked carbonate-factory dependent variations by approaching carbonates almost exclusively as a T-factory operating system characterized by highstand shedding (e.g. Catuneanu, 2020a,b).

The importance of determining the type of carbonate factory when interpreting depositional patterns in seismic-scale outcrops and seismic profiles, was for example extensively discussed for: (i) the Carboniferous–Permian Sverdrup Basin with a M-factory to T-factory transition (e.g. Beauchamp & Desrochers, 1997; Beauchamp *et al.,* 2014); (ii) the Miocene in south-east Spain with C-factory to T-factory change-over (Fig. 22; e.g. Franseen *et al.,* 1997; Braga *et al.,* 2006; Kleipool *et al.*, 2017); and (iii) the Miocene Carnarvon Basin (Australia) with co-existing C-factory and T-factory systems (e.g. Anell & Wallace, 2020). In the aforementioned studies, sediment production and distribution, and slope profiles differed because of variations in the operating carbonate factory, stressing the significance of a factory-dependent approach to carbonate sedimentary systems in sequence stratigraphy.

CONCLUSIONS

The use of the carbonate factory classification system for benthic marine carbonates as defined in the literature relates to the mode of carbonate precipitation. In addition, this classification system links to a broad set of associated aspects: (i) sediment production variations; (ii) grain-size spectrum and mineralogy of the sediments produced; (iii) sediment export patterns; (iv) platform morphology; (v) platform margin type; (vi) slope angle and associated sediment composition; and (vii) sequence stratigraphic development.

Present tropical systems (T-factory) occupy the photic zone in shallow waters between 30°N and 30°S. At present, these systems build flat-topped rimmed platforms, atolls, fringing reefs or carbonate ramp systems. The T-factory tends to export vast amounts of sediments during highstands in sea-level when the platform top is flooded. These sediments usually are aragonite-rich, mud-dominated, and can be transported over large distances. In contrast, during sea-level lowstands, sediment production is sharply reduced, and sediment export is fairly coarse-grained with a mineralogy relative rich in high-magnesium calcite (HMC) and low-magnesium calcite (LMC). This sediment export pattern is called highstand shedding. Sediment can be exported over long distances; to over 50 km. The rimmed flat-topped T-factory systems have exponential slopes, and contour currents at times reorganize the sediments deposited on the slopes. The most well-known carbonate ramp today is the Arabian/Persian Gulf, which is a T-factory or biogeochemical factory.

The cold-water-coral factory (CWC-factory) occupies a vast deep-water realm throughout the world's oceans. This factory builds large mounds, either single entities or numerous mounds covering large provinces along the shelf. The CWC-factory shows episodic growth in response to changes in hydrodynamic settings or productivity changes linked to variations in nutrient input, which both correlate with sea-level fluctuations. The CWC-factory builds sturdy frameworks that are aragonite and LMC dominated. The framework building capacity of the cold-water corals together with the limited export capacity produces location-bound systems.

The cool-water factory (C-factory) has an operational system comparable to siliciclastic systems with an open shelf subjected to wave and current action removing the majority of the sediments. Sediments in this shaved shelf system are dominated by LMC components, but aragonite is also present, which, however, upon burial is quickly dissolved because of undersaturated waters. Sea-level changes impact the system as known from siliciclastic systems with the removal of sediments from the shelf and their deposition at the shelf edge during the transition towards a lowstand in sea-level. As a result, the system displays thick and well-defined lowstand successions and thinner more widespread highstand successions, comparable to a siliciclastic-type lowstand shedding system.

C-factory slopes usually have a sigmoidal shape.

With steady sediment production on the platform margin to upper slopes, the microbial factory (M-factory) possesses a different sediment production profile compared with the other factories. The microbial character of the system not only stabilizes the slopes but also results in the production of coarse-grained sediments that are able to maintain linear shaped slopes with steeper angles than known from the other factories. The M-factory may consist of single mounds, but also may form flat-topped carbonate platforms with a basin inclined platform edge. Sediment production and export is fairly continuous, while the main production area occupies the upper slope and can adapt to sea-level changes, and hence is called slope shedding. The mineralogy of the system is HMC dominated and fairly coarse-grained.

The planktic factory (P-factory) represents the steady background sediment input within the marine realm marked by seasonal variations. Present-day input depends on planktic foraminifera and coccoliths, which both first evolved in the Mesozoic, as well as pteropods from the Cenozoic, together with radiolarians and diatoms. The geochemical signals in the skeletons provide ample information on past, present and future climate variations.

Applying the carbonate factory classification scheme not only assigns the operational mode of the system, but at the same time describes a vast set of sedimentological parameters that determine the variability of the individual system in its response to short-term and long-term environmental changes, from temperature variations in seawater to sea-level changes, and to tectonic processes. Bearing in mind which factory one is dealing with helps in understanding the great variety of associated features that can be observed in outcrop, seismic and logs. It also will help to understand the possible variations in petrophysical, geochemical and diagenetic characteristics and modifications.

ACKNOWLEDGEMENTS

REFERENCES

Adams, E.W. and Kenter, J.A.M. (2014) So different, yet so similar: comparing and contrasting siliciclastic and carbonate slopes. In: *Deposits, Architecture and Controls of Carbonate Margin, Slope and Basinal Settings* (Eds Verwer, K., Playton, T.E. and Harris, P.M.), *SEPM Special Publication*, **105**, pp. 14–25.SEPM (Society for Sedimentary Geology). Tulsa, Oklahoma, USA.

Aitken, S.A., Collom, C.J., Henderson, C.M. and Johnston, P.A. (2002) Stratigraphy, paleoecology, and origin of Lower Devonian (Emsian) carbonate mud buildups, Hamar Laghdad, eastern Anti-Atlas, Morocco, Africa. *Bull. Can. Pet. Geol.*, **50**, 217–243.

Amado-Filho, G.M., Moura, R.L., Bastos, A.C., Salgado, L.T., Sumida, P.Y., Guth, A.Z., Francini-Filho, R.B., Pereira-Filho, G.H., Abrantes, D.P., Brasileiro, P.S., Bahia, R.G., Lea, R.N., Kaufman, L., Kleypas, J.A., Farina, M. and Thompson, F.L. (2012) Rhodolith beds are major CaCO3 bio-factories in the tropical South West Atlantic. *PLoS One*, **7**, e35171.

Anastas, A.S., Dalrymple, R.W., James, N.P. and Nelson, C.S. (1997) Cross-stratified calcarenites from New Zealand: subaqueous dunes in a cool-water, Oligo-Miocene seaway. *Sedimentology*, **44**, 869–891.

Andresen, N., Reijmer, J.J.G. and Droxler, A.W. (2003) Timing and distribution of calciturbidites around a deeply submerged carbonate platform in a seismically active setting (Pedro Bank, Northern Nicaragua Rise, Caribbean Sea). *Int. J. Earth Sci. Geol. Rundschau*, **92**, 573–592.

Anell, I. and Wallace, M.W. (2020) A fine balance: accommodation dominated control of contemporaneous cool-carbonate shelf-edge clinoforms and tropical reef-margin trajectories, North Carnarvon Basin, Northwestern Australia. *Sedimentology*, **67**, 96–117.

Atkinson, M.J., Carlson, B. and Crow, G.L. (1995) Coral growth in high-nutrient, low-ph seawater: a case study of corals cultured at Waikiki Aquarium, Honolulu. *Hawaii. Coral Reefs*, **14**, 215–223.

Bádenas, B., Aurell, M. and Bosence, D. (2010) Continuity and facies heterogeneities of shallow carbonate ramp cycles (Sinemurian, Lower Jurassic, North-east Spain). *Sedimentology*, **57**, 1021–1048.

Bahamonde, J.R., Colmenero, J.R. and Vera, C. (1997) Growth and demise of Late Carboniferous carbonate platforms in the eastern Cantabrian Zone, Asturias, northwestern Spain. *Sed. Geol.*, **110**, 99–122.

Bahamonde, J.R., Kenter, J.A.M., Della Porta, G., Keim, L., Immenhauser, A. and Reijmer, J.J.G. (2004) Lithofacies and depositional processes on a high, steep-margined Carboniferous (Bashkirian-Moscovian) carbonate platform slope, Sierra del Cuera, NW Spain. *Sed. Geol.*, **166**, 145–156.

Bahamonde, J.R., Vera, C. and Colmenero, J.R. (2000) A steep-fronted Carboniferous carbonate platform: clinoformal geometry and lithofacies (Picos de Europa, NW Spain). *Sedimentology*, **47**, 645–664.

Bassant, P., Van Buchem, F.S.P., Strasser, A. and Görür, N. (2005) The stratigraphic architecture and evolution of the Burdigalian carbonate–siliciclastic sedimentary systems of the Mut Basin, Turkey. *Sed. Geol.*, **173**, 187–232.

Bathurst, R.G.C. (1971) *Carbonate Sediments and their Diagenesis.* Elsevier, Amsterdam, 439 pp.

Bauch, T., Reijmer, J.J.G., McNeill, D.F. and Schäfer, P. (2011) Development of a Pliocene mixed-carbonate / lhword> siliciclastic reef (Limon, Costa Rica). *Sed. Geol.*, **239**, 37–47.

Beaman, R.J., Bridge, T.C.L., Lüter, C., Reitner, J. and Wörheide, G. (2016) Spatial patterns in the distribution of benthic assemblages across a large depth gradient in the Coral Sea, Australia. *Mar. Biodivers.*, **46**, 795–808.

Beauchamp, B. and Desrochers, A. (1997) Permian warm- to very cold-water carbonates and cherts in Northwest Pangea. In: *Cool-Water Carbonates* (Eds James, N.P. and Clarke, J.A.D.), *SEPM Special Publication*, **56**, pp. 327–348. SEPM (Society for Sedimentary Geology). Tulsa, Oklahoma, USA.

Beauchamp, B., Henderson, C.M., Grasby, S.E., Gates, L.T., Beatty, T.W., Utting, J. and James, N.P. (2009) Late permian sedimentation in the Sverdrup Basin, Canadian Arctic: the lindström and black stripe formations. *Bull. Can. Pet. Geol.*, **57**, 167–191.

Beauchamp, B., Shultz, C.V. and Anderson, K.D. (2014) Warm- vs. cool-water carbonate factories and adjacent slopes: Pennsylvanian-Early Permian Sverdrup Basin, Arctic Canada. In: *Deposits, Architecture, and Controls of Carbonate Margin, Slope and Basinal Settings* (Eds Verwer, K., Playton, T.E. and Harris, P.M.), *SEPM Special Publication*, **105**, 114–141.

Berger, A. (1989) The spectral characteristics of Pre-Quaternary climate records, an example of the relationship between astronomical theory and geosciences. In: *Climate*

and Geo-Sciences, a Challenge for Sciences and Society in the 21st Century (Eds Berger, A., Schneider, S. and Duplessy, J.C.), pp. 47–76.Kluwer Academic Publishers, Dordrecht, The Netherlands.

Berger, W.H. (1978) Deep-sea carbonate: pteropod distribution and the aragonite compensation depth. *Deep Sea Research*, **25**, 447–452.

Betzler, C., **Brachert, T.C.** and **Nebelsick, J.** (1997a) The warm temperate carbonate province: a review of the facies, zonations, and delimitations. *Cour. Forsch.-Inst. Senckenberg*, **201**, 83–99.

Betzler, C., **Brachert, T.C.**, **Braga, J.C.** and **Martin, J.M.** (1997b) Nearshore, temperate, carbonate depositional systems (lower Tortonian, Agua Amarga Basin, southern Spain): implications for carbonate sequence stratigraphy. *Sed. Geol.*, **113**, 27–53.

Betzler, C., **Eberli, G.**, **Alvarez Zarikian, C.**, **Alons-Goarcía, M.**, **Bialik, O.**, **Blättler, C.**, **Guo, J.**, **Haffen, S.**, **Horozal, S.**, **Inoue, M.**, **Jovane, L.**, **Kroon, D.**, **Lanci, L.**, **Laya, J.**, **Ling Hui Mee, A.**, **Lüdmann, T.**, **Nakakuni, M.**, **Nath, B.**, **Niino, K.**, **Petruny, L.**, **Pratiwi, S.**, **Reijmer, J.**, **Reolid, J.**, **Slagle, A.**, **Sloss, C.**, **Su, X.**, **Swart, P.**, **Wright, J.**, **Yao, Z.** and **Young, Z.** (2017) Expedition 359 summary. In: *Proceedings of the International Ocean Discovery Program* (Eds Betzler, C., Eberli, G. and Alvarez-Zarikian, C. and the Expedition 359 Scientists), **359**. International Ocean Discovery Program, College Station, TX.

Betzler, C., **Eberli, G.P.**, **Lüdmann, T.**, **Reolid, J.**, **Kroon, D.**, **Reijmer, J.J.G.**, **Swart, P.K.**, **Wright, J.**, **Young, J.R.**, **Alvarez-Zarikian, C.**, **Alonso-García, M.**, **Bialik, O.M.**, **Blättler, C.L.**, **Guo, J.A.**, **Haffen, S.**, **Horozal, S.**, **Inoue, M.**, **Jovane, L.**, **Lanci, L.**, **Laya, J.C.**, **Hui Mee, A.L.**, **Nakakuni, M.**, **Nath, B.N.**, **Niino, K.**, **Petruny, L.M.**, **Pratiwi, S.D.**, **Slagle, A.L.**, **Sloss, C.R.**, **Su, X.** and **Yao, Z.** (2018) Refinement of Miocene sea level and monsoon events from the sedimentary archive of the Maldives (Indian Ocean). *Progress in Earth and Planetary Science*, **5**, 5.

Betzler, C., **Furstenau, J.**, **Lüdmann, T.**, **Hubscher, C.**, **Lindhorst, S.**, **Paul, A.**, **Reijmer, J.J.G.** and **Droxler, A.W.** (2013) Sea-level and ocean-current control on carbonate-platform growth, Maldives, Indian Ocean. *Basin Res.*, **25**, 172–196.

Betzler, C., **Hübscher, C.**, **Lindhorst, S.**, **Lüdmann, T.**, **Reijmer, J.J.G.** and **Braga, J.-C.** (2016) Lowstand wedges in carbonate platform slopes (Quaternary, Maldives, Indian Ocean). *Depos. Rec.*, **2**, 196–207.

Betzler, C., **Lindhorst, S.**, **Eberli, G.P.**, **Lüdmann, T.**, **Möbius, J.R.**, **Ludwig, J.**, **Schutter, I.**, **Wunsch, M.**, **Reijmer, J.J.G.** and **Hübscher, C.** (2014) Periplatform drift: the combined result of contour current and off-bank transport along carbonate platforms. *Geology*, **42**, 871–874.

Betzler, C., **Reijmer, J.J.G.**, **Bernet, K.**, **Eberli, G.P.** and **Anselmetti, F.S.** (1999) Sedimentary patterns and geometries of the Bahamian outer carbonate ramp (Miocene-Lower Pliocene, Great Bahama Bank). *Sedimentology*, **46**, 1127–1144.

Biddle, K.T. (1981) The basinal Cipit boulders: indicators of Middle to Upper Triassic buildup margins, Dolomite Alps, Italy. *Riv. Ital. Paleontol. Stratigr.*, **86**, 779–794.

Blanchon, P., **Granados-Corea, M.**, **Abbey, E.**, **Braga, J.C.**, **Braithwaite, C.**, **Kennedy, D.M.**, **Spencer, T.**, **Webster, J.M.** and **Woodroffe, C.D.** (2014) Postglacial fringing-reef to barrier-reef conversion on Tahiti links Darwin's reef types. *Sci. Rep.*, **4**, 4997.

Blendinger, W. (1994) The carbonate factory of Middle Triassic buildups in the Dolomites, Italy: a quantitative analysis. *Sedimentology*, **41**, 1147–1160.

Blendinger, W., **Bowlin, B.**, **Zijp, F.r.**, **Darke, G.** and **Ekroll, M.** (1997) Carbonate buildup flank deposits: an example from the Permian (Barents Sea, northern Norway) challenges classical facies models. *Sed. Geol.*, **112**, 89–103.

Blomeier, D.P.G. and **Reijmer, J.J.G.** (2002) Facies architecture of an Early Jurassic carbonate platform slope (Jbel Bou Dahar, High Atlas, Morocco). *J. Sed. Res.*, **72**, 463–476.

Bontognali, T.R.R., **Vasconcelos, C.**, **Warthmann, R.J.**, **Bernasconi, S.M.**, **Dupraz, C.**, **Strohmenger, C.J.** and **McKenzie, J.A.** (2010) Dolomite formation within microbial mats in the coastal sabkha of Abu Dhabi (United Arab Emirates). *Sedimentology*, **57**, 824–844.

Borgomano, J., **Lanteaume, C.**, **Léonide, P.**, **Fournier, F.**, **Montaggioni, L.** and **Masse, J.-P.** (2020) Quantitative carbonate sequence stratigraphy: insights from stratigraphic forward models. *Am. Assoc. Petrol. Geol. Bull.*, **104**, 1115–1142.

Borkhataria, R., **Aigner, T.**, **Poppelreiter, M.C.** and **Pipping, J.C.P.** (2005) Characterisation of epeiric "layer-cake" carbonate reservoirs: Upper Muschelkalk (Middle Triassic), the Netherlands. *J. Petrol. Geol.*, **28**, 119–145.

Bosellini, A. (1984) Progradation geometries of carbonate platforms: examples from the Triassic of the Dolomites, northern Italy. *Sedimentology*, **31**, 1–24.

Bosellini, A. (1989) Dynamics of Tethyan carbonate platforms. In: *Controls on Carbonate Platform and Basin Development* (Eds Crevello, P.D., Wilson, J.L., Sarg, J.F. and Read, J.F.), *SEPM Special Publication*, **44**, pp. 3–13.Society of Economic Paleontologists and Mineralogists, Tulsa, Oklahoma, USA.

Bosellini, A. and **Neri, C.** (1991) *The Sella Platform (Upper Triassic, Dolomites, Italy)*. pp. 30. Tourist Office, St. Ulrich, Italy.

Bosellini, A. and **Rossi, D.** (1974) Triassic carbonate buildups of the Dolomites, Northern Italy. In: *Reefs in Time and Space - Selected Examples from the Recent and Ancient* (Ed. Laporte, L.F.), SEPM Special Publication, **18**, pp. 209–233. Society of Economic Paleontologists and Mineralogists, Tulsa, Oklahoma, USA.

Bosence, D.W. (1985) The morphology and ecology of a mound-building coralline alga (*Neogoniolithon Strictum*) from the Florida Keys. *Paleontology*, **28**, 189–206.

Bosence, D.W. (1989) Biogenic carbonate production in Florida Bay. *Bull. Mar. Sci.*, **44**, 419–433.

Bosence, D.W.J., **Pomar, L.**, **Waltham, D.A.** and **Lankester, T.H.G.** (1994) Computer modeling a Miocene carbonate platform, Mallorca, Spain. *Am. Assoc. Petrol. Geol. Bull.*, **78**, 247–266.

Bosscher, H. and **Schlager, W.** (1992) Computer simulation of reef growth. *Sedimentology*, **39**, 503–512.

Bosscher, H. and **Schlager, W.** (1993) Accumulation rates of carbonate platforms. *J. Geol.*, **101**, 345–355.

Boulvain, F. (2001) Facies architecture and diagenesis of Belgian Late Frasnian carbonate mounds. *Sed. Geol.*, **145**, 269–294.

Bourget, J., **Ainsworth, R.B.** and **Nanson, R.** (2014) Origin of mixed carbonate and siliciclastic sequences at the margin of a "Giant" platform during the quaternary (Bonaparte Basin, NW Australia). In: *Deposits, Architecture, and Controls of Carbonate Margin, Slope and Basinal Settings* (Eds Verwer, K., Playton, T.E. and Harris, P.M.), *SEPM*

Special Publication, **105**, pp. 157–177.SEPM (Society for Sedimentary Geology), Tulsa, Oklahoma, USA.

Bown, P.R., **Lees, J.A.** and **Young, J.R.** (2004) Calcareous nannoplankton evolution and diversity through time. In: *Coccolithophores: From Molecular Processes to Global Impact* (Eds Thierstein, H.R. and Young, J.R.), pp. 481–508. Springer, Berlin–Heidelberg.

Brachert, T.C., **Buggisch, W.**, **Flügel, E.**, **Hüssner, H.M.**, **Joachimski, M.M.**, **Tourneur, F.** and **Walliser, O.H.** (1992) Controls of mud mound formation: the Early Devonian Kess-Kess carbonates of the Hamar Laghdad, Anti-Atlas, Morocco. *Geol. Rundsch.*, **81**, 15–44.

Brachert, T.C., **Forst, M.H.**, **Pais, J.J.**, **Legoinha, P.** and **Reijmer, J.J.G.** (2003) Lowstand carbonates, highstand sandstones? *Sed. Geol.*, **155**, 1–12.

Braga, J.C. and **Martín, J.M.** (1996) Geometries of reef advance in response to relative sea-level changes in a Messinian (uppermost Miocene) fringing reef (Cariatiz reef, Sorbas Basin, SE Spain). *Sed. Geol.*, **107**, 61–81.

Braga, J.C., **Martín, J.M.**, **Betzler, C.** and **Aguirre, J.** (2006) Models of temperate carbonate deposition in Neogene basins in SE Spain: a synthesis. In: *Cool-Water Carbonates: Depositional Systems and Palaeoenvironmental Controls* (Eds Pedley, H.M. and Carannante, G.), *Special Publication*, **255**, 121–135. Geological Society of London, London.

Brandner, R., **Flügel, E.** and **Senowbari-Daryan, B.** (1991) Microfacies of carbonate slope boulders: indicator of the source area (Middle Triassic: Mahlknecht Cliff, Western Dolomites). *Facies*, **25**, 279–296.

Brandner, R. and **Keim, L.** (2011) A 4-day geological field trip in the western dolomites. *Geo. Alp*, **8**, 76–118.

Brasileiro, P.S., **Braga, J.C.**, **Amado-Filho, G.M.**, **Leal, R.N.**, **Bassi, D.**, **Franco, T.**, **Bastos, A.C.** and **Moura, R.L.** (2018) Burial rate determines Holocene rhodolith development on the Brazilian shelf. *Palaios*, **33**, 464–477.

Broch, H. (1922) Riffkorallen im Nordmeer einst und jetzt. *Die Naturwissenschaften*, **10**, 804–806.

Broecker, W.S. and **Takahashi, T.** (1966) Calcium carbonate precipitation on the Bahama Banks. *J. Geophys. Res.*, **71**, 1575–1602.

Brookfield, M.E. (1988) A mid-Ordovician temperate carbonate shelf – the Black River and Trenton Limestone Groups of southern Ontario, Canada. *Sed. Geol.*, **60**, 137–153.

Buls, T., **Anderskouv, K.**, **Friend, P.L.**, **Thompson, C.E.L.** and **Stemmerik, L.** (2017) Physical behaviour of Cretaceous calcareous nannofossil ooze: Insight from flume studies of disaggregated chalk. *Sedimentology*, **64**, 478–507.

Burgess, P.M. and **Prince, G.D.** (2015) Non-unique stratal geometries: implications for sequence stratigraphic interpretations. *Basin Res.*, **27**, 351–365.

Busson, J., **Joseph, P.**, **Mulder, T.**, **Teles, V.**, **Borgomano, J.**, **Granjeon, D.**, **Betzler, C.**, **Poli, E.** and **Wunsch, M.** (2019) High-resolution stratigraphic forward modeling of a Quaternary carbonate margin: controls and dynamic of the progradation. *Sed. Geol.*, **379**, 77–96.

Carannante, G., **Esteban, M.**, **Milliman, J.D.** and **Simone, L.** (1988) Carbonate lithofacies as paleolatitude indicators: problems and limitations. *Sed. Geol.*, **60**, 333–346.

Carranza, A., **Muñoz, A.**, **Kitahara, M.**, **Scarabino, F.**, **Ortega, L.**, **López, G.**, **Franco-Fraguas, P.**, **De Mello, C.**, **Acosta, J.** and **Fontan, A.** (2012) Deep-water coral reefs from the Uruguayan outer shelf and slope. *Mar. Biodivers.*, **42**, 411–414.

Carvajal, C. and **Steel, R.** (2009) Shelf-edge architecture and bypass of sand to deep water: influence of shelf-edge processes, sea level and sediment supply. *J. Sed. Res.*, **79**, 652–672.

Catuneanu, O. (2006) *Principles of Sequence Stratigraphy*. pp. 375. Elsevier, Oxford, UK.

Catuneanu, O. (2019) Model-independent sequence stratigraphy. *Earth Sci. Rev.*, **188**, 312–388.

Catuneanu, O. (2020a) Sequence stratigraphy of deep-water systems. *Mar. Petrol. Geol.*, **114**, 104238.

Catuneanu, O. (2020b) Sequence stratigraphy in the context of the 'modeling revolution'. *Mar. Petrol. Geol.*, **116**, 104309.

Catuneanu, O., **Galloway, W.E.**, **Kendall, C.G.S.C.**, **Miall, A.D.**, **Posamentier, H.W.**, **Strasser, A.** and **Tucker, M.E.** (2011) Sequence stratigraphy: methodology and nomenclature. *Newsl. Stratigr.*, **44**, 173–245.

Catuneanu, O. and **Zecchin, M.** (2013) High-resolution sequence stratigraphy of clastic shelves II: controls on sequence development. *Mar. Petrol. Geol.*, **39**, 26–38.

Chabaud, L., **Ducassou, E.**, **Tournadour, E.**, **Mulder, T.**, **Reijmer, J.J.G.**, **Conesa, G.**, **Giraudeau, J.**, **Hanquiez, V.**, **Borgomano, J.** and **Ross, L.** (2016) Sedimentary processes determining the modern carbonate periplatform drift of Little Bahama Bank. *Mar. Geol.*, **378**, 213–229.

Chazottes, V., **Le Campion-Alsumard, T.** and **Peyrot-Clausade, M.** (1995) Bioerosion rates on coral reefs: interactions between macroborers, microborers and grazers (Moorea, French Polynesia). *Palaeogeogr. Palaeoclimatol. Palaeoecol.*, **113**, 189–198.

Chazottes, V., **Le Campion-Alsumard, T.**, **Peyrot-Clausade, M.** and **Cuet, P.** (2002) The effects of eutrophication-related alterations to coral reef communities on agents and rates of bioerosion (Reunion Island, Indian Ocean). *Coral Reefs*, **21**, 375–390.

Chazottes, V., **Reijmer, J.J.G.** and **Cordier, E.** (2008) Sediment characteristics in reef areas influenced by eutrophication-related alterations of benthic communities and bioerosion processes. *Mar. Geol.*, **250**, 114–127.

Coles, S.L. and **Jokiel, P.L.** (1978) Synergistic effects of temperature, salinity and light on the hermatypic coral Montipora verrucosa. *Mar. Biol.*, **49**, 187–195.

Collins, J., **Narr, W.**, **Harris, P.M.**, **Playton, T.E.D.**, **Jenkins, S.**, **Tankersley, T.** and **Kenter, J.A.M.** (2014) Lithofacies, depositional environments, burial diagenesis, and dynamic field behavior in a carboniferous slope reservoir, tengiz field (Republic of Kazakhstan), and comparison with outcrop analogs. In: *Deposits, Architecture, and Controls of Carbonate Margin, Slope and Basinal Settings* (Eds Verwer, K., Playton, T.E. and Harris, P.M.), *SEPM Special Publication*, **105**, 50–83.SEPM (Society for Sedimentary Geology), Oklahoma, USA.

Collins, L.B., **Zhu, Z.R.**, **Wyrwoll, K.H.**, **Hatcher, B.G.**, **Playford, P.E.**, **Eisenhauer, A.**, **Chen, J.H.**, **Wasserburg, G.J.** and **Bonani, G.** (1993) Holocene growth history of reef complex on a cool-water carbonate margin: easter Group of the Houtman Abrolhos, Eastern Indian Ocean. *Mar. Geol.*, **115**, 29–46.

Collins, L.B., **Zhu, Z.R.**, **Wyrwoll, K.-H.** and **Eisenhauer, A.** (2003) Late quaternary structure and development of the northern Ningaloo Reef, Australia. *Sed. Geol.*, **159**, 81–94.

Correa, T.B.S., **Grasmueck, M.**, **Eberli, G.P.**, **Reed, J.K.**, **Verwer, K.** and **Purkis, S.** (2012) Variability of cold-water coral mounds in a high sediment input and tidal current regime, Straits of Florida. *Sedimentology*, **59**, 1278–1304.

Counts, J.W., Jorry, S.J., Leroux, E., Miramontes, E. and Jouet, G. (2018) Sedimentation adjacent to atolls and volcano-cored carbonate platforms in the Mozambique Channel (SW Indian Ocean). *Mar. Geol.*, 404, 41–59.

Counts, J.W., Jorry, S.J., Vazquez Riveiros, N., Jouet, G., Giraudeau, J., Cheron, S., Boissier, A. and Miramontes, E. (2019) A late Quaternary record of highstand shedding from an isolated carbonate platform (Juan de Nova, southern Indian Ocean). *Depos. Rec.*, 5, 540–557.

Crevello, P.D. (1990) *Stratigraphic evolution of Lower Jurassic carbonate platforms: record of rift tectonics and eustasy, Central and Eastern High Atlas, Morocco.* Ph.D. Thesis (unpublished), Colorado School of Mines, Golden, USA, 456 pp.

Crossland, C.J. (1988) Latitudinal comparisons of coral reef structure and function. In: *6th International Coral Reef Symposium* (Eds Choat, J.H., Barnes, D., Borowitzka, M., Coll, J.C., Davies, P.J., Flood, P., Hatcher, B.G., Hopley, D., Hutchings, P.A., Kinsey, D., Orme, G.R., Pichon, M., Sale, P.F., Sammarco, P., Wallace, C.C., Wilkinson, C., Wolanski, E. and Bellwood, O.), Proceedings of the 6th International Coral Reef Symposium: Vol. 1: Plenary Addressess and Status review. ICRS, Townsville, Australia.

Cuevas Castell, J.M., Betzler, C., Rössler, J., Hüssner, H. and Peinl, M. (2007) Integrating outcrop data and forward computer modelling to unravel the development of a Messinian carbonate platform in SE Spain (Sorbas Basin). *Sedimentology*, 54, 423–441.

De Haas, H., Mienis, F., Frank, N., Richter, T.O., Steinacher, R., de Stigter, H., van der Land, C. and van Weering, T.C.E. (2009) Morphology and sedimentology of (clustered) cold-water coral mounds at the south Rockall Trough margins, NE Atlantic Ocean. *Facies*, 55, 1–26.

De Mol, B., Van Rensbergen, P., Pillen, S., Van Herreweghe, K., Van Rooij, D., McDonnell, A., Huvenne, V., Ivanov, M., Swennen, R. and Henriet, J.P. (2002) Large deep-water coral banks in the Porcupine Basin, southwest of Ireland. *Mar. Geol.*, 188, 193–231.

De Mol, L., Van Rooij, D., Pirlet, H., Greinert, J., Frank, N., Quemmerais, F. and Henriet, J.-P. (2011) Cold-water coral habitats in the Penmarc'h and Guilvinec Canyons (Bay of Biscay): deep-water versus shallow-water settings. *Mar. Geol.*, 282, 40–52.

De Vargas, C., Aubry, M.-P., Probert, I.A.N. and Young, J. (2007) Chapter 12 - Origin and evolution of coccolithophores: from coastal hunters to oceanic farmers. In: *Evolution of Primary Producers in the Sea* (Eds Falkowski, P.G. and Knoll, A.H.), pp. 251–285. Academic Press, Burlington, UK.

Della Porta, G. (2015) Carbonate build-ups in lacustrine, hydrothermal and fluvial settings: comparing depositional geometry, fabric types and geochemical signature. In: *Microbial Carbonates in Space and Time: Implications for Global Exploration and Production* (Eds Bosence, D.W.J., Gibbons, K.A., Le Heron, D.P., Morgan, W.A., Pritchard, T. and Vining, B.A.), Special Publication, 418, pp. 17–68. Geological Society of London, London.

Della Porta, G., Kenter, J.A.M., Immenhauser, A. and Bahamonde, J.R. (2002) Lithofacies character and architecture across a Pennsylvanian inner-platform transect (Sierra de Cuera, Asturias, Spain). *J. Sed. Res.*, 72, 898–916.

Della Porta, G., Kenter, J.A.M., Bahamonde, J.R., Immenhauser, A. and Villa, E. (2003) Microbial boundstone dominated carbonate slope (Upper Carboniferous, N Spain): Microfacies, lithofacies distribution and stratal geometry. *Facies*, 49, 175–208.

Della Porta, G., Kenter, J.A.M. and Bahamonde, J.R. (2004) Depositional facies and stratal geometry of an Upper Carboniferous prograding and aggrading high-relief carbonate platform (Cantabrian Mountains, N. Spain). *Sedimentology*, 51, 267–295.

Della Porta, G., Oscar, M.-T., Kenter, J.A.M. and Verwer, K. (2014) Lower Jurassic microbial and skeletal carbonate factories and platform geometry (Djebel Bou Dahar, High Atlas, Morocco). In: *Deposits, Architecture, and Controls of Carbonate Margin, Slope, and Basinal Settings* (Eds Verwer, K., Playton, T.E. and Harris, P.M.), *SEPM Special Publication*, 105, pp. 238–264.SEPM (Society for Sedimentary Geology), Tulsa, Oklahoma, USA.

Diaz, M.R. and Eberli, G.P. (2019) Decoding the mechanism of formation in marine ooids: a review. *Earth Sci. Rev.*, 190, 536–556.

Diaz, M.R., Norstrand, J.D., Eberli, G.P., Piggot, A.M., Zhou, J. and Klaus, J.S. (2014) Functional gene diversity of oolitic sands from Great Bahama Bank. *Geobiology*, 12, 231–249.

Diaz, M.R., Swart, P.K., Eberli, G.P., Oehlert, A.M., Devlin, Q., Saeid, A. and Altabet, M.A. (2015) Geochemical evidence of microbial activity within ooids. *Sedimentology*, 62, 2090–2112.

Dorschel, B., Hebbeln, D., Foubert, A., White, M. and Wheeler, A.J. (2007) Hydrodynamics and cold-water coral facies distribution related to recent sedimentary processes at Galway Mound west of Ireland. *Mar. Geol.*, 244, 184–195.

Dravis, J. (1979) Rapid and widespread generation of recent oolitic hardgrounds on a high energy Bahamian platform, Eleuthera Bank, Bahamas. *J. Sediment. Petrol.*, 49, 195–208.

Dravis, J.J. (1996) Rapidity of freshwater calcite cementation - implications for carbonate diagenesis and sequence stratigraphy. *Sed. Geol.*, 107, 1–10.

Droste, H. (1990) Depositional cycles and source rock development in an epeiric intra-platform basin: the Hanifa Formation of the Arabian Peninsula. *Sed. Geol.*, 69, 281–296.

Droxler, A.W. and Schlager, W. (1985) Glacial versus interglacial sedimentation rates and turbidite frequency in the Bahamas. *Geology*, 13, 799–802.

Drummond, C.N. and Wilkinson, B.H. (1996) Stratal thickness frequencies and the prevalence of orderedness in stratigraphic sequences. *J. Geol.*, 104, 1–18.

Duane, M.J. and Al-Zamel, A.Z. (1999) Syngenetic textural evolution of modern sabkha stromatolites (Kuwait). *Sed. Geol.*, 127, 237–245.

Duce, S., Dechnik, B., Webster, J.M., Hua, Q., Sadler, J., Webb, G.E., Nothdurft, L., Salas-Saavedra, M. and Vila-Concejo, A. (2020) Mechanisms of spur and groove development and implications for reef platform evolution. *Quatern. Sci. Rev.*, 231, 106155.

Duce, S., Vila-Concejo, A., Hamylton, S.M., Webster, J.M., Bruce, E. and Beaman, R.J. (2016) A morphometric assessment and classification of coral reef spur and groove morphology. *Geomorphology*, 265, 68–83.

Duineveld, G.C.A., Lavaleye, M.S.S., Bergman, M.J.N., de Stigter, H. and Mienis, F. (2007) Trophic structure of a cold-water coral mound community (Rockall Bank, NE Atlantic) in relation to the near-bottom particle supply and current regime. *Bull. Mar. Sci.*, 81, 449–467.

Dullo, W.-C. (2005) Coral growth and reef growth: a brief review. *Facies*, **51**, 33–48.

Dullo, W.-C., **Reijmer, J.J.G.**, **Schuhmacher, H.**, **Eisenhauer, A.**, **Hassan, M.** and **Heiss, G.A.** (1996) Holocene reef growth and recent carbonate production in the Red Sea. In: *Global and regional controls on biogenic sedimentation. I. Reef evolution. Research Reports* (Eds Reitner, J., Neuweiler, F. and Gunkel, F.), 1, Göttinger Arbeiten zur Geologie und Paläontologie - Sonderband 2, pp. 13–17. Geologisches Institut der Georg-August-Universität Göttingen, Göttingen.

Dunbar, G.B. and **Dickens, G.R.** (2003) Massive siliciclastic discharge to slopes of the Great Barrier Reef Platform during sea-level transgression: constraints from sediment cores between 15°S and 16°S latitude and possible explanations. *Sed. Geol.*, **162**, 141–158.

Dunham, R.J. (1962) Classification of carbonate rocks according to depositional texture. In: *Classification of Carbonate Rocks – A Symposium* (Ed. Ham, W.E.), AAPG Memoir, **1**, pp. 108–121. American Association of Petroleum Geologists, Tulsa, Oklahoma, USA.

Dupraz, C., **Reid, R.P.**, **Braissant, O.**, **Decho, A.W.**, **Norman, R.S.** and **Visscher, P.T.** (2009) Processes of carbonate precipitation in modern microbial mats. *Earth-Sci. Rev.*, **96**, 141–162.

Dupraz, C., **Visscher, P.T.**, **Baumgartner, L.K.** and **Reid, R.P.** (2004) Microbe–mineral interactions: early carbonate precipitation in a hypersaline lake (Eleuthera Island, Bahamas). *Sedimentology*, **51**, 745–765.

Eberli, G.P. and **Betzler, C.** (2019) Characteristics of modern carbonate contourite drifts. *Sedimentology*, **66**, 1163–1191.

Eberli, G.P. and **Ginsburg, R.N.** (1987) Segmentation and coalescence of platform, Tertiary, NW Great Bahama Bank. *Geology*, **15**, 75–79.

Eberli, G.P. and **Ginsburg, R.N.** (1989) Cenozoic progradation of northwestern Great Bahama Bank, a record of lateral platform growth and sea-level fluctuations. In: *Controls on Carbonate Platform and Basin Development* (Eds Crevello, P.D., Wilson, J.L., Sarg, J.F. and Read, J.F.), *SEPM Special Publication*, **44**, 339–351.

Eberli, G.P., **Swart, P.K.**, **McNeill, D.F.**, **Kenter, J.A.M.**, **Anselmetti, F.S.**, **Melim, L.A.** and **Ginsburg, R.N.** (1997) A synopsis of the Bahamas Drilling Project: results from two deep core borings drilled on the Great Bahama Bank. In: *Proceedings of the Ocean Drilling Program. Initial Reports.* Vol. **166** (Eds Eberli, G.P., Swart, P.K., Malone, M.J. and *et al.*), pp. 23–41. Ocean Drilling Program, College Station, TX.

Edgcomb, V.P., **Bernhard, J.M.**, **Beaudoin, D.**, **Pruss, S.**, **Welander, P.V.**, **Schubotz, F.**, **Mehay, S.**, **Gillespie, A.L.** and **Summons, R.E.** (2013) Molecular indicators of microbial diversity in oolitic sands of Highborne Cay, Bahamas. *Geobiology*, **11**, 234–251.

Eisele, M., **Hebbeln, D.** and **Wienberg, C.** (2008) Growth history of a cold-water coral covered carbonate mound—Galway Mound, Porcupine Seabight, NE-Atlantic. *Mar. Geol.*, **253**, 160–169.

Emiliani, C. (1952) Nomenclature and grammar. *J. Wash. Acad. Sci.*, **42**, 137–141.

Emiliani, C. (1991) Planktic/planktonic, nektic/nektonic, benthic/benthonic. *J. Paleontol.*, **65**, 329.

Emmerich, A. (2001) *Fazies und geometrische Entwicklung am Slope einer Mitteltriassischen Karbonatplattform der Latemar (Dolomiten, Italien)*. MSc thesis, GAEA heidelbergensis 9 (CD-Rom), Geologisch-Paläontologisches Institut Ruprechts-Karls-Universität, Heidelberg, Germany.

Emmerich, A. (2004) *Controlling factors of two Middle Triassic carbonate platforms: Latemar and Rosengarten (Dolomites, Northern Italy)*. PhD thesis, Ruprecht – Karls – Universität Heidelberg, Heidelberg, 172 pp.

Emmerich, A., **Glasmacher, U.A.**, **Bauer, F.**, **Bechstädt, T.** and **Zühlke, R.** (2005a) Meso-/Cenozoic basin and carbonate platform development in the SW-Dolomites unraveled by basin modelling and apatite FT analysis: Rosengarten and Latemar (Northern Italy). *Sed. Geol.*, **175**, 415–438.

Emmerich, A., **Zamparelli, V.**, **Bechstädt, T.** and **Zühlke, R.** (2005b) The reefal margin and slope of a Middle Triassic carbonate platform: the Latemar (Dolomites, Italy). *Facies*, **50**, 573–614.

Emmermann, P.P., **Reijmer, J.J.G.** and **Andresen, N.** (1999) Sedimentation rates of Late Quaternary periplatform sediments based on aragonite/calcite ratios: Sudanese Red Sea vs. Pedro Bank (Caribbean). In: *On the Determination of Sediment Accumulation Rates* (Eds Bruns, P. and Hass, H.C.), *GeoResearch Forum* **5**, pp. 67–86.Trans Tech Publications, Switzerland.

Enos, P. (1974) *Surface sediment facies of the Florida-Bahamas Plateau Map Series MC-5 no. 4 edn.* Geological Society of America.

Enos, P. (1991) Sedimentary parameters for computer modeling. In: *Sedimentary Modeling: Computer Simulations and Methods for Improved Parameter Definition* (Eds Franseen, E.K., Watney, W.L., Kendall, C.G.S.C. and Ross, W.), Kansas Geological Survey Bulletin **233**, pp. 63–99.

Enríquez, S. and **Schubert, N.** (2014) Direct contribution of the seagrass Thalassia testudinum to lime mud production. *Nat. Commun.*, **5**, 3835.

Esker, D., **Eberli, G.P.** and **McNeill, D.F.** (1998) The structural and sedimentological controls on the reoccupation of Quaternary incised valleys, Belize southern lagoon. *Am. Assoc. Petrol. Geol. Bull.*, **82**, 2075–2109.

Etnoyer, P. and **Morgan, L.E.** (2005) Habitat-forming deep-sea corals in the Northeast Pacific Ocean. In: *Cold-Water Corals and Ecosystems* (Eds Freiwald, A. and Roberts, J.M.), pp. 331–343.Springer-Verlag, Berlin, Heidelberg, Germany.

Feary, D.A. and **James, N.P.** (1998) Seismic stratigraphy and geological evolution of the Cenozoic, cool-water, Eucla Platform, Great Australian Bight. *Am. Assoc. Petrol. Geol. Bull.*, **82**, 792–816.

Ferro, C.E., **Droxler, A.W.**, **Anderson, J.B.** and **Mucciarone, D.** (1999) Late Quaternary shift of mixed siliciclastic-carbonate environments induced by glacial eustatic sea-level fluctuations in Belize. In: *Advanves in Carbonate Sequence Stratigraphy: Application to Reservoirs, Outcrops and Models* (Eds Harris, P.M., Saller, A.H. and Simo, T.), *SEPM Special Publication*, **63**, pp. 385–411.SEPM (Society for Sedimentary Geology), Tulsa, Oklahoma, USA.

Fink, H.G., **Wienberg, C.**, **Hebbeln, D.**, **McGregor, H.V.**, **Schmiedl, G.**, **Taviani, M.** and **Freiwald, A.** (2012) Oxygen control on Holocene cold-water coral development in the eastern Mediterranean Sea. *Deep Sea Res. Part I*, **62**, 89–96.

Fink, H.G., **Wienberg, C.**, **De Pol-Holz, R.**, **Wintersteller, P.** and **Hebbeln, D.** (2013) Cold-water coral growth in the Alboran Sea related to high productivity during the Late Pleistocene and Holocene. *Mar. Geol.*, **339**, 71–82.

Floquet, M. and **Hennuy, J.** (2003) Evolutionary gravity flow deposits in the Middle Turonian – Early Coniacian

Southern Provence Basin (SE France): Origins and depositional processes. In: *Submarine Mass Movements and Their Consequences* (Eds Locat, J. and Mienert, J.), Natural and Technical Hazard Research Series, pp. 417–424.Kluwer Academic Publishers, Dordrecht, The Netherlands.

Flügel, E. (1982) Evolution of Triassic reefs: current concepts and problems. *Facies*, **6**, 297–328.

Flügel, E. (2002) Triassic reef patterns. In: *Phanerozoic Reef Patterns* (Eds Kiessling, W., Flügel, E. and Golonka, J.), *SEPM Special Publication*, **72**, pp. 391–463.SEPM (Society for Sedimentary Geology), Tulsa, Oklahoma, USA.

Flügel, E. (2004) *Microfacies of Carbonate Rocks*. Springer, Berlin, 976 pp.

Flügel, E. (2010) *Microfacies of Carbonate Rocks – Analysis, Interpretation and Application*. Springer, Heidelberg-Dordrecht-London-New York. 984 pp.

Folk, R.L. (1959) Practical petrographic classification of limestones. *Am. Assoc. Petrol. Geol. Bull.*, **43**, 1–38.

Folk, R.L. (1974) *Petrology of Sedimentary Rocks*. Hemphill Publishing Company, Austin, Texas, USA, 182 pp.

Fornos, J.J. and Ahr, W.M. (1997) Temperate carbonates on a modern, low-energy, isolated ramp: the Balearic Platform, Spain. *J. Sed. Res. Sect. B Stratigraphy Glob. Stud.*, **67**, 364–373.

Fornos, J.J., Forteza, V., Jaume, C. and Martinez-Taberner, A. (1992) Present-day Halimeda carbonate sediments in temperate Mediterranean embayments: Fornells, Balearic Islands. *Sed. Geol.*, **75**, 283–293.

Foster, M.S. (2001) Rhodoliths: between rocks and soft places. *J. Phycol.*, **37**, 659–667.

Foubert, A., Depreiter, D., Beck, T., Maignien, L., Pannemans, B., Frank, N., Blamart, D. and Henriet, J.-P. (2008) Carbonate mounds in a mud volcano province off north-west Morocco: Key to processes and controls. *Mar. Geol.*, **248**, 74–96.

Frank, N., Ricard, E., Lutringer-Paquet, A., van der Land, C., Colin, C., Blamart, D., Foubert, A., Van Rooij, D., Henriet, J.-P., de Haas, H. and van Weering, T. (2009) The Holocene occurrence of cold water corals in the NE Atlantic: implications for coral carbonate mound evolution. *Mar. Geol.*, **266**, 129–142.

Frank, T.D., James, N.P., Bone, Y., Malcolm, I. and Bobak, L.E. (2014) Late Quaternary carbonate deposition at the bottom of the world. *Sed. Geol.*, **305**, 1–16.

Frank, T.D., James, N.P. and Shultis, A.I. (2020) Lack of synsedimentary chemical alteration in polar carbonates (Ross Sea, Antarctica): resolution of a conundrum. *J. Sed. Res.*, **90**, 449–467.

Frank, T.D., Pritchard, J.M., Fielding, C.R. and Mory, A.J. (2012) Cold-water carbonate deposition in a high-latitude, glacially influenced Permian seaway (Southern Carnarvon Basin, Western Australia). *Aust. J. Earth Sci.*, **59**, 479–494.

Freiwald, A., Fosså, J.H., Grehan, A., Koslow, T. and Roberts, J.M. (2004) *Cold-water Coral Reefs*. UNEP-WCMC, Cambridge.

Franseen, E.K., Goldstein, R.H. and Farr, M.R. (1997) Substrate-slope and temperature controls on carbonate ramps: revelations from Upper Miocene Outcrops, SE Spain. In: *Cool-Water Carbonates* (Eds James, N.P. and Clarke, J.A.D.), *SEPM Special Publication*, **56**, pp. 271–292.SEPM (Society for Sedimentary Geology), Tulsa, Oklahoma, USA.

Freiwald, A., Beuck, L., Rüggeberg, A., Taviani, M., Hebbeln, D. and R/V Meteor M70-1 Participants. (2009)

The white coral community in the central mediterranean sea - revealed by RO V surveys. *Oceanography*, **22**, 36–52.

Freiwald, A., Fosså, J.H., Grehan, A., Koslow, T. and Roberts, J.M. (2004) *Cold-Water Coral Reefs*. UNEP-WCMC, Cambridge, UK.

Freiwald, A., Henrich, R. and Pätzold, J. (1997) Anatomy of a deep-water coral reef mound from Stjernsund, West Finnmark, Northern Norway. In: *Cool-Water Carbonates* (Eds James, N.P. and Clarke, J.A.D.), *SEPM Special Publication*, **56**, pp. 141–162.SEPM (Society for Sedimentary Geology), Tulsa, Oklahoma, USA.

Freiwald, A. and Roberts, J.M., (Eds). (2005) *Cold-Water Corals and Ecosystems*. Springer-Verlag Berlin Heidelberg, Erlangen, Germany, pp. 1242.

Frost, E.L. and Kerans, C. (2009) Platform-Margin trajectory as a control on syndepositional fracture patterns, Canning Basin, Western Australia. *J. Sediment. Res.*, **79**, 44–55.

Gaetani, M., Fois, E., Jadoul, F. and Nicora, A. (1981) Nature and evolution of Middle Triassic carbonate buildups in the Dolomites (Italy). *Mar. Geol.*, **44**, 25–57.

Gale, A., Anderskouv, K., Surlyk, F. and Whalley, J. (2015) Slope failure of chalk channel margins: implications of an Upper Cretaceous mass transport complex, southern England. *J. Geol. Soc.*, **172**, 763–776.

Gattuso, J.-P., Frankignoulle, M., Bourge, I., Romaine, S. and Buddemeier, R.W. (1998) Effect of calcium carbonate saturation of seawater on coral calcification. *Global Planet Change*, **18**, 37–46.

Ginsburg, R.N., Lloyd, R.M., McCallum, J.S., Stockman, K.W. and Moody, R.A. (1958) *Surface Sediments of Great Bahama Bank*. Shell Development Company, Houston, Texas, USA.

Ginsburg, R.N. and Lowenstam, H.A. (1958) The influence of marine bottom communities on the depositional environment of sediments. *J. Geol.*, **66**, 310–318.

Gischler, E. and Hudson, J.H. (2019) Holocene tropical reef accretion and lagoon sedimentation: a quantitative approach to the influence of sea-level rise, climate and subsidence (Belize, Maldives, French Polynesia). *Depos. Rec.*, **5**, 515–539.

Gläser, I. and Betzler, C. (2002) Facies partitioning and sequence stratigraphy of cool-water, mixed carbonate-siliciclastic sediments (Upper Miocene Guadalquivir Domain, southern Spain). *Int. J. Earth Sci.*, **91**, 1041–1053.

Glaser, K.S. and Droxler, A.W. (1991) High production and highstand shedding from deeply submerged carbonate banks, northern Nicaragua Rise. *J. Sediment. Petrol.*, **61**, 128–142.

Glaser, K.S. and Droxler, A.W. (1993) Controls and development of late Quaternary periplatform carbonate stratigraphy in Walton Basin (northern Nicaragua Rise, Caribbean Sea). *Paleoceanography*, **8**, 243–274.

Goedert, J.L., Thiel, V., Schmale, O., Rau, W.W., Michaelis, W. and Peckmann, J. (2003) The late eocene "Whyskey Creek" methane-seep deposit (Western Washington State) part I: geology, paleontology, and molecular geobiology. *Facies*, **48**, 223–240.

Goldhammer, R.K., Dunn, P.A. and Hardie, L.A. (1990) Depositional cycles, composite sea-level changes, cycle stacking patterns, and the hierarchy of stratigraphic forcing: examples from Alpine Triassic platform carbonates. *Geol. Soc. Am. Bull.*, **102**, 535–562.

Goldhammer, R.K., Oswald, E.J. and Dunn, P.A. (1991) Hierarchy of stratigraphic forcing: example from Middle Pennsylvanian shelf carbonates of the Paradox basin. In:

Sedimentary Modeling: Computer Simulations and Methods for Improved Parameter Definition (Eds Franseen, E.K., Watney, W.L., Kendall, C.G.S.C. and Ross, W.), *Kansas Geological Survey Bulletin*, **233**, pp. 361–413.

Grammer, G.M., Crescini, C.M., McNeill, D.F. and Taylor, L.H. (1999) Quantifying rates of syndepositional marine cementation in deeper platform environments - new insight into a fundamental process. *J. Sed. Res.*, **69**, 202–207.

Grammer, G.M., Ginsburg, R.N., Swart, P.K., McNeill, D.F., Jull, A.J.T. and Prezbindowski, D.R. (1993) Rapid growth rates of syndepositional marine aragonite cements in steep marginal slope deposits, Bahamas and Belize. *J. Sediment. Petrol.*, **63**, 983–989.

Grasmueck, M., Eberli, G.P., Viggiano, D.A., Correa, T., Rathwell, G. and Luo, J. (2006) Autonomous underwater vehicle (AUV) mapping reveals coral mound distribution, morphology, and oceanography in deep water of the Straits of Florida. *Geophys. Res. Lett.*, **33**, L23616.

Gravier, C. (1908) Sur quelques traits de la biologie des récifs coralliens. *Revue Sci.*, **5**, 385–393.

Grigg, R.W. (1982) Darwin point: a threshold for atoll formation. *Coral Reefs*, **1**, 29–34.

Grigyalis, A. and Gorbachik, T.N. (1980) Morphology and taxonomy of Jurassic and Early Cretaceous representatives of the superfamily Globigerinacea (Favusellidae). *J. Foramin. Res.*, **10**, 180–190.

Haak, A.B. and Schlager, W. (1989) Compositional variations in calciturbidites due to sea-level fluctuations, late Quaternary, Bahamas. *Geol. Rundsch.*, **78**, 477–486.

Halfar, J., Godinez-Orta, L., Mutti, M., Valdez-Holguín, J.E. and Borges, J.M. (2004) Nutrient and temperature controls on modern carbonate production. An example from the Gulf of California, Mexico. *Geology*, **32**, 213–216.

Halfar, J., Godinez-Orta, L., Mutti, M., Valdez-Holguin, J.E. and Borges, J.M. (2006a) Carbonates calibrated against oceanographic parameters along a latitudinal transect in the Gulf of California, Mexico. *Sedimentology*, **53**, 297–320.

Halfar, J., Gordinez-Orta, L. and Ingle, J.C. (2000) Microfacies analysis of recent carbonate environments in the southern Gulf of California, Mexico - a model for warm-temperate to subtropical carbonate formation. *Palaios*, **15**, 323–342.

Halfar, J., Strasser, M., Riegl, B. and Godinez-Orta, L. (2006b) Oceanography, sedimentology and acoustic mapping of a bryomol carbonate factory in the northern Gulf of California, Mexico. In: *Cool-Water Carbonates: Depositional Systems and Palaeoenvironmental Controls* (Eds Pedley, H.M. and Carannante, G.), *Special Publication*, **255**, 197–215.

Hallock, P. (1985) Why are larger foraminifera large? *Paleobiology*, **11**, 195–208.

Hallock, P. (2005) Global change and modern coral reefs: new opportunities to understand shallow-water carbonate depositional processes. *Sed. Geol.*, **175**, 19–33.

Hallock, P. and Schlager, W. (1986) Nutrient excess and the demise of coral reefs and carbonate platforms. *Palaios*, **1**, 389–398.

Hanz, U., Wienberg, C., Hebbeln, D., Duineveld, G., Lavaleye, M., Juva, K., Dullo, W.C., Freiwald, A., Tamborrino, L., Reichart, G.J., Flögel, S. and Mienis, F. (2019) Environmental factors influencing benthic communities in the oxygen minimum zones on the Angolan and Namibian margins. *Biogeosciences*, **16**, 4337–4356.

Haq, B.U. and Boersma, A. (1978) *Introduction to Marine Micropaleontology*, pp. 376 Elsevier, New York, USA.

Harris, M.T. (1993) Reef fabrics, biotic crusts and syndepositional cements of the Latemar reef margin (Middle Triassic), northern Italy. *Sedimentology*, **40**, 383–402.

Harris, M.T. (1994) The foreslope and toe-of slope facies of the Middle Triassic Latemar build up (Dolomites, Northern Italy). *J. Sed. Res.*, **B64**, 132–145.

Harris, P.M., Ellis, J. and Purkis, S.J. (2013) Assessing the extent of carbonate deposition in early rift settings. *Am. Assoc. Petrol. Geol. Bull.*, **97**, 27–60.

Harris, P.M., Purkis, S.J., Ellis, J., Swart, P.K. and Reijmer, J.J.G. (2015) Mapping bathymetry and depositional facies on Great Bahama Bank. *Sedimentology*, **62**, 566–589.

Haug, G.H. and Tiedemann, R. (1998) Effect of the formation of the Isthmus of Panama on Atlantic Ocean thermohaline circulation. *Nature*, **393**, 673–676.

Hebbeln, D., Bender, M., Gaide, S., Titschack, J., Vandorpe, T., Van Rooij, D., Wintersteller, P. and Wienberg, C. (2019) Thousands of cold-water coral mounds along the Moroccan Atlantic continental margin: distribution and morphometry. *Mar. Geol.*, **411**, 51–61.

Hebbeln, D. and Samankassou, E. (2015) Where did ancient carbonate mounds grow—in bathyal depths or in shallow shelf waters? *Earth Sci. Rev.*, **145**, 56–65.

Hebbeln, D., Wienberg, C., Wintersteller, P., Freiwald, A., Becker, M., Beuck, L., Dullo, C., Eberli, G.P., Glogowski, S., Matos, L., Forster, N., Reyes-Bonilla, H. and Taviani, M. (2014) Environmental forcing of the Campeche cold-water coral province, southern Gulf of Mexico. *Biogeosciences*, **11**, 1799–1815.

Heckel, P.H. (1972) Recognition of ancient shallow marine environments. In: *Recognition of Ancient Sedimentary Environments* (Eds Rigby, J.K. and Hamblin, W.K.), *SEPM Special Publication*, **16**, pp. 226–286.SEPM (Society for Sedimentary Geology), Tulsa, Oklahoma, USA.

Hemleben, C., Spindler, M. and Anderson, O.R. (1989) *Modern Planktonic Foraminifera*, pp. 363. Springer, New York, USA.

Hennuy, J. (2003) *Sédimentation carbonatée et silicoclastique sous côntrole tectonique, le Bassin Sud-Provençal et sa plate-forme carbonatée du Turonien moyen au Coniacien moyen - Evolution séquentielle, diagénétique, paléogéographique*. PhD thesis, Université de Provence (Aix-Marseille I), Marseille, 252 pp plus 42 plates.

Henrich, R., Freiwald, A., Betzler, C., Bader, B., Schäfer, P., Samtleben, C., Brachert, T.C., Wehrmann, A., Zankl, H. and Kühlman, D. (1995) Controls on modern carbonate sedimentation on warm-temperate to Arctic coasts, shelves and seamounts in the northern hemisphere: implications for fossil counterparts. *Facies*, **32**, 71–108.

Henrich, R., Hartmann, M., Reitner, J., Schäfer, P., Freiwald, A., Steinmetz, S., Dietrich, P. and Thiede, J. (1992) Facies belts and communities of the Arctic Vesterisbanken Seamount (Central Greenland Sea). *Facies*, **27**, 71–104.

Henriet, J.P., Hamoumi, N., Da Silva, A.C., Foubert, A., Lauridsen, B.W., Rüggeberg, A. and Van Rooij, D. (2014) Carbonate mounds: from paradox to World Heritage. *Mar. Geol.*, **352**, 89–110.

Hohenegger, J. (2005) Estimation of environmental paleogradient values based on presence/absence data: a case study using benthic foraminifera for paleodepth

estimation. *Palaeogeogr. Palaeoclimatol. Palaeoecol.*, **217**, 115–130.

Holbourn, A., **Kuhnt, W.** and **Xu, J.** (2011) Indonesian Throughflow variability during the last 140 ka: the Timor Sea outflow. In: *The SE Asian Gateway: History and Tectonics of the Australia–Asia Collision* (Eds Hall, R., Cottam, M.A. and Wilson, M.E.J.), **355,** pp. 283–303. Geological Society, London.

Humphreys, A.F., **Halfar, J.**, **Rivera, F.**, **Manzello, D.**, **Reymond, C.E.**, **Westphal, H.** and **Riegl, B.** (2016) Variable El Niño-Southern Oscillation influence on biofacies dynamics of eastern Pacific shallow-water carbonate systems. *Geology*, **44**, 571–574.

Humphreys, A.F., **Halfar, J.**, **Ingle, J.C.**, **Manzello, D.**, **Reymond, C.E.**, **Westphal, H.** and **Riegl, B.** (2018) Effect of seawater temperature, pH, and nutrients on the distribution and character of low abundance shallow water benthic foraminifera in the Galápagos. *PLoS One*, **13**, e0202746.

Huvenne, V., **Bailey, W.**, **Shannon, P.**, **Naeth, J.**, **di Primio, R.**, **Henriet, J.**, **Horsfield, B.**, **de Haas, H.**, **Wheeler, A.** and **Olu-Le Roy, K.** (2007) The Magellan mound province in the Porcupine Basin. *Int. J. Earth Sci.*, **96**, 85–101.

Huvenne, V., **Masson, D.** and **Wheeler, A.** (2009) Sediment dynamics of a sandy contourite: the sedimentary context of the Darwin cold-water coral mounds, Northern Rockall Trough. *Int. J. Earth Sci.*, **98**, 865–884.

James, N.P. (1997) The cool-water carbonate depositional realm. In: *Cool-Water Carbonates: Society for Sedimentary Geology Special Publication* (Eds James, N.P. and Clarke, A.D.), *SEPM Special Publication*, **56**, pp. 1–20.SEPM (Society for Sedimentary Geology), Tulsa, Oklahoma, USA.

James, N.P. and **Bone, Y.** (2011) *Neritic Sedimentary Facies*, pp. 85–108.Springer, Netherlands.

James, N.P., **Boreen, T.D.**, **Bone, Y.** and **Feary, D.A.** (1994) Holocene carbonate sedimentation on the west Eucla Shelf, Great Australian Bight: a shaved shelf. *Sed. Geol.*, **90**, 161–177.

James, N.P., **Collins, L.B.**, **Bone, Y.** and **Hallock, P.** (1999) Subtropical carbonates in a temperate realm: modern sediments on the southwest Australian Shelf. *J. Sed. Res.*, **69**, 1297–1321.

James, N.P., **Feary, D.A.**, **Betzler, C.**, **Bone, Y.**, **Holbourn, A.E.**, **Li, Q.**, **Machiyama, H.**, **Simo, J.A.** and **Surlyk, F.** (2004) Origin of Late Pleistocene Bryozoan reef mounds; Great Australian Bight. *J. Sed. Res.*, **74**, 20–48.

James, N.P., **Frank, T.D.** and **Fielding, C.R.** (2009) Carbonate sedimentation in a permian high-latitude, subpolar depositional realm: Queensland, Australia. *J. Sed. Res.*, **79**, 125–143.

James, N.P. and **Jones, B.** (2015) *Origin of Carbonate Rocks*. AGU-Wiley-Blackwell, Chichester (West Sussex), U.K.

James, N.P., **Seibel, M.J.**, **Dalrymple, R.W.**, **Besson, D.** and **Parize, O.** (2014) Warm-temperate, marine, carbonate sedimentation in an Early Miocene, tide-influenced, incised valley; Provence, south-east France. *Sedimentology*, **61**, 497–534.

Janson, X., **Eberli, G.P.**, **Bonnaffe, F.**, **Gaumet, F.** and **De Casanove, V.** (2007) Seismic expressions of a Miocene prograding carbonate margin, Mut Basin, Turkey. *Am. Assoc. Petrol. Geol. Bull.*, **91**, 685–713.

Jiang, L.-Q., **Feely, R.A.**, **Carter, B.R.**, **Greeley, D.J.**, **Gledhill, D.K.** and **Arzayus, K.M.** (2015) Climatological distribution of aragonite saturation state in the global oceans. *Glob. Biogeochem. Cycles*, **29**, 1656–1673.

Jo, A., **Eberli, G.P.** and **Grasmueck, M.** (2015) Margin collapse and slope failure along southwestern Great Bahama Bank. *Sed. Geol.*, **317**, 43–52.

Jorry, S.J., **Droxler, A.W.** and **Francis, J.M.** (2010) Deepwater carbonate deposition in response to re-flooding of carbonate bank and atoll-tops at glacial terminations. *Quatern. Sci. Rev.*, **29**, 2010–2026.

Jorry, S.J., **Jouet, G.**, **Edinger, E.N.**, **Toucanne, S.**, **Counts, J.W.**, **Miramontes, E.**, **Courgeon, S.**, **Riveiros, N.V.**, **Le Roy, P.** and **Camoin, G.F.** (2020) From platform top to adjacent deep sea: new source-to-sink insights into carbonate sediment production and transfer in the SW Indian Ocean (Glorieuses archipelago). *Mar. Geol.*, **423**, 106144.

Joubin, L. (1922) Distribution géographique de quelques coraux abyssaux dand les mers occidentales européenes. *Acad. Sci. Paris Comptes Rendus*, **175**, 930–933.

Kano, A., **Ferdelman, T.G.**, **Williams, T.**, **Henriet, J.-P.**, **Ishikawa, T.**, **Kawagoe, N.**, **Takashima, C.**, **Kakizaki, Y.**, **Abe, K.**, **Sakai, S.**, **Browning, E.L.**, **Li, X.** Integrated Ocean Drilling Program Expedition 307 Scientists (2007) Age constrains on the origin and growth history of a deep-water coral mound in the northeast Atlantic drilled during Integrated Ocean Drilling Program Expedition 307. *Geology*, **35**, 1051–1054.

Keim, L. and **Schlager, W.** (1999) Automicrite facies on steep slopes (Triassic, Dolomites, Italy). *Facies*, **41**, 15–26.

Keim, L. and **Schlager, W.** (2001) Quantitative compositional analysis of a Triassic carbonate platform (Southern Alps, Italy). *Sed. Geol.*, **139**, 261–283.

Kenig, F., **Huc, A.Y.**, **Purser, B.H.** and **Oudin, J.-L.** (1990) Sedimentation, distribution and diagenesis of organic matter in a recent carbonate environment, Abu Dhabi, U.A.E. *Org. Geochem.*, **16**, 735–747.

Kenter, J.A.M. (1990) Carbonate platform flanks: slope angle and sediment fabric. *Sedimentology*, **37**, 777–794.

Kenter, J.A.M. and **Campbell, A.E.** (1991) Sedimentation on a Lower Jurassic carbonate platform flank: geometry, sediment fabric and related depositional structures (Djebel Bou Dahar, High Atlas, Morocco). *Sed. Geol.*, **72**, 1–34.

Kenter, J.A.M., **Harris, P.M.** and **Della Porta, G.** (2005) Steep microbial boundstone-dominated platform margins— examples and implications. *Sed. Geol.*, **178**, 5–30.

Kenter, J.A.M. and **Schlager, W.** (1989) A comparison of shear strength in calcareous and siliciclastic marine sediments. *Mar. Geol.*, **88**, 145–152.

Kenter, J.A.M. and **Schlager, W.** (2009) Slope angle and basin depth of the Triassic platform-basin transition at the Gosaukamm. *Austria. Aust. J. Earth Sci.*, **102**, 15–22.

Kerans, C. and **Harris, P.M.** (1993) Outer shelf and shelf crest. In: *Guide to the Permian Reef Geology Trail, McKittrick Canyon, Guadalupe Mountains National Park, Texas* (Eds Bebout, D.G. and Kerans, C.), Guidebook **26**, pp. 32–43.Texas Bureau of Economic Ecology - Bureau of Economic Geology - University of Texas, Austin, Texas.

Kenyon, N.H., **Akhmetzhanov, A.M.**, **Wheeler, A.J.**, **van Weering, T.C.E.**, **de Haas, H.** and **Ivanov, M.K.** (2003) Giant carbonate mud mounds in the southern Rockall Trough. *Mar. Geol.*, **195**, 5–30.

Kievman, C.M. (1998) Match between Late Pleistocene Great Bahama Bank and deep-sea oxygen isotope records of sea level. *Geology*, **26**, 635–638.

Kindler, P. and **Wilson, M.E.J.** (2010) Carbonate grain associations: their use and environmental significance, a brief review. In: *Carbonate Systems During the Oligocene-*

Miocene Climate Transition (Eds Mutti, M., Pliller, W.E. and Betzler, C.), *Int. Assoc. Sedimentol. Spec. Publ.* **42**, pp. 35–48.International Association of Sedimentologists/Wiley-Blackwell, Chichester (West Sussex), UK.

Kirkby, M.J. (1987) General models of long-term slope evolution through mass movement. In: *Slope Stability, Geotechnical Engineering and Geomorphology* (Eds Anderson, M.G. and Richards, K.S.), pp. 359–379.John Wiley and Sons, London.

Kleipool, L.M., de Jong, K., de Vaal, E.L. and **Reijmer, J.J.G.** (2017) Seismic characterization of switching platform geometries and dominant carbonate producers (Miocene, Las Negras, Spain). *Sedimentology*, **64**, 1676–1707.

Klicpera, A., Michel, J. and **Westphal, H.** (2015) Facies patterns of a tropical heterozoan carbonate platform under eutrophic conditions: the Banc d'Arguin, Mauritania. *Facies*, **61**, 421.

Kucera, M. (2007) Planktonic foraminifera as tracers of past oceanic environments. *Dev. Mar. Geol.*, **1**, 213–262.

Lantzsch, H., Roth, S., Reijmer, J.J.G. and **Kinkel, H.** (2007) Sea-level related resedimentation processes on the northern slope of Little Bahama Bank (Middle Pleistocene to Holocene). *Sedimentology*, **54**, 1307–1322.

Laugié, M., Michel, J., Pohl, A., Poli, E. and **Borgomano, J.** (2019) Global distribution of modern shallow-water marine carbonate factories: a spatial model based on environmental parameters. *Sci. Rep.*, **9**, 16432.

Le Goff, J., Reijmer, J.J.G., Cerepi, A., Loisy, C., Swennen, R., Heba, G., Cavailhes, T. and **De Graaf, S.** (2019) The dismantling of the Apulian carbonate platform during the late Campanian – early Maastrichtian in Albania. *Cretac. Res.*, **96**, 83–106.

Le Goff, J., Slootman, A., Mulder, T., Cavailhes, T., Ducassou, E., Hanquiez, V., Jaballah, J. and **Reijmer, J.J.G.** (2020) On the architecture of intra-formational mass-transport deposits: insights from the carbonate slopes of Great Bahama Bank and the Apulian Carbonate Platform. *Mar. Geol.*, **427**, 106205.

Lees, A. (1964) The structure and origin of the Waulsortian (Lower Carboniferous) 'Reefs' of West-Central Eire. *Philos. Trans. R. Soc. London. Ser B, Biol. Sci.*, **247**, 483–531.

Lees, A. (1975) Possible influence of salinity and temperatures on modern shelf carbonate sedimentation. *Mar. Geol.*, **19**, 159–198.

Lees, A. and **Buller, A.T.** (1972) Modern temperate-water and warm-water shelf carbonate sediments contrasted. *Mar. Geol.*, **13**, M67–M73.

Lees, A. and **Miller, J.** (1995) Waulsortian banks. In: *Carbonate Mud-Mounds - Their Origin and Evolution* (Eds Monty, C.L.V., Bosence, D.W.J., Bridges, P.H. and Pratt, B.R.), *Int. Assoc. Sedimentol. Special Publication*, **23**, pp. 191–271. International Association of Sedimentologists/Wiley, Oxford, UK.

Leonard, J.E., Cameron, B., Pilkey, O.H. and **Friedman, G.M.** (1981) Evaluation of cold-water carbonates as a possible paleoclimatic indicator. *Sed. Geol.*, **28**, 1–28.

Lewis, S.K. (2001) *An Examination of the Effects of Environmental Stresses on Stony Corals*. PhD Thesis, University of Georgia, Athens, 175 pp.

Liebetrau, V., Augustin, N., Kutterolf, S., Schmidt, M., Eisenhauer, A., Garbe-Schönberg, D. and **Weinrebe, W.** (2014) Cold-seep-driven carbonate deposits at the Central American forearc: contrasting evolution and timing in escarpment and mound settings. *Int. J. Earth Sci.*, **103**, 1845–1872.

Lindhorst, S., Betzler, C., Wunsch, M., Lüdmann, T. and **Kuhn, G.** (2019) Carbonate drifts as marine archives of aeolian dust (Santaren Channel, Bahamas). *Sedimentology*, **66**, 1386–1409.

Lokier, S.W. and **Al Junaibi, M.** (2016) The petrographic description of carbonate facies: are we all speaking the same language? *Sedimentology*, **63**, 1843–1885.

Lokier, S.W., Court, W.M., Onuma, T. and **Paul, A.** (2018) Implications of sea-level rise in a modern carbonate ramp setting. *Geomorphology*, **304**, 64–73.

Lokier, S.W., Knaf, A. and **Kimiagar, S.** (2013) A quantitative analysis of recent arid coastal sedimentary facies from the Arabian Gulf Coastline of Abu Dhabi, United Arab Emirates. *Mar. Geol.*, **346**, 141–152.

Long, D.J. and **Baco, A.R.** (2014) Rapid change with depth in megabenthic structure-forming communities of the Makapu'u deep-sea coral bed. *Deep Sea Res. Part II*, **99**, 158–168.

Lowenstam, H.A. (1981) Minerals formed by organisms. *Science*, **211**, 1126–1131.

Lowenstam, H.A. and **Weiner, S.** (1989) *On Biomineralization*. Oxford University Press, New York, USA, 336 pp.

Lüdmann, T., Betzler, C., Eberli, G.P., Reolid, J., Reijmer, J.J.G., Sloss, C.R., Bialik, O.M., Alvarez-Zarikian, C.A., Alonso-García, M., Blättler, C.L., Guo, J.A., Haffen, S., Horozal, S., Inoue, M., Jovane, L., Kroon, D., Lanci, L., Laya, J.C., Mee, A.L.H., Nakakuni, M., Nath, B.N., Niino, K., Petruny, L.M., Pratiwi, S.D., Slagle, A.L., Su, X., Swart, P.K., Wright, J.D., Yao, Z. and **Young, J.R.** (2018a) Carbonate delta drift: a new sediment drift type. *Mar. Geol.*, **401**, 98–111.

Lüdmann, T., Betzler, C., Eberli, G.P., Reolid, J., Reijmer, J.J.G., Sloss, C.R., Bialik, O.M., Alvarez-Zarikian, C.A., Alonso-García, M., Blättler, C.L., Guo, J.A., Haffen, S., Horozal, S., Inoue, M., Jovane, L., Kroon, D., Lanci, L., Laya, J.C., Mee, A.L.H., Nakakuni, M., Nath, B.N., Niino, K., Petruny, L.M., Pratiwi, S.D., Slagle, A.L., Su, X., Swart, P.K., Wright, J.D., Yao, Z. and **Young, J.R.** (2018b) Corrigendum to "Carbonate delta drift: a new sediment drift type" [Mar. Geol. 401 (2018) 98–111]. *Mar. Geol.*, **406**, 214–215.

Lüdmann, T., Paulat, M., Betzler, C., Möbius, J., Lindhorst, S., Wunsch, M. and **Eberli, G.P.** (2016) Carbonate mounds in the Santaren Channel, Bahamas: a current-dominated periplatform depositional regime. *Mar. Geol.*, **376**, 69–85.

Malone, P.G. and **Dodd, J.R.** (1967) Temperature and salinity effects on calcification rate in Mytilus edulis and its paleoecological implicatons. *Limnol. Oceanogr.*, **12**, 432–436.

Maloof, A.C. and **Grotzinger, J.P.** (2012) The Holocene shallowing-upward parasequence of north-west Andros Island, Bahamas. *Sedimentology*, **59**, 1375–1407.

Mann, S. (1983) Mineralization in biological systems. In: *Inorganic Elements in Biochemistry* (Eds Connett, P.H., Follmann, H., Lammers, M., Mann, S., Odom, J.D. and Wetterhahn, K.E.), pp. 125–174.Springer Berlin Heidelberg, Berlin, Heidelberg, Germany.

Markello, J., Koepnick, R., Waite, L. and **Collins, J.** (2008) The Carbonate Analogs Through Time (CATT) Hypothesis and the Global Atlas of Carbonate Fields — A Systematic and Predictive Look at Phanerozoic Carbonate Systems. In: *Controls on Carbonate Platform and Reef Development* (Eds Lukasik, J. and Simo, J.A.), *SEPM Special*

Publication, **89**, 15–45. SEPM (Society for Sedimentary Geology), Tulsa, Oklahoma, USA.

Matsuda, S. (1989) Succession and growth rates of encrusting crustose coralline algae (Rhodophyta, Cryptonemiales) in the upper fore-reef environment off Ishigaki Island, Ryukyu Islands. *Coral Reefs*, **7**, 185–195.

Matsuda, S. and **Iryu, Y.** (2011) Rhodoliths from deep fore-reef to shelf areas around Okinawa-jima, Ryukyu Islands, Japan. *Mar. Geol.*, **282**, 215–230.

Maurer, F. (2000) Growth mode of Middle Triassic carbonate platforms in the Western Dolomites (Southern Alps, Italy). *Sed. Geol.*, **134**, 275–286.

McNeill, D.F., **Coates, A.G.**, **Budd, A.F.** and **Borne, P.F.** (2000) Integrated paleontologic and paleomagnetic stratigraphy of the upper Neogene deposits around Limon, Costa Rica: a coastal emergence record of the Central American Isthmus. *Geol. Soc. Am. Bull.*, **112**, 963–981.

Mergner, H. and **Schuhmacher, H.** (1974) Morphologie, Ökologie und Zonierung von Korallenriffen bei Aqaba, (Golf von Aqaba, Rotes Meer). *Helgoländer wissenschaftliche Meeresuntersungen*, **26**, 238–358.

Mergner, H. and **Schuhmacher, H.** (1981) Quantitative analyse der Korallenbesiedlung eines Vorriffareals bei Aqaba (Rotes Meer). *Helgoländer wissenschaftliche Meeresuntersungen*, **34**, 337–354.

Merino-Tomé, Ó., **Della Porta, G.**, **Pierre, A.**, **Kenter, J.A.M.**, **Durlet, C.** and **Verwer, K.** (2017) Intact seismic-scale platforms and ramps in the Lower to Middle Jurassic of Morocco: implications for stratal anatomy and lithofacies partitioning. *AAPG Bulletin.*, **101**, 505–513.

Merino-Tomé, Ó., **Della Porta, G.**, **Kenter, J.A.M.**, **Verwer, K.**, **Harris, P.M.**, **Adams, E.W.**, **Playton, T.E.** and **Corrochano, D.** (2012) Sequence development in an isolated carbonate platform (Lower Jurassic, Djebel Bou Dahar, High Atlas, Morocco): influence of tectonics, eustacy and carbonate production. *Sedimentology*, **59**, 118–155.

Michel, J., **Borgomano, J.** and **Reijmer, J.J.G.** (2018) Heterozoan carbonates: When, where and why? A synthesis on parameters controlling carbonate production and occurrences. *Earth Sci. Rev.*, **182**, 50–67.

Michel, J., **Laugié, M.**, **Pohl, A.**, **Lanteaume, C.**, **Masse, J.-P.**, **Donnadieu, Y.** and **Borgomano, J.** (2019) Marine carbonate factories: a global model of carbonate platform distribution. *Int. J. Earth Sci.*, **108**, 1773–1792.

Michel, J., **Vicens, G.M.** and **Westphal, H.** (2011) Modern heterozoan carbonates from a eutrophic tropical shelf (Mauritania). *J. Sed. Res.*, **81**, 641–655.

Mienis, F., **Duineveld, G.C.A.**, **Davies, A.J.**, **Ross, S.W.**, **Seim, H.**, **Bane, J.** and **van Weering, T.C.E.** (2012) The influence of near-bed hydrodynamic conditions on cold-water corals in the Viosca Knoll area. *Gulf Mexico Deep Sea Res. Part I Oceanogr. Res. Pap.*, **60**, 32–45.

Mienis, F., **Duineveld, G.C.A.**, **Lavaleye, M.S.S.** and **van Weering, T.C.E.** (2014) Proceedings ISDSC5. *Deep Sea Res. Part II Topic. Stud. Oceanogr.*, **99**, 1–5.

Mienis, F., **van der Land, C.**, **de Stigter, H.C.**, **Van de Vorstenbosch, M.**, **de Haas, H.**, **Richter, T.** and **van Weering, T.C.E.** (2009a) Sediment accumulation on a cold-water carbonate mound at the Southwest Rockall trough margin. *Mar. Geol.*, **265**, 40–50.

Mienis, F., **de Stigter, H.C.**, **White, M.**, **Duineveld, G.**, **de Haas, H.** and **van Weering, T.C.E.** (2007) Hydrodynamic controls on cold-water coral growth and carbonate-mound development at the SW and SE Rockall Trough Margin, NE Atlantic Ocean. *Deep Sea Res. Part I Oceanogr. Res. Pap.*, **54**, 1655–1674.

Mienis, F., **de Stigter, H.C.**, **de Haas, H.** and **van Weering, T.C.E.** (2009b) Near-bed particle deposition and resuspension in a cold-water coral mound area at the Southwest Rockall Trough margin, NE Atlantic. *Deep Sea Res. I Oceanogr. Res. Pap.*, **56**, 1026–1038.

Mienis, F., **van Weering, T.**, **de Haas, H.**, **de Stigter, H.**, **Huvenne, V.** and **Wheeler, A.** (2006) Carbonate mound development at the SW Rockall Trough margin based on high resolution TOBI and seismic recording. *Mar. Geol.*, **233**, 1–19.

Milliman, J.D. (1974) *Marine Carbonates.* Springer Verlag, Berlin-Heidelberg-New York, USA, 375 pp.

Mitchell, J.K., **Holdgate, G.R.**, **Wallace, M.W.** and **Gallagher, S.J.** (2007) Marine geology of the Quaternary Bass Canyon system, southeast Australia: a cool-water carbonate system. *Mar. Geol.*, **237**, 71–96.

Morse, J.W. and **Mackenzie, F.T.** (1990) *Geochemistry of Sedimentary Carbonates.* Elsevier, Amsterdam, 707 pp.

Mulder, T., **Ducassou, E.**, **Eberli, G.P.**, **Hanquiez, V.**, **Gonthier, E.**, **Kindler, P.**, **Principaud, M.**, **Fournier, F.**, **Leonide, P.**, **Billeaud, I.**, **Marsset, B.**, **Reijmer, J.J.G.**, **Bondu, C.**, **Joussiaume, R.** and **Pakiades, M.** (2012) New insights into the morphology and sedimentary processes along the western slope of Great Bahama Bank. *Geology*, **40**, 603–606.

Mulder, T., **Ducassou, E.**, **Hanquiez, V.**, **Principaud, M.**, **Fauquembergue, K.**, **Tournadour, E.**, **Chabaud, L.**, **Reijmer, J.**, **Recouvreur, A.**, **Gillet, H.**, **Borgomano, J.**, **Schmitt, A.** and **Moal, P.** (2019) Contour current imprints and contourite drifts in the Bahamian archipelago. *Sedimentology*, **66**, 1192–1221.

Müller, M.N. (2019) On the genesis and function of coccolithophore calcification. *Front. Mar. Sci.*, **6**, 49.

Muñoz, A., **Cristobo, J.**, **Rios, P.**, **Druet, M.**, **Polonio, V.**, **Uchupi, E.** and **Acosta, J.** (2012) Sediment drifts and cold-water coral reefs in the Patagonian upper and middle continental slope. *Mar. Pet. Geol.*, **36**, 70–82.

Murris, R.J. (1980) Middle East: stratigraphic evolution and oil habitat. *AAPG Bull.*, **64**, 597–618.

Muthiga, N.A. and **Szmant, A.M.** (1987) The effect of salinity stress on the rates of aerobic respiration and photosynthesis in the hermatypic coral *Siderastrea Siderea*. *Biol. Bull.*, **173**, 539–551.

Mutti, M. and **Hallock, P.** (2003) Carbonate systems along nutrient and temperature gradients: some sedimentological and geochemical constraints. *Int. J. Earth Sci.*, **92**, 465–475.

Nelson, C.S. (1988) An introductory perspective on non-tropical shelf carbonates. *Sed. Geol.*, **60**, 3–12.

Nelson, J.E. and **Ginsburg, R.N.** (1986) Calcium carbonate production by epibionts on Thalassia in Florida Bay. *J. Sediment. Petrol.*, **56**, 622–628.

Neuweiler, F. (1995) *Dynamische Sedimentationsvorgänge, Diagenese und Biofazies unterkretazischer Plattformränder: (Apt/Alb; Soba-Region, Prov. Cantabria, N-Spanien).* Selbstverlag Fachbereich Geowissenschaften, E17, FU Berlin, Berlin, 235 pp.

Neuweiler, F., **Gautret, P.**, **Thiel, V.**, **Lange, R.**, **Michaelis, W.** and **Reitner, J.** (1999) Petrology of Lower Cretaceous carbonate mud mounds (Albian, N. Spain): insights into organomineralic deposits of the geological record. *Sedimentology*, **46**, 837–860.

Neves, B.M., **Du Preez, C.** and **Edinger, E.** (2014) Mapping coral and sponge habitats on a shelf-depth environment

using multibeam sonar and ROV video observations: Learmonth Bank, northern British Columbia, Canada. *Deep Sea Res. Part II*, **99**, 169–183.

Nordgaard, O. (1930) Faunistic notes on marine evertebrates VI. On the distribution of some Madreporarian corals in Northern Norway. *Kong. Norslze Vidensli. Selsli. Forliandl.*, **2**, 102–113.

Opdyke, B.N. and Wilkinson, B.H. (1990) Paleolatitude distribution of phanerozoic marine ooids and cements. *Palaeogeogr. Palaeoclimatol. Palaeoecol.*, **78**, 135–148.

Opdyke, B.N. and Wilkinson, B.H. (1993) Carbonate mineral saturation state and cratonic limestone accumulation. *Am. J. Sci.*, **293**, 217–234.

Pacton, M., Ariztegui, D., Wacey, D., Kilburn, M.R., Rollion-Bard, C., Farah, R. and Vasconcelos, C. (2012) Going nano: a new step toward understanding the processes governing freshwater ooid formation. *Geology*, **40**, 547–550.

Paul, A., Reijmer, J.J.G., Fürstenau, J., Kinkel, H. and Betzler, C. (2012) Relationship between Late Pleistocene sea-level variations, carbonate platform morphology and aragonite production (Maldives, Indian Ocean). *Sedimentology*, **59**, 1640–1658.

Paulat, M., Lüdmann, T., Betzler, C. and Eberli, G.P. (2019) Neogene palaeoceanographic changes recorded in a carbonate contourite drift (Santaren Channel, Bahamas). *Sedimentology*, **66**, 1361–1385.

Peckmann, J., Gischler, E., Oschmann, W. and Reitner, J. (2001) An early carboniferous seep community and hydrocarbon-derived carbonates from the Harz Mountains, Germany. *Geology*, **29**, 271–274.

Peckmann, J., Goedert, J.L., Heinrichs, T., Hoefs, J. and Reitner, J. (2003) The late eocene "Whyskey Creek" methane-seep deposit (Western Washington State) part II: petrology, stable isotopes, and biogeochemistry. *Facies*, **48**, 241–254.

Pedley, M. and Grasso, M. (2002) Lithofacies modelling and sequence stratigraphy in microtidal cool-water carbonates: a case study from the Pleistocene of Sicily, Italy. *Sedimentology*, **49**, 533–553.

Perry, C.T. (2003) Coral reefs in a high-latitude, siliciclastic barrier island setting: reef framework and sediment production at Inhaca Island, southern Mozambique. *Coral Reefs*, **22**, 485–497.

Perry, C.T. (2005) Structure and development of detrital reef deposits in turbid nearshore environments, Inhaca Island, Mozambique. *Mar. Geol.*, **214**, 143–161.

Perry, C.T. and Beavington-Penney, S.J. (2005) Epiphytic calcium carbonate production and facies development within sub-tropical seagrass beds, Inhaca Island, Mozambique. *Sed. Geol.*, **174**, 161–176.

Piller, W.E. and Mansour, A.M. (1990) The northern Bay of Safaga (Red Sea, Egypt): an actuopaleontological approach. II: sediment analysis and sedimentary facies. *Beiträge zur Paläontologie von Österreich*, **16**, 1–102.

Piller, W.E. and Mansour, A.M. (1994) Origin and transport mechanisms of non-carbonate sediments in a carbonate-dominated environment (northern Safaga Bay, Red Sea, Egypt). *Abhandlungen der Geologischen Bundesanstalt von Österreich*, **50**, 369–379.

Piller, W.E. and Pervesler, P. (1989) The northern Bay of Safaga (Red Sea, Egypt): an actuopaleontological approach. I. Topography and bottom facies. *Beiträge zur Paläontologie von Österreich*, **15**, 103–147.

Piller, W.E. and Rasser, M. (1996) Rhodolith formation induced by reef erosion in the Red Sea, Egypt. *Coral Reefs*, **15**, 191–198.

Pires, D.O., Silva, J.C. and Bastos, N.D. (2014) Reproduction of deep-sea reef-building corals from the southwestern Atlantic. *Deep Sea Res. Part II*, **99**, 51–63.

Playford, P.E. (1980) Devonian "Great Barrier Reef" of canning basin, Western Australia. *Bull. Am. Assoc. Petrol. Geol.*, **64**, 814–840.

Playford, P.E., Hocking, R.M. and Cockbain, A.E. (2009) *Devonian Reef Complexes of the Canning Basin, Western Australia*. Geological Survey of Western Australia, Perth, Western Australia, 444 pp.

Playford, P.E., Hurley, N.F., Kerans, C. and Middleton, M.F. (1989) Reefal platform development, Devonian of the Canning Basin, western Australia. In: *Controls on Carbonate Platform and Basin Development* (Eds Crevello, P.D., Wilson, J.L., Sarg, J.F. and Read, J.F.), *SEPM Special Publication*, **44**, pp. 187–202.Society of Economic Paleontologists and Mineralogists, Tulsa, Oklahoma, USA.

Playton, T., Janson, X. and Kerans, C. (2010) 18. Carbonate slopes. In: *Facies 4* (Eds James, N.P. and Dalrymple, R.W.), pp. 449–476. Geological Association of Canada, St. John's.

Playton, T.E. and Kerans, C. (2015a) Late devonian carbonate margins and foreslopes of the lennard shelf, Canning Basin, Western Australia, part A: development during backstepping and the aggradation-to-progradation transition. *J. Sed. Res.*, **85**, 1334–1361.

Playton, T.E. and Kerans, C. (2015b) Late devonian carbonate margins and foreslopes of the lennard shelf, Canning Basin, Western Australia, part B: development during progradation and across the frasnian-famennian biotic crisis. *J. Sed. Res.*, **85**, 1362–1392.

Playton, T.E. and Kerans, C. (2018) Architecture and genesis of prograding deep boundstone margins and debris-dominated carbonate slopes: examples from the Permian Capitan Formation, Southern Guadalupe Mountains, West Texas. *Sed. Geol.*, **370**, 15–41.

Pohl, A., Donnadieu, Y., Godderis, Y., Lanteaume, C., Hairabian, A., Frau, C., Michel, J., Laugie, M., Reijmer, J.J.G., Scotese, C.R. and Borgomano, J. (2020) Carbonate platform production during the Cretaceous. *GSA Bull.*, **132**, 2606–2610.

Pohl, A., Laugié, M., Borgomano, J., Michel, J., Lanteaume, C., Scotese, C.R., Frau, C., Poli, E. and Donnadieu, Y. (2019) Quantifying the paleogeographic driver of Cretaceous carbonate platform development using paleoecological niche modeling. *Palaeogeogr. Palaeoclimatol. Palaeoecol.*, **514**, 222–232.

Pomar, L. (1991) Reef geometries, erosion surfaces and high-frequency sea-level changes, upper Miocene Reef Complex, Mallorca, Spain. *Sedimentology*, **38**, 243–269.

Pomar, L. (2001) Types of carbonate platforms: a genetic approach. *Basin Res.*, **13**, 313–334.

Pomar, L. and Hallock, P. (2008) Carbonate factories: a conundrum in sedimentary geology. *Earth Sci. Rev.*, **87**, 134–169.

Porter, J.W., Lewis, S.K. and Porter, K.G. (1999) The effect of multiple stressors on the florida keys coral reef ecosystem: a landscape hypothesis and a physiological test. *Limnol. Oceanogr.*, **44**, 941–949.

Poulton, A.J., Stinchcombe, M.C., Achterberg, E.P., Bakker, D.C.E., Dumousseaud, C., Lawson, H.E., Lee, G.A., Richier, S., Suggett, D.J. and Young, J.R. (2014) Coccolithophores on the north-west European shelf: calcification rates and environmental controls. *Biogeosciences*, **11**, 3919–3940.

Pratt, B.R. (2001) Calcification of cyanobacterial filaments: *Girvanella* and the origin of lower Paleozoic lime mud. *Geology*, **29**, 763–766.

Preto, N. (2012) Petrology of carbonate beds from the stratotype of the Carnian (Stuores Wiesen section, Dolomites, Italy): the contribution of platform-derived microbialites. *Geo. Alp*, **9**, 12–29.

Preto, N., **Hinnov, L.A.**, **Hardie, L.A.** and **De Zanche, V.** (2001) Middle Triassic orbital signature recorded in the shallow-marine Latemar carbonate buildup (Dolomites, Italy). *Geology*, **29**, 1123–1126.

Principaud, M., **Mulder, T.**, **Gillet, H.** and **Borgomano, J.** (2015) Large-scale carbonate submarine mass-wasting along the northwestern slope of the Great Bahama Bank (Bahamas): morphology, architecture, and mechanisms. *Sed. Geol.*, **317**, 27–42.

Principaud, M., **Ponte, J.-P.**, **Mulder, T.**, **Gillet, H.**, **Robin, C.** and **Borgomano, J.** (2017) Slope-to-basin stratigraphic evolution of the northwestern Great Bahama Bank (Bahamas) during the Neogene to Quaternary: interactions between downslope and bottom currents deposits. *Basin Res.*, **29**, 699–724.

Pruvot, G. (1894) Essai sur la topographie et la constitution des fonds sous-marins de la region Banyuls. *Arch. Zoologie Experim. Gen.*, **3**(2), 599–672.

Pruvot, G. (1895) Coup d'oeil sur la distribution generale des invertebres dans la region de Banyuls (Golfe de Lion). *Arch. Zoologie Experim. et Gen.*, **3**, 629–658.

Puga-Bernabéu, Á., **Beaman, R.J.**, **Webster, J.M.**, **Thomas, A.L.** and **Jacobsen, G.** (2017) Gloria Knolls Slide: a prominent submarine landslide complex on the Great Barrier Reef margin of north-eastern Australia. *Mar. Geol.*, **385**, 68–83.

Puga-Bernabéu, Á., **Martín, J.M.**, **Braga, J.C.** and **Aguirre, J.** (2014) Offshore remobilization processes and deposits in low-energy temperate-water carbonate-ramp systems: examples from the Neogene basins of the Betic Cordillera (SE Spain). *Sed. Geol.*, **304**, 11–27.

Purdy, E.G. (1963a) Recent calcium carbonate facies of the Great Bahama Bank. 1. Petrography and reaction groups. *J. Geol.*, **71**, 334–355.

Purdy, E.G. (1963b) Recent calcium carbonate facies of the Great Bahama Bank. 2. Sedimentary facies. *J. Geol.*, **71**, 472–497.

Purkis, S.J. and **Harris, P.M.** (2016) The extent and patterns of sediment filling of accommodation space on Great Bahama Bank. *J. Sed. Res.*, **86**, 294–310.

Purser, B.H. (1973) *The Persian Gulf: Holocene Carbonate Sedimentation and Diagenesis in a Shallow Epicontinental Sea*. Springer-Verlag, New York–Heidelberg–Berlin, 471 pp.

Rankey, E.C. (2002) Spatial patterns of sediment accumulation on a Holocene carbonate tidal flat, Northwest Andros Island, Bahamas. *J. Sed. Res.*, **72**, 591–601.

Rao, C.P. (1981) Criteria for recognition of cold-water carbonate sedimentation; Berriedale Limestone (Lower Permian), Tasmania, Australia. *J. Sed. Res.*, **51**, 491–506.

Rao, C.P. (1996) *Modern Carbonates: Tropical, Temperate, Polar*. Tasmanian Government Printers, Hobart, Tasmania, Australia.

Razin, P., **Taati, F.** and **van Buchem, F.S.P.** (2010) Sequence stratigraphy of Cenomanian–Turonian carbonate platform margins (Sarvak Formation) in the High Zagros, SW Iran: an outcrop reference model for the Arabian Plate. In: *Mesozoic and Cenozoic Carbonate Systems of the Mediterranean and the Middle East: Stratigraphic and Diagenetic Reference Models* (Eds Van Buchem, F.S.P., Gerdes, K.D. and Esteban, M.), Special Publication, **329**, 187–218. Geological Society of London, London.

Read, J.F. (1985) Carbonate platform facies models. *Am. Assoc. Petrol. Geol. Bull.*, **69**, 1–21.

Reijmer, J.J.G. (1998) Compositional variations during phases of progradation and retrogradation of a Triassic carbonate platform (Picco di Vallandro/Dürrenstein, Dolomites, Italy). *Geol. Rundsch.*, **87**, 436–448.

Reijmer, J.J.G. (2016) Carbonate factories. In: *Encyclopedia of Marine Geosciences* (Eds Harff, J., Meschede, M., Petersen, S. and Thiede, J.), pp. 80–84.Springer, The Netherlands.

Reijmer, J.J.G. and **Andresen, N.** (2007) Mineralogy and grain size variations along two carbonate margin-to-basin transects (Pedro Bank, Northern Nicaragua Rise). *Sed. Geol.*, **198**, 327–350.

Reijmer, J.J.G., **Bauch, T.** and **Schäfer, P.** (2012a) Carbonate facies patterns in surface sediments of upwelling and non-upwelling shelf environments (Panama, East Pacific). *Sedimentology*, **59**, 32–56.

Reijmer, J.J.G., **Betzler, C.**, **Kroon, D.**, **Tiedemann, R.** and **Eberli, G.P.** (2002) Bahamian carbonate platform development in response to sea-level changes and the closure of the Isthmus of Panama. *Int. J. Earth Sci.*, **91**, 482–489.

Reijmer, J.J.G., **Palmieri, P.** and **Groen, R.** (2012b) Compositional variations in calciturbidites and calcidebrites in response to sea-level fluctuations (Exuma Sound, Bahamas). *Facies*, **58**, 493–507.

Reijmer, J.J.G., **Palmieri, P.**, **Groen, R.** and **Floquet, M.** (2015) Calciturbidites and calcidebrites: sea-level variations or tectonic processes? *Sed. Geol.*, **317**, 53–70.

Reijmer, J.J.G., **Schlager, W.** and **Droxler, A.W.** (1988) Site 632: Pliocene-Pleistocene sedimentation cycles in a Bahamian basin. In: *Proceedings of the Ocean Drilling Program, Scientific Results Leg 101* (Eds Austin Jr., J.A., Schlager, W. and et al.), **101**, pp. 213–220.Ocean Drilling Program, College Station, TX, USA.

Reijmer, J.J.G., **Sprenger, A.**, **Ten Kate, W.G.H.Z.**, **Schlager, W.** and **Krystyn, L.** (1994) Periodicities in the composition of Late Triassic calciturbidites (Eastern Alps, Austria). In: *Orbital Forcing and Cyclic Sequences* (Eds De Boer, P.L. and Smith, D.G.), *Int. Assoc. Sedimentol.* Special Publication, **19**, 323–343. International Association of Sedimentologists - Blackwell, London.

Reijmer, J.J.G., **Swart, P.K.**, **Bauch, T.**, **Otto, R.**, **Reuning, L.**, **Roth, S.** and **Zechel, S.** (2009) A re-evaluation of facies on Great Bahama Bank I: new facies maps of western Great Bahama Bank. In: *Perspectives in Carbonate Geology: A Tribute to the Career of Robert Nathan Ginsburg* (Eds Swart, P.K., Eberli, G.P. and McKenzie, J.A.), Int. Assoc. Sedimentol. Special Publication, **41**, 29–46.Wiley-Blackwell-IAS, Oxford, UK.

Reijmer, J.J.G., **Ten Kate, W.G.H.Z.**, **Sprenger, A.** and **Schlager, W.** (1991) Calciturbidite composition related to exposure and flooding of a carbonate platform (Triassic, Eastern Alps). *Sedimentology*, **38**, 1059–1074.

Reiss, Z. and **Hottinger, L.** (1984) *The Gulf of Aqaba - Ecologic Micropaleontology*. Springer-Verlag, Berlin–Heidelberg.

Rendle, R.H., **Reijmer, J.J.G.**, **Kroon, D.** and **Henderson, G.M.** (2000) Mineralogy and sedimentology of the Pleistocene to Holocene on the leeward margin of Great Bahama Bank. In: *Proceedings of the Ocean Drilling*

Program, Scientific Results Leg 166 (Eds Eberli, G.P., Swart, P.K., Malone, M.J. and et al.), **166**, pp. 61–76.Ocean Drilling Program, College Station, TX, USA.

Rendle, R.H. and **Reijmer, J.J.G.** (2002) Quaternary slope development of the western, leeward margin of the Great Bahama Bank. *Mar. Geol.*, **185**, 143–164.

Rendle-Bühring, R.H. and **Reijmer, J.J.G.** (2005) Controls on grain-size patterns in periplatform carbonates: marginal setting versus glacio-eustacy. *Sed. Geol.*, **175**, 99–113.

Reolid, J., **Betzler, C.**, **Braga, J.**, **Martín, J.**, **Lindhorst, S.** and **Reijmer, J.G.** (2014) Reef slope geometries and facies distribution: controlling factors (Messinian, SE Spain). *Facies*, **60**, 737–753.

Reolid, J., **Betzler, C.**, **Eberli, G.P.** and **Grammer, G.M.** (2017) The importance of microbial binding in Neogene-Quaternary steep slopes. *J. Sediment. Res.*, **87**, 567–577.

Reuning, L., **Reijmer, J.J.G.** and **Betzler, C.** (2002) Sedimentation cycles and their diagenesis on the slope of a Miocene carbonate ramp (Bahamas, ODP Leg 166). *Mar. Geol.*, **185**, 121–142.

Reymond, C.E., **Zihrul, K.-S.**, **Halfar, J.**, **Riegl, B.**, **Humphreys, A.** and **Westphal, H.** (2016) Heterozoan carbonates from the equatorial rocky reefs of the Gal_apagos Archipelago. *Sedimentology*, **63**, 940–958.

Riding, R. and **Liang, L.** (2005) Geobiology of microbial carbonates: metazoan and seawater saturation state influences on secular trends during the Phanerozoic. *Palaeogeogr. Palaeoclimatol. Palaeoecol.*, **219**, 101–115.

Riding, R., **Martin, J.M.** and **Braga, J.C.** (1991) Coral-stromatolite reef framework, Upper Miocene, Almeria, Spain. *Sedimentology*, **38**, 799–818.

Robbins, L.L. and **Blackwelder, P.L.** (1992) Biochemical and ultrastructural evidence for the origin of whitings: a biologically induced calcium carbonate precipitation mechanism. *Geology*, **20**, 464–468.

Roberts, J.M., **Wheeler, A.J.**, **Freiwald, A.** and **Cairns, S.D.** (2009) *Cold-Water Corals - The Biology and Geology of Deep-Sea Coral Habitats*. Cambridge University Press, Cambridge, UK, 333 pp.

Roth, S. and **Reijmer, J.J.G.** (2004) Holocene Atlantic climate variations deduced from carbonate periplatform sediments (leeward margin, Great Bahama Bank). *Paleoceanography*, **19**, PA1003. https://doi.org/10.1029/2003PA000885.

Roth, S. and **Reijmer, J.J.G.** (2005) Holocene millennial to centennial carbonate cyclicity recorded in slope sediments of the Great Bahama Bank and its climatic implications. *Sedimentology*, **52**, 161–181.

Rüggeberg, A., **Dullo, C.**, **Dorschel, B.** and **Hebbeln, D.** (2007) Environmental changes and growth history of a cold-water carbonate mound (Propeller Mound, Porcupine Seabight). *Int. J. Earth Sci.*, **96**, 57–72.

Rüggeberg, A., **Flögel, S.**, **Dullo, W.-C.**, **Hissmann, K.** and **Freiwald, A.** (2011) Water mass characteristics and sill dynamics in a subpolar cold-water coral reef setting at Stjernsund, northern Norway. *Mar. Geol.*, **282**, 5–12.

Russo, F., **Neri, C.**, **Mastandrea, A.** and **Baracca, A.** (1997) The mud mound nature of the Cassian platform margins of the Dolomites. A case history: the cipit boulders from Punta Grohmann (Sasso Piatto Massif, Northern Italy). *Facies*, **36**, 25–36.

Saxena, S. and **Betzler, C.** (2003) Genetic sequence stratigraphy of cool water slope carbonates (Pleistocene Eucla Shelf, southern Australia). *Int. J. Earth Sci.*, **92**, 482–493.

Scheibner, C. and **Reijmer, J.J.G.** (1999) Facies patterns within a lower Jurassic upper slope to inner platform transect (Jbel Bou Dahar, Morocco). *Facies*, **41**, 55–80.

Schiebel, R. and **Hemleben, C.** (2005) Modern planktic foraminifera. *Paläontologische Zeitschrift*, **79**, 135–148.

Schlager, W. (2000) Sedimentation rates and growth potential of tropical, cool-water and mud-mound carbonate systems. In: *Carbonate Platform Systems: Components and Interactions* (Eds Skelton, P.W. and Palmer, T.J.), *Special Publication*, **178**, pp. 217–227. Geological Society of London, London.

Schlager, W. (2003) Benthic carbonate factories of the Phanerozoic. *Int. J. Earth Sci.*, **92**, 445–464.

Schlager, W. (2005) *Carbonate Sedimentology and Sequence Stratigraphy*. SEPM (Society for Sedimentary Geology), Tulsa, Oklahoma, USA, 200 pp.

Schlager, W. and **James, N.P.** (1978) Low-magnesian calcite limestones forming at the deep-sea floor (Tongue of the Ocean, Bahamas). *Sedimentology*, **25**, 675–702.

Schlager, W., **Reijmer, J.J.G.** and **Droxler, A.W.** (1994) Highstand shedding of carbonate platforms. *J. Sed. Res.*, **B64**, 270–281.

Schlager, W. and **Reijmer, J.J.G.** (2009) Carbonate platform slopes of the Alpine Triassic and the Neogene - a comparison. *Aust. J. Earth Sci.*, **102**, 4–14.

Schnyder, J.S.D., **Eberli, G.P.**, **Kirby, J.T.**, **Shi, F.**, **Tehranirad, B.**, **Mulder, T.**, **Ducassou, E.**, **Hebbeln, D.** and **Wintersteller, P.** (2016) Tsunamis caused by submarine slope failures along western Great Bahama Bank. *Sci. Rep.*, **6**, 35925.

Scholle, P.A. and **Ulmer-Scholle, D.S.** (2003) *A Color Guide to the Petrography of Carbonate Rocks*. American Association of Petroleum Geologists, Tulsa, Oklahoma, USA. 474 pp.

Schwarzacher, W. and **Haas, J.** (1986) Comparative statistical analysis of some Hungarian and Austrian Upper Triassic peritidal carbonate sequences. *Acta Geol. Hung*, **29**, 175–196.

Séard, C., **Camoin, G.**, **Yokoyama, Y.**, **Matsuzaki, H.**, **Durand, N.**, **Bard, E.**, **Sepulcre, S.** and **Deschamps, P.** (2011) Microbialite development patterns in the last deglacial reefs from Tahiti (French Polynesia; IODP Expedition #310): Implications on reef framework architecture. *Mar. Geol.*, **279**, 63–86.

Smith, S.V. and **Buddemeier, R.W.** (1992) Global change and coral reef ecosystems. *Annu. Rev. Ecol. Syst.*, **23**, 89–118.

Spence, G.H. and **Tucker, M.E.** (1997) Genesis of limestone megabreccias and their significance in carbonate sequence stratigraphic models: a review. *Sed. Geol.*, **112**, 163–193.

Stefani, M., **Furin, S.** and **Gianolla, P.** (2010) The changing climate framework and depositional dynamics of Triassic carbonate platforms from the Dolomites. *Palaeogeogr. Palaeoclimatol. Palaeoecol.*, **290**, 43–57.

Stephens, D.W. (1990) Changes in lake levels, salinity and the biological community of Great Salt Lake (Utah, USA), 1847–1987. *Hydrobiologia*, **197**, 139–146.

Stone, R.P. (2006) Coral habitat in the Aleutian Islands of Alaska: depth distribution, fine-scale species associations, and fisheries interactions. *Coral Reefs*, **25**, 229–238.

Strasser, A. (2015) Hiatuses and condensation: an estimation of time lost on a shallow carbonate platform. *Depos. Rec.*, **1**, 91–117.

Stuut, J.-B., **Zabel, M.**, **Ratmeyer, V.**, **Helmke, P.**, **Schefuß, E.**, **Lavik, G.** and **Schneider, R.** (2005) Provenance of

present-day eolian dust collected off NW Africa. *J. Geophys. Res. Atmos.*, **110**.

Surlyk, F. and Lykke-Andersen, H. (2007) Contourite drifts, moats and channels in the Upper Cretaceous chalk of the Danish Basin. *Sedimentology*, **54**, 405–422.

Suzuki, A., Nakamori, T. and Kayanne, H. (1995) The mechanism of production enhancement in coral reef carbonate systems: model and empirical results. *Sed. Geol.*, **99**, 259–280.

Swart, P.K., Oehlert, A.M., Mackenzie, G.J., Eberli, G.P. and Reijmer, J.J.G. (2014) The fertilization of the Bahamas by Saharan dust: a trigger for carbonate precipitation? *Geology*, **42**, 671–674.

Swart, P.K., Reijmer, J.J.G. and Otto, R. (2009) A re-evaluation of facies on Great Bahama Bank II: variations in the δ13C, δ18O and mineralogy of surface sediments. In: *Perspectives in Carbonate Geology: A Tribute to the Career of Robert Nathan Ginsburg* (Eds Swart, P.K., Eberli, G.P. and McKenzie, J.A.), *Int. Assoc. Sedimentol. Special Publication*, **41**, pp. 47–59. Wiley-Blackwell-IAS, Oxford.

Tcherepanov, E.N., Droxler, A.W., Lapointe, P. and Mohn, K. (2008) Carbonate seismic stratigraphy of the Gulf of Papua mixed depositional system: neogene stratigraphic signature and eustatic control. *Basin Res.*, **20**, 185–209.

Tcherepanov, E.N., Droxler, A.W., Lapointe, P., Dickens, G.R., Bentley, S.J., Beaufort, L., Peterson, L.C., Daniell, J. and Opdyke, B.N. (2008) Neogene evolution of the mixed carbonate-siliciclastic system in the Gulf of Papua, Papua New Guinea. *J. Geophys. Res. Earth Surface*, **113**, F01S21.

Tcherepanov, E.N., Droxler, A.W., Lapointe, P., Mohn, K. and Larsen, O.A. (2010) Siliciclastic influx and burial of the Cenozoic carbonate system in the Gulf of Papua. *Mar. Petrol. Geol.*, **27**, 533–554.

Teichert, C. (1958) Cold- and deep-water coral banks. *Am. Assoc. Petrol. Geol. Bull.*, **42**, 1064–1082.

Thompson, J.B. (2000) Microbial whitings. In: *Microbial Sediments* (Eds Riding, R.E. and Awramik, S.M.), pp. 250–260.Springer-Verlag, Berlin – Heidelberg, Germany.

Tinker, S.W. (1998) Shelf-to-basin facies distributions and sequence stratigraphy of a steep-rimmed carbonate margin: capitan depositional system, McKittrick Canyon, New Mexico and Texas. *J. Sed. Res.*, **68**, 1146–1174.

Titschack, J., Fink, H.G., Baum, D., Wienberg, C., Hebbeln, D. and Freiwald, A. (2016) Mediterranean cold-water corals – an important regional carbonate factory? *Depos. Rec.*, **2**, 74–96.

Tsuji, Y. (1993) Tide influenced high energy environments and rhodolith-associated carbonate deposition on the outer shelf and slope off the Miyako Islands, southern Ryukyu Islands Arc, Japan. *Mar. Geol.*, **113**, 255–271.

Tucker, M.E. and Wright, V.P. (1990) *Carbonate Sedimentology*. Blackwell Scientific Publications, Oxford, UK, 482 pp.

Twiggs, E.J. and Collins, L.B. (2010) Development and demise of a fringing coral reef during Holocene environmental change, eastern Ningaloo Reef, Western Australia. *Mar. Geol.*, **275**, 20–36.

van Buchem, F.S.P., Al-Husseini, M.I., Maurer, F. and Droste, H.J. (Eds). (2010) *Barremian – Aptian Stratigraphy and Hydrocarbon Habitat of the Eastern Arabian Plate. GeoArabia Special Publication*, **4**, Gulf PetroLink, Manama, Bahrain, 614 pp (**2** volumes).

van Buchem, F.S.P., Razin, P., Homewood, P.W., Oterdoom, W.H. and Philip, J. (2002) Stratigraphic organization of carbonate ramps and organic-rich intrashelf basins: Natih formation (middle Cretaceous) of northern Oman. *Am. Assoc. Petrol. Geol. Bull.*, **86**, 21–53.

van Buchem, F., Smit, F., Buijs, G., Trudgill, B. and Larsen, P.H. (2018) Tectono-stratigraphic framework and depositional history of the Cretaceous-Danian succession of the Danish Central Graben (North Sea) – new light on a mature area. In: *Petroleum Geology of NW Europe: 50 Years of Learning – Proceedings of the 8th Petroleum Geological Conference* (Eds Bowman, M. and Levell, B.), pp. 9–46. Geological Society of London, London.

van der Kooij, B., Immenhauser, A., Steuber, T., Rionda, J.R.B. and Tome, O.M. (2010) Controlling factors of volumetrically important marine carbonate cementation in deep slope settings. *Sedimentology*, **57**, 1491–1525.

van der Land, C., Eisele, M., Mienis, F., de Haas, H., Hebbeln, D., Reijmer, J.J.G. and van Weering, T.C.E. (2014) Carbonate mound development in contrasting settings on the Irish margin. *Deep Sea Res. Part II*, **99**, 297–306.

van der Land, C., Mienis, F., de Haas, H., Frank, N., Swennen, R. and van Weering, T.C.E. (2010) Diagenetic processes in carbonate mound sediments at the south-west Rockall Trough margin. *Sedimentology*, **57**, 912–931.

van der Land, C., Mienis, F., de Haas, H., de Stigter, H.C., Swennen, R., Reijmer, J.J.G. and van Weering, T.C.E. (2011) Paleo-redox fronts and their formation in carbonate mound sediments from the Rockall Trough. *Mar. Geol.*, **284**, 86–95.

van der Land, C., Wood, R., Wu, K., van Dijke, M.I.J., Jiang, Z., Corbett, P.W.M. and Couples, G. (2013) Modelling the permeability evolution of carbonate rocks. *Mar. Petrol. Geol.*, **48**, 1–7.

van Weering, T.C.E., de Haas, H., de Stigter, H.C., Lykke-Andersen, H. and Kouvaev, I. (2003) Structure and development of giant carbonate mounds at the SW and SE Rockall Trough margins, NE Atlantic Ocean. *Mar. Geol.*, **198**, 67–81.

Verwer, K., Della Porta, G., Merino-Tomé, O. and Kenter, J.A.M. (2009) Controls and predictability of carbonate facies architecture in a Lower Jurassic three-dimensional barrier-shoal complex (Djebel Bou Dahar, High Atlas, Morocco). *Sedimentology*, **56**, 1801–1831.

Viana, A.R., Faugeres, J.C., Kowsmann, R.O., Lima, J.A.M., Caddah, L.F.G. and Rizzo, J.G. (1998) Hydrology, morphology and sedimentology of the Campos continental margin, offshore Brazil. *Sed. Geol.*, **115**, 133–157.

Villalobos, M. and Braga, J.C. (Eds). (2003) *Geology of the Arid Zone of Almeria (Southeast Spain) - An Educational Field Guide*. State Water Company for the Southern Basin SA (ACUSUR). 165 pp.

Wallace, M.W., Holdgate, G.R., Daniels, J., Gallagher, S.J. and Smith, A. (2002) Sonic velocity, submarine canyons, and burial diagenesis in Oligocene-Holocene cool-water carbonates, Gippsland Basin, southeast Australia. *Am. Assoc. Petrol. Geol. Bull.*, **86**, 1593–1607.

Warrlich, G., Bosence, D. and Waltham, D. (2005) 3D and 4D controls on carbonate depositional systems: sedimentological and sequence stratigraphic analysis of an attached carbonate platform and atoll (Miocene, Níjar Basin, SE Spain). *Sedimentology*, **52**, 363–389.

Warrlich, G.M.D., Waltham, D.A. and Bosence, D.W.J. (2002) Quantifying the sequence stratigraphy and drowning mechanisms of atolls using a new 3-D forward stratigraphic modelling program (CARBONATE 3D). *Basin Res.*, **14**, 379–400.

Webster, J.M., **Beaman, R.J.**, **Puga-Bernabéu, Å.**, **Ludman, D.**, **Renema, W.**, **Wust, R.A.J.**, **George, N.P.J.**, **Reimer, P.J.**, **Jacobsen, G.E.** and **Moss, P.** (2012) Late Pleistocene history of turbidite sedimentation in a submarine canyon off the northern Great Barrier Reef, Australia. *Palaeogeogr. Palaeoclimatol. Palaeoecol.*, **331–332**, 75–89.

Webster, J.M., **George, N.P.J.**, **Beaman, R.J.**, **Hill, J.**, **Puga-Bernabéu, Å.**, **Hinestrosa, G.**, **Abbey, E.A.** and **Daniell, J.J.** (2016) Submarine landslides on the Great Barrier Reef shelf edge and upper slope: a mechanism for generating tsunamis on the north-east Australian coast? *Mar. Geol.*, **371**, 120–129.

Weij, R., **Reijmer, J.J.G.**, **Eberli, G.P.** and **Swart, P.K.** (2019) The limited link between accommodation space, sediment thickness, and inner platform facies distribution (Holocene–Pleistocene, Bahamas). *Depos. Rec.*, **5**, 400–420.

Weiner, S. and **Dove, P.M.** (2003) An overview of biomineralization processes and the problem of the vital effect. *Rev. Mineral. Geochem.*, **54**, 1–29.

Wendt, J., **Belka, Z.**, **Kaufmann, B.**, **Kostrewa, R.** and **Hayer, J.** (1997) The world's most spectacular carbonate mud mounds (Middle Devonian, Algerian Sahara). *J. Sed. Res.*, **67**, 424–436.

Westphal, H., **Halfar, J.** and **Freiwald, A.** (2010) Heterozoan carbonates in subtropical to tropical settings in the present and past. *Int. J. Earth Sci.*, **99**, 153–169.

Wienberg, C., **Hebbeln, D.**, **Fink, H.G.**, **Mienis, F.**, **Dorschel, B.**, **Vertino, A.**, **Correa, M.L.** and **Freiwald, A.** (2009) Scleractinian cold-water corals in the Gulf of Cadiz-First clues about their spatial and temporal distribution. *Deep Sea Res. Part 1 Oceanogr. Res. Pap.*, **56**, 1873–1893.

Wienberg, C. and **Titschack, J.** (2017) Framework-forming scleractinian cold-water corals through space and time: a late Quaternary North Atlantic perspective. In: *Marine Animal Forests: The Ecology of Benthic Biodiversity Hotspots* (Eds Rossi, S., Bramanti, L., Gori, A. and Orejas-Saco-del-Valle, C.), pp. 699–732.Springer International Publishing Switzerland, Cham, Switzerland.

Wienberg, C., **Titschack, J.**, **Freiwald, A.**, **Frank, N.**, **Lundälv, T.**, **Taviani, M.**, **Beuck, L.**, **Schröder-Ritzrau, A.**, **Krengel, T.** and **Hebbeln, D.** (2018) The giant Mauritanian cold-water coral mound province: oxygen control on coral mound formation. *Quatern. Sci. Rev.*, **185**, 135–152.

Wilber, R.J., **Milliman, J.D.** and **Halley, R.B.** (1990) Accumulation of bank-top sediment on the western slope of Great Bahama Bank: rapid progradation of a carbonate megabank. *Geology*, **18**, 970–974.

Williams, H.D., **Burgess, P.M.**, **Wright, V.P.**, **Della Porta, G.** and **Granjeon, D.** (2011) Investigating carbonate platform types: multiple controls and a continuum of geometries. *J. Sediment. Res.*, **81**, 18–37.

Wilson, P.A. and **Roberts, H.H.** (1992) Carbonate-periplatform sedimentation by density flows: a mechanism for rapid off-bank and vertical transport of shallow-water fines. *Geology*, **20**, 713–716.

Wilson, P.A. and **Roberts, H.H.** (1995) Density cascading: off-shelf sediment transport, evidence and implications, Bahama Banks. *J. Sed. Res.*, **A65**, 45–56.

Wright, V.P. and **Burchette, T.P.** (1998) *Carbonate Ramps*. Geological Society of London, London, 465 pp.

Wunsch, M., **Betzler, C.**, **Lindhorst, S.**, **Lüdmann, T.** and **Eberli, G.P.** (2017) Sedimentary dynamics along carbonate slopes (Bahamas archipelago). *Sedimentology*, **64**, 631–657.

Wunsch, M., **Betzler, C.**, **Eberli, G.P.**, **Lindhorst, S.**, **Lüdmann, T.** and **Reijmer, J.J.G.** (2018) Sedimentary dynamics and high-frequency sequence stratigraphy of the southwestern slope of Great Bahama Bank. *Sed. Geol.*, **363**, 96–117.

Yates, K.K. and **Robbins, L.L.** (1998) Production of carbonate sediments by a unicellular green alga. *Am. Mineral.*, **83**, 1503–1509.

Zhang, J., **Kim, W.**, **Olariu, C.** and **Steel, R.** (2019) Accommodation- versus supply-dominated systems for sediment partitioning to deep water. *Geology*, **47**, 419–422.

Zhang, J., **Steel, R.** and **Olariu, C.** (2017) What conditions are required for deltas to reach the shelf edge during rising sea level? *Geology*, **45**, 1107–1110.

Zhou, K. and **Pratt, B.R.** (2019a) Upper Devonian (Frasnian) stromatactis-bearing mud mounds, western Alberta, Canada: reef framework dominated by peloidal microcrystalline calcite. *J. Sed. Res.*, **89**, 833–848.

Zhou, K. and **Pratt, B.R.** (2019b) Composition and origin of stromatactis-bearing mud-mounds (Upper Devonian, Frasnian), southern Rocky Mountains, western Canada. *Sedimentology*, **66**, 2455–2489.